INTERNATIONAL STANDARD

ISO 21650

First edition
2007-10-15

Actions from waves and currents on coastal structures

Effets des vagues et des courants sur les structures côtières

Reference number
ISO 21650:2007(E)

ISO copyright office
Case postale 56 • CH-1211 Geneva 20
Tel. + 41 22 749 01 11
Fax + 41 22 749 09 47
E-mail copyright@iso.org
Web www.iso.org

Published in Switzerland

Contents

Page

Foreword

ISO (the International Organization for Standardization) is a worldwide federation of national standards bodies (ISO member bodies). The work of preparing International Standards is normally carried out through ISO technical committees. Each member body interested in a subject for which a technical committee has been established has the right to be represented on that committee. International organizations, governmental and non-governmental, in liaison with ISO, also take part in the work. ISO collaborates closely with the International Electrotechnical Commission (IEC) on all matters of electrotechnical standardization.

International Standards are drafted in accordance with the rules given in the ISO/IEC Directives, Part 2.

The main task of technical committees is to prepare International Standards. Draft International Standards adopted by the technical committees are circulated to the member bodies for voting. Publication as an International Standard requires approval by at least 75 % of the member bodies casting a vote.

Attention is drawn to the possibility that some of the elements of this document may be the subject of patent rights. ISO shall not be held responsible for identifying any or all such patent rights.

ISO 21650 was prepared by Technical Committee ISO/TC 98, *Bases for design of structures*, Subcommittee SC 3, *Loads, forces and other actions*.

Introduction

This International Standard, which deals with the actions from waves and currents on structures in the coastal zone and in estuaries, is the first of its kind. Waves and currents and actions from waves and currents on structures in deeper water, especially structures for the petroleum industry, are dealt with in ISO 19901-1 and ISO 19902, ISO 19903 and ISO 19904-1. Some of the structural elements for deeper water structures and coastal structures are the same, especially elements with cylindrical shapes. There will thus be, to some extent, an overlap between this International Standard and other ISO standards on the wave and current actions on cylindrical structural elements. There is though, a difference in wave conditions and wave kinematics between coastal waves and deeper water waves.

Actions from waves and currents on coastal structures

1 Scope

This International Standard describes the principles of determining the wave and current actions on structures of the following types in the coastal zone and estuaries:

- breakwaters:
  - rubble mound breakwaters;
  - vertical and composite breakwaters;
  - wave screens;
  - floating breakwaters;
- coastal dykes;
- seawalls;
- cylindrical structures (jetties, dolphins, lighthouses, pipelines etc.).

For the rubble mound structures it is not possible to determine the forces on and the stability of each individual armour unit because of the complex flow around and between each armour unit. But there are formulae and principles to estimate the necessary armour unit mass given the design wave conditions. Coefficients in these formulae are based on hydraulic model tests. Since the rubble mound structures are heavily used, they are included in this International Standard, although they may not be treated exactly in accordance with ISO 2394.

This International Standard does not include breakwater layout for harbours, layout of structures to manage sediment transport, scour and beach stability or the response of flexible dynamic structures, except vortex induced vibrations.

Design will be performed at different levels of detail:

- concepts;
- feasibility;
- detailed design.

This International Standard is aimed at serving the detailed design.

It is pointed out that the annexes are only informative and are not guidelines/manuals. The annexes have no regulatory power.

Wave and current conditions vary for different construction sites. It is very important to assess the wave and current conditions at a given site. Assessment procedures for these conditions and for their uncertainties are included.

2 Terms and definitions

For the purposes of this document, the following terms and definitions apply.

2.1
actions
force (load) applied to the structure by waves and/or currents

2.2
anchors
units placed on the seabed, such as ship anchors, piles driven into the seabed or concrete blocks, to which mooring lines are attached to restrain a floating object from excessive movements

2.3
annual maximum method
method of estimating extreme wave heights based on a sample of annual maximum wave heights

2.4
armour layer
protective layer on a breakwater, seawall or other rubble mound structures composed of armour units

2.5
armour unit
relatively large quarry stone or concrete shaped unit that is selected to fit specified geometric characteristics and density

2.6
astronomical tide
phenomenon of the alternate rising and falling of sea surface solely governed by the astronomical conditions of the sun and the moon, which is predicted with the tidal constituents determined from harmonic analysis of tide level readings over a long period

2.7
breakwater
structure protecting a shore area, harbour, anchorage and/or basin from waves

2.8
buoyancy
resultant of upward forces, exerted by the water on a submerged or floating body, equal to the weight of the water displaced by this body

2.9
chart datum
CD
reference level for soundings in navigation charts

2.10
core
inner portion of a breakwater, dyke and rubble mound structures, often with low permeability

2.11
crest
1. highest point of a coastal structure

2. highest point of a wave profile

2.12
crown wall
concrete superstructure on a rubble mound

2.13
datum level
reference level for survey, design, construction and maintenance of coastal and maritime structures, often set at a chart datum or national geodetic datum

2.14
deep water
water of such a depth that surface waves are little affected by bottom topography, being larger than about one-half the wavelength

2.15
design water level
DWL
water level selected for functional design, structural design and stability analysis of marine structures

NOTE Generally it is the water level that mostly affects the safety of the structures/facilities in question. DWL is chosen in view of the acceptable level of risk of failure/damage.

2.16
density driven currents
currents induced by horizontal gradients of water density generated by changes in the salinity and/or temperature, which are caused by the influx of fresh water from run-off from land through an estuary, heat flux from coastal power stations, or other reasons

2.17
diffractions coefficient
ratio of the height of diffracted waves to the height of incident waves

2.18
directional spreading function
function expressing the relative distribution of wave energy in the directional domain

2.19
directional wave spectrum
function expressing the energy density distribution of waves in the frequency and directional domains, being expressed as the product of frequency wave spectrum and the directional spreading function

2.20
drag coefficient
coefficient used in the Morison equation to determine the drag force

2.21
dyke berms
nearly horizontal area in the seaward and landward dyke slope which are primarily built to provide access for maintenance and amenity and which reduce wave run-up and overtopping

2.22
dyke toe
part of a dyke that terminates the base of the dyke on its seaward face

NOTE Various toe constructions are used to prevent undermining of the dyke.

2.23
extreme sea state
extreme waves
state of waves occurring a few dozen times a year to once in many years, expressed with the significant wave height and the mean or significant wave period at the peak of storm event

2.24
filter
intermediate layer, preventing fine materials of an underlayer from being washed through the voids of an upper layer

2.25
floating breakwater
moored floating object to reduce wave heights in the area behind the floating breakwater

2.26
foreshore
shallow water zone near the shore on which coastal dykes, seawalls and other structures are built

NOTE In beach morphology the term foreshore is used to denote the part of the shore lying between the crest of the seaward berm and the ordinary low water mark.

2.27
frequency wave spectrum
function expressing the energy density distribution of waves in the frequency domain

2.28
geotextile
synthetic fabric which may be woven or non-woven used as a filter

2.29
highest astronomical tide
HAT
tide at the highest level that can be predicted to occur under average meteorological conditions and under any combination of astronomical conditions

NOTE HAT is not reached every year and does not represent the highest sea level that can be reached, because storm surges and tsunamis may cause considerably higher levels to occur.

2.30
highest wave height
height of the highest wave of a given wave record or that in a wave train under a given sea state

2.31
impulsive wave pressure
water pressure of high peak intensity with a very short duration induced by the collision of the front surface of a breaking wave with a structure or the collision of a rising wave surface with a horizontal or slightly inclined deck of a pier

2.32
inertia coefficient
coefficient used in the Morison equation to determine the inertia force

2.33
international marine chart datum
IMCD
chart datum set at the lowest astronomical tide level, as adopted by the International Hydrographic Organization (IHO)

2.34
jetty GB
pier US
deck structure supported by vertical and possibly inclined piles extending into the sea, frequently in a direction normal to the coastline

2.35
lift coefficient
coefficient used to determine the lift force

2.36
lowest astronomical tide
LAT
tide at the lowest level that can be predicted to occur under average meteorological conditions and under any combination of astronomical conditions

NOTE LAT is not reached every year and does not represent the lowest sea level which can be reached, because storm surges (negative) and tsunamis may cause considerably lower levels to occur.

2.37
mean high water springs
MHWS
average height of high waters, occurring at the time of spring tides

2.38
mean low water springs
MLWS
average height of low waters occurring at the time of the spring tides

2.39
mean sea level
MSL
average height of the sea level for all stages of the tide over a 19-year period, generally determined from hourly height readings

2.40
mean water level
MWL
average elevation of the water surface over a given time period, usually determined from hourly tidal level readings

NOTE The monthly mean water level varies around seasons by a few tens of centimetres.

2.41
mean wave period
average period of all waves among a given wave record

NOTE The mean wave period is often estimated from the spectral information obtained from a wave record. See 5.2.1.

2.42
moorings
ropes, wires or chains to hold a floating object in position

2.43
overtopping
passing of water over the top of a structure as a result of wave run-up or surge actions

NOTE This definition could serve as a general definition and should not be given individually for each structure.

2.44
parapet
low wall built along the crest of a seawall

2.45
peaks-over-threshold method
POT method
method of estimating extreme wave heights based on a sample of peak heights of storm waves exceeding some threshold level

2.46
peak wave period
period corresponding to the peak of frequency wave spectrum

2.47
permeability
capacity of bulk material (sand, crushed rock, soft rock *in situ*) in permitting movement of water through its pores

2.48
pipeline
structure for carrying water, oil, gas, sewage, etc.

2.49
piping
erosion of closed flow channels caused by water flowing through soil usually underneath the dyke body

NOTE Soil particles are carried about by seepage flow, thus endangering the stability of the dyke.

2.50
pore pressure
interstitial pressure of water within a mass of soil or rock

2.51
porosity
percentage of the total volume of a soil and/or granular material occupied by air/gas and water

2.52
pulsating wave pressure
wave pressure with a period comparable with the wave period

2.53
refraction coefficient
ratio of the height of waves having been affected by the refraction effect in shallow water to their height in deep water with the shoaling effect eliminated

2.54
reflection coefficient
ratio of the height of reflected waves to the height of incident waves

2.55
revetment
cladding of concrete slabs, asphalt, clay, grass and other materials to protect the surface of a sea dyke against erosion

2.56
rip-rap
usually, well-graded quarry stone, randomly placed as an armour layer to prevent erosion

2.57
rock
aggregate of one or more minerals

2.58
run-up/run-down
phenomenon of waves running up and down the seaward slope of a sloping structure, their height being measured as the vertical distance from the still water level

2.59
***R*-year wave height**
extreme wave height corresponding to the return period of R years

NOTE When used, the specific value of R is indicated such as 100-year wave height.

2.60
scour
removal of underwater sand and stone material by waves and currents, especially at the base or toe of a structure

2.61
sea state
condition of sea surface within a short time span, being expressed with characteristic wave heights, periods and directions

2.62
seaward dyke slope
slope of the dyke on the seaward side that is generally flatter than 1:4 to reduce wave run-up, protected by a revetment made of clay and grass, concrete slabs, asphalt, or stones to prevent erosion

2.63
shallow water
water of such a depth that surface waves are noticeably affected by bottom topography, being less than about one-half the wavelength

NOTE Region of water in which waves propagate is sometimes classified into three categories of deep water, intermediate depth, and shallow water. According to this classification, shallow water represents the zone of depth less than about one-twentieth of the wavelength.

2.64
shoaling coefficient
ratio of the height of waves affected by the depth change in shallow water to their height in deep water with the refraction effect eliminated

2.65
shoreward dyke slope
slope of dyke on the landward side, generally no steeper than 1:3 to prevent erosion by wave overtopping

NOTE It is generally protected by a revetment made of clay/grass.

2.66
significant wave height
average height of the one-third highest waves of a given wave record

NOTE The significant wave height is often estimated from the spectral information obtained from a wave record. See 5.2.1.

2.67
significant wave period
average period of the one-third highest waves of a given wave record

2.68
slamming actions
actions when a water surface and a structure suddenly collide

2.69
still water level
SWL
level of water surface in the absence of any wave and wind actions, is also called the undisturbed water level

2.70
stone
quarried or artificially broken rock for use in construction, either as an aggregate or cut into shaped blocks as dimension stone

2.71
storm surge
phenomenon of the rise of the sea surface above astronomical water level on the open coast, bays and on estuaries due to the action of wind stresses on the water surface, the atmospheric pressure reduction, storm-induced seiches, wave set-up and others

2.72
swell
wind-generated waves that have advanced out of the wave generating area and are no longer affected by winds

2.73
tidal currents
alternative or circulating currents associated with tidal variation

NOTE Tides and tidal currents are generally strongly modified by the coastline.

2.74
toe
lowest part of sea- and port-side breakwater slope, generally forming the transition to the seabed

2.75
total sample method
method of estimating extreme wave heights by extrapolating a distribution of all the wave heights measured at a site of interest

2.76
tsunami
long waves with the period of several minutes to one hour and the height up to a few tens of meters, which are generated by the vertical movement of sea floor associated with a submarine earthquake, by plunging of large mass of earth into water by land slide or volcanic eruption, and other causes

2.77
uplift
upward water pressure exerted up the base of a structure or pavement due to waves, excluding buoyancy

2.78
vortex induced vibration
VIV
vibration induced by vortexes shed alternatively from either side of a cylinder in a current and/or waves

2.79
wave climate
description of wave conditions at a particular location over months, seasons or years, usually expressed by the statistics of significant wave height, mean or significant wave period, and wave direction

2.80
wave induced currents
currents in the nearshore zone, which are induced by the horizontal gradient of wave energy flux being attenuated by wave breaking

2.81
wave pressure
water pressure exerted on a structure induced by the action of waves, excluding hydrostatic pressure

2.82
wave set-up
rise of water level near the shoreline associated with wave decay by breaking

NOTE Wave set-up may amount to more than 10 % of the offshore significant wave height.

2.83
wave transmission coefficient
ratio of the height of waves transmitted behind a structure to the height of incident waves

2.84
wind waves
waves generated by and/or developed by wind

2.85
wind driven current
currents induced by the wind stress on the sea surface

NOTE In coastal waters, wind driven currents are influenced by the bottom topography and the presence of the coastline.

2.86
wind set-up
rise of water level at the leeward side of a water body caused by wind stresses on the water surface

3 Symbols

$H_{1/3}$ significant wave height or the average height of highest one-third waves

H_{max} highest wave height

H_{m0} significant wave height estimated from wave spectrum

m_n n-th moment of wave spectrum such as m_0 and m_2

$T_{1/3}$ significant wave period

T_m mean wave period

$T_{m0,2}$ mean wave period estimated from the zero-th and second moments of wave spectrum

T_p period corresponding to the peak of frequency wave spectrum

4 Basic variables for actions from waves and currents

4.1 Water levels

4.1.1 Tides

The astronomical tide levels at a design site shall be calculated with the tidal constituents obtained through the harmonic analysis of a long-term tide record at the site or those estimated from a nearby tide station.

The highest and lowest water levels that have occurred at or near the site should be taken into account in the evaluation of the actions from waves and currents.

The datum level for maritime structures shall be established with reference to the International Marine Chart Datum and/or the national geodetic datum levels.

4.1.2 Storm surges and tsunamis

The characteristics of storm surges at a design site should be duly investigated and be taken into consideration in evaluation of the action of waves and currents.

Investigation of storm surges may include data collection and hindcasting of storm surges in the past, and numerical evaluation of hypothetical storm surges in the future.

Sets of storm surge water levels and/or storm tides should statistically be analysed for extreme distribution functions so as to determine R-year storm surge levels.

In the locality where the action of a tsunami is not negligible, tsunami characteristics at the site should be duly investigated by means of data collection and hindcasting of tsunamis in the past, and/or numerical evaluation of hypothetical tsunamis in the future.

4.1.3 Joint probability of waves and high water level

Evaluation of the action of waves should be made with due consideration for the joint probability of wave height and water level, especially at a site where the water is relatively shallow and breaker heights are controlled by the depth of water under influence of the tide.

The wave measurement data obtained at the location where the largest wave height is limited by the water depth should not be used for extreme statistical analysis for the estimation of storm wave conditions at the water deeper than the site of measurements.

4.2 Waves

4.2.1 Wave heights and periods

The characteristic heights of wind waves and swell for evaluation of the action of waves should be the significant wave height $H_{1/3}$ and the highest wave height H_{max}, which are defined by the zero-crossing method in the time domain analysis. Other definitions of wave heights may be used as the characteristic wave heights when a method of evaluation requires the use of such wave heights. The significant wave height may be estimated from the zero-th moment of wave spectrum, m_0, as being equal to 4,0 $m_0^{1/2}$. When this estimation is employed, the symbol Hm_0 should be used instead of $H_{1/3}$ so as to clarify the estimation method of the significant wave height, because they may differ by several percent or more (see B.1.2).

The characteristic periods of wind waves and swell for evaluation of the action of waves are the significant wave period $T_{1/3}$ and the mean period T_m, which are defined by the zero-crossing method in the time domain analysis, and the spectral peak period T_p, which is obtained from the frequency-domain analysis. The mean period may be estimated from the zero-th and second moments of wave spectrum as being equal to $(m_0/m_2)^{1/2}$. When this estimation is employed, the symbol $T_{m0,2}$ should be used so as to clarify the estimation method of the mean wave period, because the spectrally estimated mean period is generally smaller than the individually counted mean period.

Because of the random nature of wind waves and swell, the heights and periods of individual waves in a given sea state are distributed over broad ranges of variation. Statistical distributions of individual wave heights and periods should be taken into consideration when evaluating actions from waves in shallow water (see B.1).

4.2.2 Wave spectrum

Characteristics of wind waves and swell may also be represented with the directional wave spectrum, which is expressed as the product of the frequency spectral density function and the directional spreading function (see B.2).

When evaluating the action of waves, the information on the wave spectrum being employed should be clearly stated.

The extent of the directional spreading of waves becomes narrower in shallow water than in deep water because of the wave refraction effect. This change should be taken into consideration when evaluating the action of waves in shallow water.

Where wind waves and swell coexist, wave spectra exhibit multiple peaks. Wave heights may be estimated from the zero-th moment of the wave spectrum (see B.1.2). Difficulty is encountered in defining the significant wave period and the spectral peak period as well as the wave direction in case of multi-peaked wave spectra. Evaluation of the action of waves of multi-peaked spectra can be made by calculating contributions of components, constructed by superimposing the spectra of wind waves and swell in question.

4.2.3 Statistics of extreme sea state

Statistics of extreme sea state at a specific site should be established on the basis of instrumentally measured wave data and/or hindcasted wave data, coupled with necessary refraction/shoaling analysis, which cover the duration as long as possible and not less than 15 y (see B.4.1).

The method of wave hindcasting should have successfully been calibrated with several storm wave data by instrumental measurements around the site of interest.

Caution should be taken for the water depth at which waves have been measured, because a shallow water depth imposes an upper limit to the largest wave height owing to wave decay by breaking.

The preferred method of producing the data set of extreme waves is the peaks-over-threshold (POT) method. The annual maximum method may be employed, but the use of the total sample method is discouraged.

When estimating the wave height corresponding to a given return period, the confidence interval to account for sample variability should be evaluated and reported.

The wave period associated with the return wave height can be determined by referring to empirical joint distributions of wave height and period of extreme wave data.

The highest wave height corresponding to a given return period can be estimated from the result of extreme statistical analysis for the significant wave height, by converting the latter to the former on the basis of the Rayleigh distribution of individual wave heights and the wave transformation analysis.

4.2.4 Wave transformation

4.2.4.1 General

Waves undergo various transformation processes while travelling from deep water toward the shore. The processes include wave shoaling, refraction, diffraction, reflection, transmission, breaking and others. When waves propagate into a region with currents of appreciable strength, the wave heights and direction change. Considerations to be given to these wave transformation processes are described in 4.2.4.2 to 4.2.4.8.

4.2.4.2 Wave shoaling

The process of wave shoaling may be evaluated using the linear wave theory. The shoaling coefficient of wind waves and swell can be calculated by means of either the monochromatic wave method or the spectral method, because the difference between the results by the two methods is a few percent at most.

When evaluating wave loading on structures however, it is preferable to take into account the wave non-linearity effect that can cause a large increase of wave height beyond the prediction by the linear wave theory.

4.2.4.3 Wave refraction

Wave transformation by refraction should be evaluated by the directional spectral calculation. For preliminary analysis however, the calculation with monochromatic waves can be employed for the cases of simple bathymetry because of a relatively small difference between the two calculation methods for such cases (see B.5.2).

4.2.4.4 Wave diffractions

Wave transformation by diffraction behind barriers such as islands and breakwaters shall be evaluated using the directional spectral calculation. Diagrams of multidirectional random wave diffractions can be referred to for the purpose of preliminary analysis. Care should be taken for the directional spreading characteristics of wind waves and swell at the site of interest, because they are the governing factor of random wave diffraction.

When it is expected that wave diffraction takes place in association with wave refraction over shoals, an appropriate method of numerical analysis and/or hydraulic model tests should be employed (see B.5.3).

4.2.4.5 Wave reflection and transmission

The coefficients of wave reflection and transmission of a maritime structure can be estimated by means of hydraulic model tests and/or the knowledge gained through model tests of similar structures in the past.

The influence of reflected waves on harbour tranquillity, structural stability and others should be examined when evaluating the action of waves.

4.2.4.6 Wave breaking

Decay and variation of wave height caused by breaking in the nearshore zone shall be evaluated by taking into account the random nature of waves.

The nearshore zone is characterized by gradual changes in the functional shape of wave height distribution, rise of the mean water level (called wave set-up) and its long-period fluctuation (called the surf beat) by wave actions, and non-zero wave height at the initial shoreline of zero depth. A numerical model for random wave breaking in the nearshore zone should be capable of reproducing such features.

4.2.4.7 Wave transformation by currents

Changes in the heights and directions of waves by currents depend on the current strength and the angle of encounter. Appropriate numerical models and/or hydraulic model tests should be used to evaluate these changes when changes are expected to be significant.

4.2.4.8 Other transformations

Other processes of wave attenuation by bottom friction, soft subsoil damping, and others may be taken into account as necessary when evaluating the action of waves.

4.2.5 Wave crest elevation and wave kinematics

4.2.5.1 Wave crest elevation

The height of a wave crest above the still water level is larger than one half of the wave height owing to the non-linear nature of water waves. Non-linear wave theories and/or reliable laboratory test data should be referred to when estimating the crest elevation of design waves. The theory and/or laboratory data of monochromatic waves may be applied to the highest individual wave of random waves for estimation of highest wave crest elevation.

4.2.5.2 Wave kinematics

The wave kinematics, or the orbital velocities and accelerations of water particles under the action of waves, should be evaluated by means of non-linear wave theories of high accuracy, because the linear wave theory underestimates the orbital velocities especially around the wave crest.

When waves are expected to break at a location at which the action of waves are to be evaluated, special consideration should be taken when evaluating the kinematics and the form of the waves because they can be quite different to those of non-breaking waves. Use of hydraulic model tests and/or advanced numerical models is recommended for the evaluation.

4.2.5.3 Wave and current kinematics

When currents of appreciable strength coexist with waves, the vector sum of the current velocity and the orbital velocities of particles by waves may be employed in evaluating the kinematics of water particles.

4.3 Currents

4.3.1 General

Currents may have an effect on structures, directly and indirectly. Directly they exercise the drag and lift forces on the structure. Indirectly they interfere with the waves and modify the wave kinematics and thus affect the actions from waves and currents. Thus the current-wave interactions should be considered when evaluating the action of waves and currents unless the currents are weak.

Currents in coastal waters may be divided into tidal currents, wind-driven currents, density-driven currents and wave-induced currents.

Currents in coastal waters may be affected by the current in the adjacent ocean. The current velocities are in general stronger in coastal waters than in the deeper oceans.

4.3.2 Current velocity

The current velocity should be expressed in vector form, with the absolute magnitude (speed) and the direction, or with the velocity components in a coordinate system.

Current velocities at a design site should preferably be investigated by field measurements for a sufficiently long duration time. Where tidal currents are not negligible, measurements should be made at several elevations in the water, because current velocities vary vertically.

When field measurements are not feasible, numerical computations may be carried out for gaining information on currents. However, calibration of the computations model should have been made with the field measurement data at several sites in the region of the same coastal waters.

5 Wave and current action on structures

5.1 Wave action on mound breakwaters

5.1.1 Definitions

Mound breakwaters are characterized by a seaward sloping front and a porous structure. The rear side might be a slope, a vertical face structure or reclaimed land. While the core is most often made of relatively small size wide-graded stone material, the slope surfaces are generally armoured with larger well-sorted rocks or concrete blocks of various shapes. Core and armour layers are separated by filter layers. A monolithic concrete crown wall, sometimes fully or partly sheltered by armour blocks, is used for the crest when access roads are needed or by some other reason.

Berm breakwaters are a special type of rubble mound breakwater which allow a certain degree of deformation of slope surfaces under wave action and reshape themselves to gain stability against further wave actions. A berm is formed around the mean sea level on the seaward side. A horizontal berm is built at construction stage and is allowed to reshape into an S-shape.

5.1.2 Types of wave action

Waves break on the sloping front resulting in loading on the armour units, run-up, run-down as well as related pore pressure variations and porous flow inside the structure.

The impact of waves on a breakwater depends on the stage of instability of the waves, i.e. the actions from non-breaking, breaking and broken waves are different given the same significant wave height and wave steepness.

5.1.3 Wave action on seaward armour units

The stability of armour units on slope surfaces against the effect of wave actions shall be examined. The wave action on the seaward armour layer is affected by the wave reflection from the structure. The armour stability increases with the increase in porosity and permeability. Further, a low-crested structure where significant overtopping occurs experiences less wave loading on the armour units than a structure with a high freely extending crown wall exposed to direct wave actions, other things being equal.

Due to the complexity of the flow around each armour unit, it has not been possible to evaluate the wave action's effect on individual armour units. Instead the required mass for the individual armour units to be stable has been determined through some semi-theoretical concepts leading to formulae with unknown coefficients. These coefficients have been determined through model tests and in some cases prototype observations.

Assessment of armour stability may be based on semi-empirical formulae (see D.1) for less exposed structures falling into the validity range for the formulae, provided that the uncertainties of the formulae are taken into account. Otherwise hydraulic model tests should be performed.

The stability of a berm breakwater depends on the equilibrium of seaward slope shape against the action of waves during its design working life. The capability of the trunk section in maintaining stability may be checked with empirical formulae but should preferably be examined by hydraulic model tests (see D.2).

5.1.4 Wave actions on seaward toe

The stability of a seaward rubble mound toe shall be examined in relation to its supporting function. The stability is mainly affected by the wave-induced flow during run-down. In case of non-depth limited waves, the most critical situation will generally be at low water levels. Special consideration should be taken where breaking waves can act directly on the toe and where seabed scour can endanger the stability of the toe.

Empirical formulae for assessment of toe block stability, based on model tests, can be used within their validity range for standard toe solutions where no wave breaking takes place on the toe (see D.1). However, model tests are generally recommended.

5.1.5 Wave overtopping

The effect of overtopping water and spray should be considered in relation to the function of the breakwater and the activities on and behind the breakwater. Attention should be given to wave transmission, danger to traffic and vessels moored behind the breakwater and damage to infrastructure and goods on hinterlands.

Empirical formulae based on model tests for assessment of average overtopping discharge can be used within their validity range (see D.1). Where overtopping is a critical factor it is recommended to perform model tests, because the existing formulae have large uncertainties and provide no information on the distribution in time and space of the overtopping water.

5.1.6 Wave action on rear slope armour

The stability of the rear slope armour layer should be considered. Overtopping water hitting the rear slope might cause damage to the slope and thus endanger the stability of the breakwater crest. Large pore pressure gradients can enhance the effect by causing a push-out load on the rear side surface blocks. This effect is usually enhanced by the presence of crown wall structures.

Assessment of rear slope armour stability should in general be based on model tests due to the lack of reliable formulae.

5.1.7 Influence of wave action on geotechnical failures

Wave loading on the slopes together with wave-induced pore pressures in the mound, and on and in the seabed, should be considered when examining the stability against geotechnical failures.

Wave loading can be approximated by the weight of water under a wave crest above the design water level, being negative if under a trough, or by the wave pressure acting on the slopes.

Pore pressures in the mound and in the seabed can be assessed by the use of calibrated numerical models. Pore pressures in the mound can be assessed by the use of model tests with due consideration of scale effects.

5.1.8 Wave action on crown walls

A freely standing part of a crown wall can experience impulsive wave loads when directly exposed to wave actions, while a wall or part of a wall sheltered by armour blocks gets pulsating wave loads. The crown wall base will experience wave-induced forces if situated below the envelope of the phreatic surface. Uplift forces are also generated by waves hitting a recurved wall front (nose for reduction of overtopping). For assessment of the overall stability of the crown wall against sliding and slip failures, the most critical simultaneous combination of the front loading and the uplift forces should be identified.

Impulsive pressures on the crown wall front are characterized by high peak values of very short duration. The influence of impulsive pressures on the overall stability of the crown wall should be evaluated with due consideration of the dynamic interactions with the foundation. Moreover, the influence of significant air inclusions in the breaking waves hitting the crown wall might be taken into account when transforming model test loadings into prototype.

For the assessment of strength of the crown wall, the load distributions giving the largest tensile stresses in the various parts of the structure should be used. The load results from wave-induced pressures, wave loads transmitted through armour units resting against the wall, dead loads from armour units resting against the wall, and reaction forces from the foundation.

The loadings on crown wall should preferably be determined from model tests with due consideration of 3-dimensional effects caused by obliqueness of the waves and of scale effects. Formulae for wave loads of crown walls are of empirical character and based only on 2-dimensional model tests (see D.1).

5.1.9 Wave action on filter layers

Filter layers should be designed to resist migration of finer mound materials into coarser mound materials caused by wave-induced pressure gradients. Empirical formulae for gradation of filters, based on physical tests and prototype observations, can be used (see D.1).

5.1.10 Stresses in armour units

Wave action imposes direct hydraulic loads on armour units with subsequent movements like rocking and displacements of some of the units. This, together with gravity forces, impose stresses which result in breakage when stresses exceed the material strength. The problem, which is more pronounced for slender types of unreinforced concrete units, should be examined in the design.

Calibrated semi-empirical formulae for stresses can be used (see D.1).

Abrasion and breakage of armour rocks can occur where wave action causes repeated movements of the rocks. The long-term performance should be considered for such cases.

Stones for building berm breakwaters should be hard and have sufficient resistance to crushing, because stones on the seaward side are forced to roll over large distances by wave actions and are subject to abrasion and crushing.

5.1.11 Seabed scour due to waves and currents

Waves and currents may cause scour close to and around structures on an erodible seabed. The scour depth should be considered and scour protection should be provided as necessary.

5.2 Wave action on vertical and composite breakwaters

5.2.1 Definition of vertical and composite breakwaters

A vertical breakwater is a structure of rectangular or nearly rectangular cross-sections having a vertical or nearly vertical front wall extending directly from the seabed or built on top of a thin bedding layer. A composite breakwater is a combined structure with a main body of rectangular or nearly rectangular cross-section, placed on a rubble mound that is submerged at all tidal levels. The main body is made of masonry works, concrete block works or a reinforced concrete caisson filled with sand, etc. A superstructure made of placed-in concrete is constructed on top of it. The cross-section of superstructure can be different from a rectangular shape and have a sloped front or other shape. The rubble foundation has berms in front and rear of the main body, and the berms and slopes are covered with armour units for protection against wave action.

The front of the main body can be covered with a mound of concrete blocks to reduce the action of waves on the main body and reduce wave reflection.

A front part of the main body can have an open chamber that is connected with the seaside water through perforation in the front wall for the purpose of partially absorbing wave energy and decreasing the degree of wave reflection by the breakwater.

5.2.2 Types of wave action on vertical and composite breakwaters

The main action of waves on vertical and composite breakwaters are the wave pressure on the front wall and the uplift on the bottom of the main body, which govern the overall stability of the main body against sliding, overturning, and foundation failure as well as the integrity of the structural elements.

Vertical and composite breakwaters can endure a certain degree of wave overtopping without endangering their structural integrity. Composite breakwaters are susceptible to the instability of armour units on rubble foundations caused by wave-induced flows in front of their main bodies. Wave-induced flow may cause scour of the seabed at the toe of the rubble mound, which can cause damage to the rubble foundation.

5.2.3 Wave pressure, uplift and buoyancy

The action of waves on the main body of a vertical or composite breakwater should be evaluated for the wave of largest height among random trains of individual waves.

The wave pressure and uplift exerted upon the main body should be evaluated by means of hydraulic model tests or appropriate calculation models, e.g. the extended Goda formula (see E.2). The wave pressure on its rear wall may need to be considered if the waves diffracted from the head towards the rear of the breakwater are not of negligible height. Care should be taken for the difference between the wave pressures for the evaluation of overall stability and those for the design of structural elements. The buoyancy of the immersed part of the main body below the design water level shall be taken into account in the stability analysis of the breakwater.

Under a certain combination of wave conditions, breakwater geometry and bathymetric features, impulsive breaking wave pressure can be exerted on the breakwater. The impulsive pressure is characterized by high peak intensity and a very short duration. When the action of impulsive pressures on the whole or structural elements of the main body needs to be considered in the design of breakwaters, it should be evaluated by taking its duration into account together with its peak intensity.

5.2.4 Wave overtopping

Depending on the use of the area behind a breakwater, the amount of wave overtopping and the height of waves transmitted behind the breakwater should be examined by determining the crest elevation of a vertical or composite breakwater and the configuration of its superstructure.

5.2.5 Wave action on armour units of rubble foundation

Armour units covering the surface of a rubble foundation shall have the capacity to remain in position under the actions from waves. The minimum mass of armour units required should preferably be determined by means of hydraulic model tests. Three-dimensional tests are recommended for examination of the stability of armour units around a breakwater head. For empirical formulae for estimation of the required mass, see E.3.

5.2.6 Influence of wave action on geotechnical failures

The main body of a vertical or composite breakwater is subject to the wave pressure on its front wall, superstructure and the rear wall, the uplift on its bottom, and the buoyancy to its immersed part. These loadings, together with its self-weight, give an eccentric and inclined load on the seabed or the surface of the rubble foundation. The eccentric and inclined load can cause geotechnical failures within the rubble mound and/or through the seabed foundation when the bearing capacity of the rubble mound and the seabed foundation is insufficient.

Appropriate methods for stability analysis against slip failures should be employed to ensure the safety of vertical and composite breakwaters (see E.4).

5.2.7 Seabed scour due to waves and currents

Waves and currents may cause scour close to and around structures on an erodible seabed. The scour depth should be considered and scour protection should possibly be provided.

5.3 Wave actions on coastal dykes and seawalls

5.3.1 Coastal dykes

5.3.1.1 Definition

Coastal dykes are man-made sloped soil structures parallel to the shore to protect the hinterland against erosion and flooding. They may be sea dykes along coastal shorelines and estuary dykes in a river estuary. These dykes are characterized by mild slopes on the seaward side and on the shoreward side. Very often, the seaward and/or shoreward sides of the dykes have a berm which provides access for maintenance, and/or reduces wave run-up and wave overtopping (seaward side). Coastal dykes are generally built of sand and/or clay and are covered by different materials such as grass, asphalt, stone or concrete revetments, etc.

5.3.1.2 Types of wave actions

Wave and current actions on coastal dykes include:

— wave loading (including impact loading by breakers) on the seaward slope of the dyke;

— wave run-up and run-down on the seaward slope of the dyke (including layer thickness and velocities);

— wave overtopping over the dyke crest;

— infiltration due to wave run-up and run-down in the dyke core;

— internal pressure on an impermeable top layer (with open toe) on the seaward side of the dyke (in case of a high water level inside the dyke).

Wave actions on coastal dykes shall be evaluated for the design wave height and wave period (see 4.2) and for a design water level (DWL) taking into account the water depth and tidal variations in front of the dyke. If relevant, the influence of the shape of wave spectra should be accounted for.

5.3.1.3 Wave action on seaward slope

The run-up height of the seaward slope is the governing factor for the determination of the crest elevation. This run-up height shall be assessed with due consideration of wave breaking (breaker index). The run-up and run-down flow (layer thickness and velocity), infiltration, phreatic water level in the dyke body, wave induced uplift forces underneath the revetment or cover layer, and wave impact loads on the seaward side of the dyke should be considered (see Annex F) when relevant.

5.3.1.4 Wave action on seaward toe

The stability of a seaward toe at a sea dyke should be examined to ensure the support of the dyke body. Therefore, the stone mass required should be accounted for by hydraulic model tests, empirical formulae or experience. Wave-induced run-up and run-down during lower water levels will mainly affect the stability of the toe and thus need to be considered (see Annex F). In addition, the width of the toe may be important in relation to the scour hole and hence should be accounted for.

5.3.1.5 Wave overtopping

Wave-induced overtopping over the dyke crest shall be assessed since overtopping waves can induce damage to the shoreward side of the dyke. Empirical formulae can be used to predict mean and peak overtopping discharges (see Annex F). Damage to the dyke body or hazards resulting from wave overtopping can be avoided when the dyke is designed for allowable overtopping rates taking into account local conditions of the dyke and the hinterland. Where overtopping is a critical factor, hydraulic model tests are recommended since individual overtopping rates, which induce damage to the dyke body, differ significantly from mean overtopping rates.

5.3.1.6 Wave action on dyke crest and shoreward slope

The crest height of the dyke shall be sufficiently large to prevent wave overtopping rates higher than the allowable rate under the design condition. Overtopping or overflowing water may result in considerable damage of the rear slope of the dyke and may eventually lead to total collapse of the dyke body. Hydraulic model tests should be performed to assess the stability of the rear slope by providing information on the mean wave overtopping rate, individual overtopping volumes per wave, the layer thickness and velocity of the overtopping bore on both the dyke crest and inner slope. Empirical formulae to assess these parameters are given in Annex F.

5.3.1.7 Influence of wave action on geotechnical failures

Geotechnical failures may be induced by wave action on the dyke and therefore need to be examined as they affect the overall stability of the dyke body. Semi-empirical and analytical models are available to account for these processes (see Annex F).

5.3.1.8 Seabed scour due to waves and currents

Waves and currents may cause scour close to and around structures on an erodible seabed. The scour depth should be considered and scour protection should be provided as necessary.

5.3.2 Seawalls

5.3.2.1 Definition

Seawalls are onshore or foreshore structures generally parallel to the shoreline. They are built as vertical face structures such as gravity concrete walls, steel or concrete sheet pile walls, and stone filled cribworks or as sloping structures with revetment typically made of concrete slabs, concrete armour units or rock armour. The principal function of seawalls is to reinforce a part of the coastal profile and to protect land and infrastructures from the action of waves and flooding.

5.3.2.2 Classification and structural components of seawalls

With respect to the effect of wave actions, two main categorizations of seawalls should be distinguished:

a) sloping or vertical seawalls;

b) porous or non-porous seawalls.

Irrespective of the type of seawall, three main structural components shall be distinguished:

— the body (which includes the front face and the core);

— the toe;

— the crest (which includes the rear face).

5.3.2.3 Types of wave action

Wave action on seawalls shall be evaluated for the design wave height and wave period (see 4.2) and for a design water level (DWL) taking into account the water depth and tidal variations in front of the seawall. The crest height should be evaluated under due consideration of the total allowable overtopping rate and/or the wave run-up height.

The following factors associated with the stability of the structure components including body (front face, filter layer, core), toe and crest (different types of crests and rear face) shall be considered:

a) horizontal wave forces (positive and negative);

b) wave up-lift forces;

c) hydraulic stability of revetments, including filters;

d) internal water pressure in the body and seepage flow.

5.3.2.4 Wave reflection

Seawalls will reflect some proportion of the incident waves and these reflections may have significant impact on the wave pattern and the sediment transport on the coastal regime in front of the sea wall. The influence of wave reflections from seawalls should therefore be investigated. Reflection coefficients can be estimated from empirical and semi-empirical formulae for perpendicular wave attack (see Annex F).

5.3.2.5 Wave action on seaward slope

Wave action on the seaward slope of a seawall are to a large extent dependent on the type of armour used for its protection. Wave climate and type of protection shall be examined together, and armour material shall be selected accordingly. Hydraulic model tests may be required to assess the stability of the selected material on the seaward slope. Empirical or semi-empirical formulae can also be used (see Annex F).

Wave-induced run-up and run-down need to be estimated since excessive run-up leads to severe overtopping over the wall crest and both run-up and run-down may cause erosion damage on the seaward slope. Empirical and semi-empirical formulae are given in Annex F.

5.3.2.6 Wave action on seaward toe

The main purpose of the toe structure of seawalls is to prevent undermining of the body of the seawall. Failure of the toe may lead to total collapse of the seawall so that wave actions on the toe should be assessed in hydraulic model studies.

5.3.2.7 Wave overtopping

Wave-induced overtopping over seawalls may induce significant damage to the structure itself or any objects behind the wall or may generate hazards for people living or working immediately behind the structure and should thus be examined in detail. Due to the complexity of some seawall geometries where no overtopping formulae are available, hydraulic model tests or numerical modelling may be required to assess the mean overtopping rate as well as individual overtopping volumes. Semi-empirical formulae based on hydraulic model tests and prototype investigations are given in Annex F.

5.3.2.8 Wave-induced forces

Seawalls with a vertical or steep front face may be exposed to wave loadings that might endanger the overall stability of the wall. Depending on the foreshore and berm geometry, seawalls might experience both pulsating and impulsive wave loadings. Therefore, the type of wave action should be identified, followed by thorough investigation of relevant failure modes such as sliding, overturning, slip and bearing capacity failures. Critical load combinations of horizontal forces, uplift forces and high water tables shall be considered. For further relevant issues such as duration of wave impact forces and strength of the seawall see 5.1.8.

Wave-induced forces may be assessed using semi-empirical formulae for 2D situations as given in Annex F for simple geometries (vertical walls with and without berms) but need to be investigated by hydraulic model tests for more complex geometries.

5.3.2.9 Seabed scour due to waves and currents

Waves and currents may cause scour close to and around structures on an erodible seabed. The scour depth should be considered and scour protection should be provided as necessary.

5.4 Wave and current action on cylindrical members and isolated cylindrical structures

5.4.1 Definition

Cylindrical structures may be single isolated cylinders to support a platform of some kind (e.g. lighthouses) or structures composed of vertical cylindrical members supporting a platform (e.g. jetty) or a truss structure with vertical, inclined and horizontal cylindrical members, supporting a platform (e.g. oil platform) or a pipeline close to or on the seabed.

5.4.2 Types of wave and current action

Waves and currents passing a cylindrical member induce dynamic pressures different from the hydrostatic pressures on the surface of the cylinder. These pressures when integrated over the whole surface of the cylinder result in a net force on the cylinder. The wave and current actions are the drag actions, the inertia actions, diffraction actions and the vortex-shedding induced actions (vortex-induced vibrations).

5.4.3 Current action

Current action on a cylinder should be calculated with a drag force formula with an appropriate drag coefficient.

5.4.4 Wave and current action on vertical cylinders from non-breaking waves

The action of non-breaking waves and currents on small diameter cylinders and cylindrical structural elements should basically be calculated using the Morison equation with appropriate wave kinematic formulation and appropriate drag and inertia coefficients.

The action of non-breaking waves on large diameter cylinders and cylindrical structural elements may be calculated using wave diffraction theories, by numerical methods or hydraulic model tests.

5.4.5 Wave and current action on vertical, inclined and horizontal cylinders from breaking waves

Wave and current action of breaking waves on vertical, inclined cylinders in shallow water and on reefs should be calculated using appropriate formulae. Special considerations should be made regarding any wave slamming action. Hydraulic model tests should be carried out on important and critical structures on rapidly varying bathymetry.

5.4.6 Slamming action of waves on horizontal and inclined cylinders

For horizontal and inclined cylinders entering and leaving the water surface as waves pass by, slamming action should be considered.

5.4.7 Wave action on decks

Wave action, including slamming, on platform or jetty decks, shall be considered when there is a possibility of the deck being hit by waves.

5.4.8 Wave action on small diameter pipelines

Wave action and current action on small diameter pipelines on or close to the seabed should be calculated using a Morison type equation for the horizontal force and a similar equation without the inertia term for the lift force.

5.4.9 Current and wave-induced vibrations

For slender structures, e.g. pipelines in free spans, current and wave-induced, vortex-shedding induced vibrations shall be considered from the strength and the fatigue resistance point of view.

5.4.10 Seabed scour at cylinders due to waves and currents

Waves and currents may cause scour close to and around structures on an erodible seabed. The scour depth should be considered and scour protection should be provided as necessary.

5.5 Wave interaction with floating breakwaters

5.5.1 Definitions

Floating breakwaters are moored floating objects installed to reduce the height of waves approaching harbours, marinas, etc. The cross sectional form of the object may vary. The most commonly cross sectional form is the rectangular form, thus forming a box type structure of a certain length. Several such boxes may be placed in a row thus forming a breakwater of required length. Other cross sectional forms are also used.

The wave height reducing function by floating breakwaters is mainly dependent on the ratio wave length:width of the breakwater. Floating breakwaters are thus mainly used in relatively sheltered areas where only relatively short period waves are present. On open coasts with ocean waves and swell, the floating breakwater concept is not economical. To give any reasonable wave-reducing effect, the size of the breakwater will be excessively large on the open coast. An exception to this is the case in which reduction of only the short period waves of the wave spectrum is of significance, e.g. protection of fish farming devices.

The moorings of a floating breakwater are normally wires and/or chains, which are fixed at the seabed to anchors, piles or concrete units These moorings often have non-linear force-motion characteristics.

5.5.2 Types of wave and current action

Wave action on a floating breakwater induces forces on the floating "box" and in the moorings of the breakwater. Hence the dynamic system "floating breakwater/mooring" lines shall be considered. The bottom anchors, piles or concrete units should provide sufficient resistance against the tension from the mooring lines.

The floating breakwater will undergo motions in its six degrees of freedom: surge, sway, heave, roll, yaw and pitch. The wave transmission, the wave forces on, and the motion response of, the breakwater should be calculated by numerical methods or hydraulic model tests, taking into account the force-motion characteristics of the mooring system.

Slowly varying wave drift forces induce generally large horizontal motions and are the governing factor of the mooring forces of floating breakwaters.

Current actions should be calculated with a drag force formula. The value of the drag coefficient should be appropriately selected by taking the draft:water depth ratio into consideration.

If necessary combined wave-current actions should be considered.

5.6 Wave action on wave screens

5.6.1 Definition

Wave screens include a wide range of structures consisting of one or more thin vertical walls used to form a fixed or rigid breakwater to protect a harbour or marina from wave actions. Wave screens consist of thin wall panel sections, used to limit wave actions, which are then attached to a supporting structure, usually a pier or separate pile-supported structure. Wave screens can be solid or permeable, and extend to mid-depth with a gap at the bottom or to the seabed without a gap. Other names for these structures include wave barriers, wave fences, wave “skirts”, baffle breakwaters and curtain walls.

5.6.2 Type of wave action

The main action of waves on wave screens are the oscillatory wave pressures on the front and back of the screen. These integrated pressures result in horizontal forces and related moments which have to be taken by the panels and support structures. Wave loading is generally due to wind-waves or boat-generated waves.

5.6.3 Wave forces

Horizontal wave forces on a wave screen may be computed by an integration of dynamic pressures from mathematical models for wave-structure interactions, by verified empirical formulae or by extrapolation of results from physical model tests. Wave forces should be evaluated for the wave of largest height among trains of individual waves for the design wave conditions (see Annex I). Wave screens may be considered “brittle” compared to vertical or rubble mound breakwaters and due consideration should be taken when selecting safety factors. Vertical loads due to buoyant forces shall also be included.

5.6.4 Wave slamming action

Wave screens are usually designed for situations where slamming loads do not occur and where wave loading is periodic in nature. Wave slamming action from breaking waves should be examined in physical model tests if such conditions are expected to occur.

5.6.5 Wave transmission, reflection and overtopping

The degree of wave transmission under or through the wave screen, the wave reflection and the degree of overtopping, should be examined when determining the draft, porosity, and crest elevation of a wave screen. Effects of waves diffracted from the ends of wave screens should also be considered. Wave interactions with wave screens should be examined using mathematical models or hydraulic model tests. An evaluation should consider irregular waves and should consider both low and high water level conditions.

5.6.6 Seabed scour at wave screens due to waves and currents

Waves and currents may cause scour close to and around structures on an erodible seabed. The scour depth should be considered and scour protection should be provided as necessary.

6 Probabilistic analysis of performance of structures exposed to action from waves and currents

6.1 Examination of uncertainties related to wave and current action

Action from waves and currents is classified as variable action by the definition given in ISO 2394. The related basic variables are the hydraulic parameters characterizing water levels, waves and currents, given in Clause 5. They are all random variables given by probability distributions, except the astronomical tide level which can be predicted accurately once the time and the location are specified. However, it should be treated as a random variable when the times of wave and current action are uncertain. For design of coastal structures, the action of waves and currents appear in calculations either as hydrodynamic loading in terms of pressure on the structures, or only indirectly as a response of the structure. The first case applies to loading on walls and piles, whereas the second case applies to structural response such as rubble mound armour stability and integrity, seabed scour, and to hydraulic response such as wave run-up and overtopping, wave transmission and reflection. In both cases the methods of estimation of action and the response to action contain uncertainty besides the random variability of the hydraulic basic variables. Major sources contributing to the uncertainties are as follows (see J.1 for discussion).

— Statistical variability of basic natural variables.

— Errors related to measurement, hindcast or visual observation of hydraulic basic variables.

— Sample variability due to limited sample size of the available data of basic variables.

— Choice of distribution as a representative of the unknown true long-term distributions for hydraulic basic variables.

— Variability of parameter estimation for a distribution function fitted to basic hydraulic data.

— Accuracy of models for prediction of storm surge water levels.

— Accuracy of models for wave forecasting and/or hindcasting.

— Accuracy of models for transformation of waves and currents, for example from deep to shallow water.

— Accuracy of models for prediction of action of waves and currents.

— Accuracy of models for prediction of structural and hydraulic response.

— Reliability of the results of physical model tests for the estimation of loadings and structural and hydraulic response.

— Variability of structural parameters.

The bias and standard deviation of each factor of uncertainty should be investigated and be duly taken into account in the evaluation of the action of waves and currents.

6.2 Reliability assessment of structures

Structures subject to the action of waves and currents should be assessed for their reliability at the serviceability and ultimate limit states with due consideration for their economic and social functions, environmental influences, and the consequences of failure. The nature and extents of the uncertainties in 6.1 should be duly taken into account when assessing the reliability of structures during their design working life.

All failure modes and failure mode interactions of importance for the performance of the structure should be considered.

The probability of failure during the design working life should preferably be assessed and confirmed to be less than the minimum value assigned to a specific class of structure, which is to be preset or approved by responsible agencies.

The probability of failure may be evaluated by the use of the reliability index method or with direct calculation by numerical integration of their probability density functions or Monte Carlo simulations.

For a structure that permits a certain degree of deformation at the serviceability and ultimate limit states, the expected amount of deformation should preferably be evaluated.

NOTE A caisson breakwater can function as a wave barrier even after its main body has slid over a small distance. A berm breakwater allows reshaping of its seaward slope by wave actions until it reaches a stable shape.

Annex A
(informative)

Water levels

A.1 Tide levels

Because the astronomical tide level at any location varies continuously with time, certain representative tide levels are used to provide the information on the range of tide levels. Most frequently used ones are the mean high (or low) water springs, which is the average height of high (or low) water at the time of spring tides obtained over a long period of time. It is equal to the elevation above (or below) the mean sea level by the amount equal to the sum of the largest two constituents of the same family, usually the M_2 and S_2. Because the heights of two high (or low) waters in a day usually differ, they are not the highest (lowest) water levels at spring tides. The near highest high water level is calculated by adding the amount equal to the sum of the amplitudes of the four main tidal components M_2, S_2, K_1 and O_1 to the mean sea level. The near lowest low water level is calculated by subtracting the same amount from the mean sea level. The latter is also called the low water Indian springs and has been used as a chart datum in some countries before the International Hydrographic Organization resolved to adopt the lowest astronomical tide (LAT) as the chart datum.

In addition to the above high (or low) water levels, the mean monthly highest (or lowest) water level, which is the annual mean of the highest (or lowest) water levels within five days after the day of new or full moon in respective months, may be used as representative of the high (or low) water levels of tides.

The water level at a given location can vary beyond the range of astronomical tide levels due to the occurrence of storm surges, tsunamis and others. Both storm surges and tsunamis can raise the water surface to very high elevations, but they can also cause the water surface to drop below the lowest astronomical tide.

A.2 Design water level

When evaluating the action of waves and currents on structures, the water level at the time of their action needs to be specified. It is called the design water level. The principle of selecting the design water level is to use the combination of waves, currents and water level which is most unfavourable to the stability and/or safety of the structure and/or facilities under design.

For a certain type of structure such as retaining walls, exceptionally low water at the ebb of tsunami may cause its seaward collapse owing to the earth and residual water pressures behind it. When scour of the seabed in front of a structure is apprehended, a low water level can become a critical condition. Impulsive breaking wave pressures may be exerted on a vertical or composite breakwater when the water level is intermediate or low, depending on the geometry of the breakwater. However, most cases of structural design set the design water level at a rather high elevation.

The methodology of selecting the design water level at high elevation is not established yet, depending on the available data, design practices in use, local situations and others. Several methods are cited in a) to d).

a) Use of the highest record of high water level

   This method is sometimes used for the case of tsunamis with the addition of a certain allowance, because the statistical analysis of tsunami heights is difficult owing to the rare occurrence of tsunamis.

b) Extreme statistical analysis of storm surge levels

   This can be done for both the absolute level of the highest water above the datum level and the deviation of highest water level from the astronomical tide at the time of storm surges. The analysis can yield the

return water level corresponding to a designated return period. When the R-year storm surge deviation is evaluated, it is added to the near highest high water level or some other high water levels. The designation or return period is the matter decided by the owner of the facilities.

c) Numerical simulation of the past worst storm surge or tsunami, around the locality

The storm surge or tsunami that inflicted the worst damage on the locality is selected, and the temporal and spatial variations of water level along the coastline are computed for design consideration. Sometimes, the strongest storm is chosen as a design storm and its track is shifted so as to yield the worst storm surge at the design site. Selection of the astronomical tide level when a design storm passes depends on the analyst in charge.

d) Probabilistic analysis

All the basic variables related to design of structures including the water level are given statistical variability and various combinations of variables are analysed with their occurrence probabilities. Monte Carlo simulation techniques are often employed and economical and/or risk optimisation can be made.

Annex B
(informative)

Wave action parameters

B.1 Wave variability and wave parameters

B.1.1 Variability of waves in the sea

Wind waves and swell in the sea are essentially random in time and space. Heights and periods of individual waves in a short time span vary randomly over wide ranges. It is necessary to define individual waves with some criteria and calculate characteristic wave heights and periods in a statistical manner in the time domain analysis. The zero-upcrossing or zero-downcrossing method is the standard technique to define individual waves, in which the two successive crossing points of the wave surface profile with the mean water level (zero-line) mark the start and the end of one individual wave, respectively. The significant wave height $H_{1/3}$ is the mean of the highest one-third waves thus defined.

The state of wave activities on the surface of the sea varies gradually with time. The condition of the sea surface in a short time span is termed the sea state, which is generally expressed with the significant wave height and the mean wave period or other period parameter, and the principal wave direction. Statistical analysis of the sea state over months, seasons and years yields a long-term description of wave conditions at a particular site, which is called the wave climate. The subject is discussed in Clause B.3.

Analysis of individual waves of a wave record is generally made for a time span of 20 min or so. The length of time span is chosen as the result of compromise between the requirement of a short duration to guarantee the constancy of sea state during the recording time and that of a long duration to have a sufficient number of waves necessary for reliable estimates of significant wave height and other characteristic wave heights and periods.

B.1.2 Marginal distribution of individual wave heights in a short time span

The distribution of individual wave heights in a short time span can be approximated using the Rayleigh distribution. The Rayleigh distribution is approximately applicable to any sea state inclusive of wind waves, swell, and coexisting state of both, regardless of frequency spectral shapes; e.g. see Goda[88] (pp. 40-41 and pp. 261-265).

The assumption of the Rayleigh distribution enables the estimation of significant wave height from spectral information as below

$$H_{1/3} = H_{m0} = 4{,}0\,\eta_{\mathrm{rms}} = 4{,}0\sqrt{m_0} \tag{B.1}$$

where η_{rms} denotes the root-mean-square surface elevation and m_0 is the zero-th moment of frequency wave spectrum defined by

$$m_n = \int_0^\infty f^n S(f)\,\mathrm{d}f \tag{B.2}$$

where $S(f)$ denotes the frequency spectral density function.

Although the Rayleigh distribution provides a good approximation to the wave height distribution, the latter in deep water is slightly narrower than the Rayleigh, resulting in the empirical relationship of $H_{1/3} \cong 3{,}8\eta_{\mathrm{rms}}$ or $H_{1/3} \cong 0{,}95H_{m0}$. In relatively shallow water outside the nearshore zone, on the other hand, the wave height distribution becomes as broad as or broader than the Rayleigh owing to the enhanced effect of wave non-linearity.

In the outer part to middle of the nearshore zone where waves begin to break randomly owing to depth-controlled limitation to large wave heights, the marginal distribution of wave heights becomes much narrower than the Rayleigh. As waves proceed toward the shoreline however, the distribution of wave heights becomes broad again owing to the stationary rise of the mean water level (wave set-up) and its temporal variation (surf beat).

B.1.3 Highest wave height in relation to significant wave height

A specific value of the highest wave height H_{max} in a group of waves is subject to random variation governed by its own probability of appearance. Its ensemble mean is the function of the number of waves within duration of a given sea state and expressed relative to the significant wave height as given below.

$$\left(\frac{H_{max}}{H_{1/3}}\right)_{mean} \cong 0{,}706\left[\sqrt{\ln N_0} + \frac{0{,}577\,2}{\sqrt{\ln N_0}}\right] \tag{B.3}$$

where N_0 denotes the number of waves.

The most probable value is given by the first term of the right-hand side of Equation (B.3).

Equation (B.3) is based on the Rayleigh distribution of wave heights. There are some reports in which extremely large waves were observed with heights beyond what might be expected from the statistical distribution of $H_{max}/H_{1/3}$. These waves are called freak waves. It is an unsettled question whether the probability of freak wave appearance remains within a range predicted by the theory of Rayleigh distribution of wave heights or if they are caused by some effects not accounted for in currently available theories of wave statistics.

B.1.4 Distribution of individual wave periods in a short time span

The distribution of individual wave periods needs to be examined in the light of the joint distribution between wave heights and periods, because the characteristic wave periods such as the significant wave period are defined in association with the wave heights ranked by their magnitudes. The joint distribution of individual wave heights and periods is strongly affected by the functional shape of the frequency wave spectrum. No reliable theoretical model is available for the joint distribution of wave heights and periods for versatile spectral shapes. Waves of sharply-peaked spectra exhibit a narrow spread of period distribution around the spectral peak period, while a combined sea state of wind waves and swell shows multiple peaks in the distribution of wave periods.

For wind waves with single-peak spectra, the following empirical relationships hold for the wave periods defined by the zero-upcrossing or zero-downcrossing method.

$$T_{max} \cong T_{1/3} \cong 1{,}2T_m \tag{B.4}$$

where T_{max}, $T_{1/3}$, and T_m denote the periods of highest wave, significant wave, and the mean wave period, respectively. The relationship between the significant wave period and the spectral peak period is affected by the spectral shape. For fully-grown wind waves, the mean relationship of $T_{1/3} \cong 0.9T_p$ is applicable. Further information can be found in Table 2.4 of Goda[88].

The mean wave period can be estimated from the frequency wave spectrum with the zero-th and second moments as below.

$$T_m \equiv T_{m0,2} = \sqrt{m_0 / m_2} \tag{B.5}$$

where the spectral moments m_0 and m_2 are calculated by Equation (B.2).

Equation B.5 is based on the condition that the wave spectrum is comprised of all the free linear frequency components. Because actual waves contain a certain amount of non-linear spectral components in the high frequency ranges, the mean period $T_{m0,2}$ estimated by Equation (B.5) becomes shorter than the mean period T_m calculated by the zero-crossing technique; the difference is enhanced in shallow water and can reach up to 20 %.

B.2 Wave spectra

B.2.1 Directional wave spectra

A detailed structure of wind waves and swell is represented with the directional wave spectrum, which can be expressed as the product of the frequency wave spectrum $S(f)$ and the directional spreading function $D(\theta|f)$. The term f denotes the frequency and θ is the azimuth measured from some fixed axis of direction.

The frequency wave spectrum or the frequency spectral density function, $S(f)$, expresses the distribution of wave energy density (being divided by the unit weight of water) in the frequency domain and has the dimension of m^2s or equivalent units. The directional spreading function, $D(\theta|f)$, expresses the distribution of wave energy density in the directional domain at a specific frequency f, relative to the spectral density at that frequency. Thus the directional spreading function has no dimensions and its integration over the full range of azimuth is set at unity for every frequency.

Details of directional wave spectra can only be examined through multiple-component wave measurements. However, some standard functional forms are available for evaluation of the actions from waves as described in B.2.2 to B.2.4. Directional spectral functions of wind waves and swell can be expressed with the input of characteristic wave height, period and direction. For the sea state of coexisting wind waves and swell, the respective spectral densities can be linearly superposed so as to yield the directional wave spectrum of the combined sea state.

Spectral analysis of wind waves and swell is based on the concept of linear superposition of component waves. When the characteristic wave height becomes large compared with wavelength and/or water depth, non-linear interactions between component waves are enhanced and a wave spectrum begins to include an appreciable amount of non-linear spectral components. Use of wave spectra in very shallow water should be made with due caution for the effect of non-linear components on wave actions.

B.2.2 Frequency spectra of wind waves and swell

Various functional forms of frequency wave spectra have been analysed on the basis of many field measurements, and several standard functions have been proposed. Some frequency spectra are expressed as the function of wind speed for the purpose of wave forecasting. They include the Pierson-Moskowitz, the JONSWAP and the TMA spectra. For evaluation of the action of waves, it is more convenient to express a frequency spectrum as the function of characteristic wave height and period.

For fully-grown wind waves, the Bretschneider-Mitsuyasu frequency spectrum, as follows, can be employed:

$$S(f) = 0{,}257 H_{1/3}^2 T_{1/3}^{-4} f^{-5} \exp[-1{,}03 (T_{1/3} f)^{-4}] \tag{B.6}$$

The functional dependence of the Bretschneider-Mitsuyasu spectrum with respect to frequency is the same as that of the Pierson-Moskowitz spectrum. Its constants have been set to satisfy the condition of $H_{1/3} = 4{,}0\sqrt{m_0}$ and the relationship of $T_p = 1{,}05 T_{1/3}$, which was derived by Mitsuyasu based on his field measurements of wind waves with the presence of some low frequency components.

For versatile functional shapes of single-peak wave spectra, the modified JONSWAP, as follows, is often employed:

$$S(f) = \beta_J H_{1/3}^2 T_p^{-4} f^{-5} \exp[-1{,}25 (T_p f)^{-4}] \gamma^{\exp[-(T_p f - 1)^2 / 2\sigma^2]} \tag{B.7}$$

in which

$$\beta_J = \frac{0{,}062\,4}{0{,}230 + 0{,}033\,6\gamma - 0{,}185 (1{,}9 + \gamma)^{-1}} [1{,}094 - 0{,}019\,15 \ln \gamma] \tag{B.8}$$

$$T_p \cong T_{1/3} / [1 - 0{,}132 (\gamma + 0{,}2)^{-0{,}559}] \tag{B.9}$$

$$\sigma \cong \begin{cases} 0{,}07 & : f \leqslant f_{\mathrm{p}} \\ 0{,}09 & : f \geqslant f_{\mathrm{p}} \end{cases} \tag{B.10}$$

in which $f_{\mathrm{p}} = 1/T_{\mathrm{p}}$ denotes the frequency at the spectral peak.

The term γ is called the peak enhancement factor, which was given the value between 1 and 7 in the original proposal of the JONSWAP spectrum. In using Equation (B.7) however, the value of γ can be chosen between 1 and 10, depending on the wave characteristics. For fully-grown wind waves, $\gamma = 1$ is appropriate because it yields the frequency spectrum equivalent to the Pierson-Moskowitz spectrum. For swell, the value should be increased in proportion to the distance of travel, but $\gamma = 10$ can be regarded as appropriate for swell having travelled over several thousand kilometres (see Goda[88], p. 30).

Equation (B.7) is due to Goda[86], who also derived the functional form of the modified Wallops spectrum having a free parameter of the exponent of the power of frequency.

B.2.3 Directional spreading function

B.2.3.1 Standard directional spreading functions

Various functional forms have been proposed for the directional spreading function of wind waves. Some functions are based on the analysis of field data, while some others are without validation by field data. Due to an insufficient number of field measurements of directional wave spectra, selection of a directional spreading function is left to the judgment of an analyst of the wave action. In this subclause, two functional forms are introduced, but other functional forms can also be used in the analysis.

The directional spreading function based on field data is the Mitsuyasu type as follows:

$$D(\theta | f) = D_0 \cos^{2s}\left(\frac{\theta - \theta_0}{2}\right) \tag{B.11}$$

in which

$$D_0 = \left[\int_{\theta_{\min}}^{\theta_{\max}} \cos^{2s}\left(\frac{\theta - \theta_0}{2}\right)\right]^{-1} \tag{B.12}$$

where θ_0 denotes the principal wave direction measured from a given axis of direction and s is the spreading parameter that varies with the frequency as in the following:

$$s = \begin{cases} (f / f_{\mathrm{p}})^5 s_{\max} & : f \leqslant f_{\mathrm{p}} \\ (f / f_{\mathrm{p}})^{-2.5} s_{\max} & : f \geqslant f_{\mathrm{p}} \end{cases} \tag{B.13}$$

According to Mitsuyasu et al.[155], the peak value of spread parameter, $s_{\max}$, varies depending on the state of wind wave growth. A representative value for fully-grown wind waves is about $s_{\max} = 10$. With an increase in the $s_{\max}$ value, the extent of directional spreading becomes narrow. Goda[88] (p. 34) and OCDI[163] (p. 39) suggest the value of $s_{\max} = 25$ for swell with short decay distance and that of $s_{\max} = 75$ for swell with large decay distance for the case of deep-water waves.

The directional spreading function employed in some multi-directional model tests is the wrapped-normal type as expressed below.

$$D(\theta) = \frac{1}{2\pi} + \frac{1}{\pi}\sum_{n=1}^{N} \exp\left[-\frac{(n\sigma_\theta)^2}{2}\right] \cos n\theta \tag{B.14}$$

in which σ_θ represents the angular standard deviation defined by

$$\sigma_\theta^2 = \int_{\theta_{\min}}^{\theta_{\max}} (\theta - \theta_0)^2 D(\theta) d\theta \tag{B.15}$$

The number of serial terms, N, should be sufficiently large to ensure convergence of the finite series.

B.2.3.2 Mutual relationships among standard spreading functions

The Mitsuyasu type spreading function dictates the frequency dependency of directional spreading as expressed by Equation (B.13), while the wrapped-normal spreading function assumes directional spreading independent of frequency. However, mutual comparison between these spreading functions is possible by means of the angular standard deviation σ_θ. When the overall directional energy spreading of the Mitsuyasu type function is calculated by the integration of the directional spectrum with respect to the frequency, the spectrum with $s_{\max} = 10$ approximately yields $\sigma_\theta = 33°$, while $s_{\max} = 75$ yields $\sigma_\theta = 14°$. For more details of mutual comparison of several directional spreading functions, see Goda[87].

B.2.3.3 Directional spreading functions in shallow water

Owing to wave refraction effects, directional spreading of wind waves and swell becomes narrow in shallow water compared with that in deep water. Numerical analysis has been made for the refraction of directional random waves on a coast with straight, parallel depth-contours. A directional wave spectrum composed of the Bretschneider-Mitsuyasu frequency spectrum and the Mitsuyasu type spreading function was employed in the analysis. From the result of this analysis, an equivalent value of spreading parameter $s_{\max}$ was evaluated as a function of the ratio of water depth to the deepwater wavelength. A diagram for the estimation of the equivalent value of the spreading parameter has been prepared and is listed in Goda[88] (p. 36) and OCDI[163] (p. 39).

In evaluation of the actions from waves, such a change of the spreading parameter should be appropriately estimated and a corresponding value in shallow water should be employed.

B.2.4 Representative height and period of combined sea state

When a sea state is composed of wind waves and swell, the directional wave spectrum exhibits multiple peaks at different frequencies and azimuths. If the information of the characteristic heights and periods as well as the principal directions of these wind waves and swell is known, the respective directional spectra of these wind waves and swell can be estimated using the formulae in the previous subclauses. The directional wave spectrum of the combined sea state is obtained by linearly superimposing the directional spectral densities of these wind waves and swell. The action of these waves is then analysed by calculating contributions of components of the directional wave spectrum thus obtained.

The representative height of the combined sea state can be estimated as follows:

$$H_s = \sqrt{H_1^2 + H_2^2 + \cdots + H_n^2} \tag{B.16}$$

where H_s denotes the characteristic wave height of combined sea state and H_1 to H_n are the characteristic heights of wave groups. Any definition of wave height such as the significant wave height or the highest wave height is applicable to this formula, because the distribution of wave heights of the combined sea state can be approximated by the Rayleigh distribution as discussed in B.1.2.

The representative period of the combined sea state is difficult to define, because the joint distribution of wave heights and periods exhibits multiple modes that correspond to the modes of periods of respective wave groups. However, there is a formula for estimation of the significant wave period of the sea state composed of two wave groups as listed in OCDI[163] (p.70). It was proposed by Tanimoto et al.[218] for the purpose of evaluating wave loading on vertical face breakwaters.

B.3 Wave climate statistics

B.3.1 Statistical representation of wave climate

As mentioned in B.1.1, a long-term description of wave conditions at a particular site is called the wave climate. Continual wave measurements carried out every few hours provide the basic source of wave climate. The significant wave height is the characteristic height of wave climate statistics, while the characteristic wave period is either the mean period, significant wave period or spectral peak period, depending on the method of wave record analysis.

Wave climate at a particular site can be described in many ways. Time-history diagrams of characteristic height, period and direction over a month, a season or a year visualize a general trend of wave climate at a particular site. The means and standard deviations of height and period over months, seasons and years provide basic statistics of wave climate. Marginal and joint distributions of characteristic wave height and period are utilized in the analysis of long-term effects of wave actions on structures. Joint distributions of wave direction with wave height or period are also important in assessing tranquility of a harbour basin and littoral sand transport rate along a coastline. Duration statistics of calm seas and rough seas are also examined for analysis of the workability and operational efficiency of maritime facilities.

B.3.2 Marginal distributions of characteristic wave height and period

The Weibull and log-normal distributions are often fitted to the marginal distributions of characteristic wave height and period of wave climate statistics. Because the sea state varies gradually, the wave heights and periods measured at intervals of several hours are mutually correlated. Even with a time lag of 24 h, the correlation coefficient between successive significant wave heights can maintain a value of 0,3 or higher. Thus the data set for the marginal distribution of characteristic wave height or period does not constitute a sample of statistically independent data.

The upper tails of the marginal distributions often exhibit trends different from the main parts, because the data in the upper tails are samples from the population of storm waves being different from the population of medium to calm sea state. A simple extrapolation of a marginal distribution of significant wave height for an estimation of extreme wave height, such as 100 year wave height, which is called the total sample method, should not be made in the evaluation process for design wave heights because of the inherent inaccuracy involved.

B.3.3 Joint distribution of characteristic wave height and period

The pattern of the joint distribution of characteristic wave height and period is highly dependent on the nature of wave climate at locality. In the area in which wind waves are predominant throughout a year, a close correlation between wave height and period is observed and the scatter of data points is relatively small. In the area in which swell activity is strong, the data points are scattered over a broad area and the correlation between wave height and period is weak. Caution should be taken against simple application of theoretical models such as double log-normal distributions to the joint distribution data of characteristic wave height and period.

A joint distribution of characteristic wave height and period over many years can be convoluted using the Rayleigh distribution for individual wave heights so as to yield the marginal distribution of whole individual wave heights or actions during the design working life of a maritime structure. For each class of joint histograms of wave height and period, the number of individual waves expected in the time interval between successive measurements is calculated using the characteristic wave period. These waves are given respective heights according to the Rayleigh distribution, and the numbers of waves in respective classes of the height are counted and tabulated. If some information is available on the joint distribution of individual wave heights and periods at the site of interest, further refinement can be achieved.

B.4 Extreme wave statistics

B.4.1 Data set for extreme wave analysis

The database for extreme wave analysis is a long record of instrumental wave measurements and/or results of wave hindcasting projects. The accuracy of wave hindcasting is affected by the reliability of both the hindcasting model itself and the meteorological information for wind field estimation. It is necessary to employ a wave hindcasting method that has been verified to yield predictions in good agreement with instrumental wave records for several large storm waves obtained around the site of interest.

The length of data record is preferably 30 y or longer. A long record is needed so as to reduce the effect of sample variability and to minimize the influence of wave climatic changes on the prediction of extreme wave heights for a long return period such as 100 y.

The measured and/or hindcasted extreme waves should preferably be classified according to types of meteorological disturbance so that the data sets can be constructed for respective storm types. Extreme wave data of respective storm types may constitute samples from different populations of extreme waves. When an extreme wave analysis is made on a data set of mixed populations, the prediction of extreme wave height may not be reliable.

A set of extreme wave data can be prepared by two methods. One is to take the maximum significant waves in every year, and the other is to take the waves at a peak of every storm event that is defined by the level by which the significant wave height exceeds a preset threshold level. The former is called the annual maximum method, and the latter is the peaks-over-threshold (POT) method. Because the currently available databases of extreme waves in the world do not cover a sufficiently long time-span, the sample size of extreme wave data by the annual maximum method is rather small and the confidence interval of extreme wave analysis becomes relatively large. Therefore, the POT method is a preferred technique of data analysis. It should be remembered that a set of extreme wave data by the POT method does not belong to the category of extreme data in the strict sense of the statistics, because a peak height is not a maximum data among a subset of independent data such as required in the extreme statistics.

The average number of storm events, or the mean rate, is an important parameter in the extreme wave analysis when the POT method is employed. The mean rate should preferably be calculated for respective storm types.

B.4.2 Extreme distribution functions for storm wave heights

Because no consensus has been established on the population distribution of storm wave heights and the POT wave data are not the extreme data in a strict sense, several distributions are employed as the candidates for fitting to the data set of extreme wave heights.

Commonly employed distributions in extreme wave analysis are the Fisher-Tippett type I (double exponential or Gumbel), the Fisher-Tippett type II (Frechét) and the Weibull distributions (see Chapter 11 of Goda[88] for their functional forms). However, other distributions such as the Generalized Extreme Value and log-normal distributions can also be used.

B.4.3 Data fitting and selection of extreme distribution function

A data set of extreme wave heights, or a sample, is fitted to a candidate distribution for parameter estimation. The least squares method (LSM), the maximum likelihood method (MLM), and other valid methods may be employed for distribution fitting. When applying the LSM, the shape parameter of the Fisher-Tippett type II or the Weibull distribution is often fixed at a predetermined value so as to transform it into a two-parameter distribution. Care should be taken to employ the non-bias plotting position formulae for distribution functions when using the LSM.

Appropriate criteria of best fitting and/or rejection should be chosen and applied for the data set, depending on the methodology of data fitting.

B.4.4 R-year wave height and confidence interval

Once the distribution best fitted to the data set is selected, the distribution is assumed to represent the population of extreme wave heights at the site of interest. The wave height corresponding to a given return period, or R-year wave height, can be estimated by a standard procedure of extreme statistics.

A data set of extreme wave heights obtained through wave measurements and/or hindcasting represents one sample from the population of storm waves at the locality. Even with absence of climatic changes, a data set covering different but equal lengths of time will constitute a sample of the same distribution but with different statistical characteristics. This is called the sample variability of data set. Because of this variability, each sample will yield different estimates of R-year return wave height. A range of confidence interval should be estimated and indicated for every estimate of return wave height, even though the methodology of estimation is left to analysts.

Furthermore, there is no way to know the true population distribution of storm wave heights in general. A misfit of an extreme wave data set to a distribution different from the true population will yield a bias in the estimate on R-year return wave height. Analysis of storm wave data sets at multiple stations in a region of same storm characteristics can yield information on the population of storm waves (see Goda et al.[93]).

B.4.5 R-year height of highest wave

The highest wave height corresponding to a given return period is usually estimated from the R-year return significant wave height by multiplying it with a certain factor based on the Rayleigh distribution or others.

In offshore engineering, efforts are often made to estimate the R-year return height of highest wave from the marginal distribution of whole individual wave heights, which is constructed from the wave climate data being convoluted with Rayleigh distribution, as discussed in B.3.3.

B.4.6 Wave period associated with R-year wave height

Information on a wave period associated with the R-year return wave height is often needed when evaluating the action of waves. However, no established method is currently available to estimate such a wave period. Often a joint distribution of storm wave heights and periods is prepared to find out a meaningful correlation between the height and period.

For fully-grown wind waves in deep water, the following mean relationship can be quoted:

$$T_{1/3} \cong 3{,}3 H_{1/3}^{0{,}63} \tag{B.17}$$

in which the units of $T_{1/3}$ are seconds and those of $H_{1/3}$ are metres. The above relationship is due to Goda[90], based on Wilson's[267] formula for wind wave forecasting.

B.5 Wave transformations

B.5.1 Processes of wave transformation

During the propagation of waves and swell, they experience various processes of wave transformation, by which the height, period, direction and spectrum are changed. The processes mainly considered in evaluation of the actions from waves and currents are shoaling, refraction, diffraction, reflection, transmission and breaking. Wave shoaling denotes the process of changes in wavelength, wave celerity, wave height, etc. when waves propagate in water of decreasing depth. Wave refraction is the process by which wave direction and height change when the waves propagate obliquely to the depth contour. Wave diffraction is the phenomenon that waves propagate into the geometric shadow zone behind a barrier. When waves encounter a man-made or natural barrier to their propagation, waves are partially or fully reflected and there may be some waves transmitted behind the barrier. These are the phenomena of wave reflection and transmission. When the height of a wave becomes large beyond a certain threshold, which is expressed either in terms of the ratio of wave height to wavelength or the ratio of wave height to water depth, the wave cannot maintain its kinematic stability and loses a part of its energy through breaking.

When waves encounter currents, they are refracted by them if the directions of the waves and the currents are different. When waves meet the opposing currents, wave heights increase and wavelengths are shortened. When waves propagate riding on the following currents, wave heights decrease and wavelengths are elongated.

Most of these processes are linear in the sense that the wave height after transformation is linearly proportional to the wave height before a transformation, and are analysed by linear wave theories. When the relationship between the wave heights after and before a transformation is not linear, the process is called non-linear. Wave transformation by breaking is a typical non-linear process. Wave shoaling exhibits some non-linear features. The effect of wave non-linearity on wave refractions is small and neglected in most analyses.

Estimation of wave heights, periods and directions by wave transformations involves a certain degree of uncertainty due to the variability of transformation processes and the reliabilities of estimation models. When evaluating the action of waves, such uncertainty should be taken into consideration.

B.5.2 Wave shoaling

B.5.2.1 Linear shoaling coefficient

The linear wave theory provides the basis for calculating the wavelength, celerity, group velocity and shoaling coefficient in shallow water. The shoaling coefficient denotes the ratio of the height of waves having been affected by the depth change in shallow water to their height in deep water with the refraction effect eliminated. The shoaling coefficient by the linear wave theory is calculated with a closed-form function of the ratio of the water depth to the local wavelength.

For shoaling of random waves, the shoaling coefficient is first computed for a range of spectral frequency components and the results at various frequencies are utilized to construct the frequency spectrum of waves in shoaling water. The characteristic wave height in shoaling water is estimated from the zero-th moment of resultant wave spectrum by Equation (B.1) and the random shoaling coefficient is calculated by using the spectrally evaluated wave heights. The shoaling coefficient of random waves differs from the shoaling coefficient of monochromatic waves, but the difference is a few percent at most in many cases.

B.5.2.2 Nonlinear shoaling coefficient

When waves with a large height or non-linear waves propagate into quiet shallow water, the wave profile takes the form of a sharp crest and flat trough. The potential and kinetic energies for a given wave height become less than those of linear waves. Conversely, non-linear waves can have a height larger than the height of linear waves for the same energy flux. Because of this feature, the shoaling coefficient of non-linear waves becomes larger than that of linear waves. Several theories are available for evaluation of the non-linear shoaling coefficient, among which the theory by Shuto[197] is often referred to. A diagram based on this theory is listed in BSI[31], Goda[88] (p.77), and OCDI[163] (p.75).

The non-linear shoaling coefficient should be employed when evaluating wave loading on structures, because prediction of such wave loading is usually made with the input of local wave height having been affected by non-linear shoaling. However, an increase of wave height by non-linear shoaling beyond the linear shoaling process does not represent a net increase of wave energy density, as explained in the above. Therefore, the non-linear shoaling coefficient should not be used in the calculation of wave energy flux, radiation stresses, longshore currents and other energy related phenomena.

B.5.3 Wave refraction

Upon entering a region of shallow water, wind waves and swell undergo the process of wave refraction together with wave shoaling. Changes in the direction of wave propagation and wave height are often analysed using the wave ray method or equivalent methods by computer, which have been developed for regular (monochromatic) waves with a single period and direction. In the coast of simple bathymetry, such methods of wave refractions analysis can be utilized for the purpose of preliminary analysis. In principle however, wave refraction should be analysed for multidirectional random waves with the input of directional

wave spectrum. Diagrams for estimation of the height and direction of random waves refracted on a coast with straight, parallel depth-contours can be found in Goda[88] (pp. 55-56) and OCDI[163] (pp. 51-52).

Around a three-dimensional reef or other complicated bathymetry, refracted waves generate a set of diffracted waves behind the shoal. Advanced mathematical models need to be mobilized to numerically analyse the detailed distribution of waves around it. In this case, use should be made of multidirectional random waves.

B.5.4 Wave diffraction

The phenomenon of wave diffraction by breakwaters and other barriers is analysed with theoretical and/or numerical models by means of computers for monochromatic waves and multidirectional random waves. However, the results of diffraction coefficients thus obtained often differ greatly between monochromatic and random waves. Because wind waves and swell in the sea can only be represented using the concept of directional wave spectrum, the diffraction analysis with monochromatic waves should not be applied to real situations when evaluating wave action.

A diffraction diagram or a contour map of diffraction coefficients behind a barrier of multidirectional random waves can be constructed by computing diffraction coefficients of directional spectral components and by calculating the directional spectral density of diffracted waves at respective locations. Diffraction diagrams of straight barriers for multidirectional random waves can be found in BSI[31], Goda[88] and OCDI[163].

The value of the diffraction coefficient of multidirectional random waves is largely dependent on the extent of directional spreading of wave energy. Selection of the value of directional spreading parameters should be made with due caution by taking into consideration the condition of wave growth state and the shallow water effect as discussed in B.2.3.

When the area behind a barrier causing wave diffractions has a bathymetry of variable depth and/or some obstacles capable of reflecting the diffracted waves, the diffraction analysis of wave distribution in the area should be made by taking wave refractions and/or reflection into account.

B.5.5 Wave reflection and transmission

When trains of waves encounter a structure in water, a part of the wave energy is reflected toward the direction opposite to that of incidence, another part is transmitted behind the structure by overtopping and/or permeation, and the rest is dissipated by breaking, turbulence and other phenomena. The degree of wave reflection is expressed by use of the reflection coefficient, which is the ratio of characteristic height of reflected waves to that of incident wave. The degree of wave transmission is expressed by use of the wave transmission coefficient, which is the ratio of characteristic height of transmitted waves to that of incident wave.

When no energy is lost through interaction between waves and structure, the magnitudes of the reflection and transmission coefficients can be analysed theoretically. For most of prototype structures however, a certain loss of wave energy flux is inevitable. Hydraulic model tests are generally required to assess the coefficients of wave reflection and transmission of the structures concerned. It is standard in such model tests to employ irregular trains of waves with the input of an appropriate frequency spectrum.

B.5.6 Wave breaking

A train of monochromatic waves in shoaling water, breaks at a stationary location at a certain depth at which the stability and continuity of wave surface are lost and dissipation of wave energy starts. A train of irregular waves breaks randomly at various locations over a wide distance, with large waves breaking off the shore and small waves breaking near the shore. Breaking of individual waves is mainly governed by the ratio of wave height to the local water depth. The ratio is sometimes called the breaker index.

In the nearshore zone, or the surf zone, where most of wave breaking takes place, the distribution of individual wave heights deviates from the Rayleigh distribution. Just outside the nearshore zone, large waves experience a strong non-linear shoaling process and the wave height distribution may become broader than the Rayleigh. In the outer part to the middle of the nearshore zone, the wave height distribution becomes much narrower than the Rayleigh owing to the disappearance of large waves by breaking. However, the

distribution maintains a shape of gradual decrease toward the upper limit, which is controlled by the water depth, because of probabilistic variations of wave breaking phenomena. From the middle of the nearshore zone toward the shoreline, the wave height distribution becomes broad again because of reformation of individual waves after breaking, presence of temporal variations of mean water level or the surf beat phenomenon, and the rise of mean water level or the wave set-up. At the location of initial shoreline, there is an appreciable amount of surface fluctuation that yields a certain distribution of individual wave heights. The nearshore zone with non-zero wave heights at the shoreline of initial zero depth is sometime termed the unsaturated surf zone (see Goda[91] for details).

There have been proposed several numerical models to predict the variation of characteristic wave heights such as $H_{1/3}$ and H_{rms} (root-mean-square height). Only a few models have the capability of simulating the transformation of wave height distribution across the nearshore zone. For shoaling water of a uniformly inclined seabed, a set of design diagrams, together with approximation formulae, have been prepared by Goda for the variations of $H_{1/250}$ and $H_{1/3}$, in which $H_{1/250}$ denotes the mean of highest 1/250 waves and has the relationship of $H_{1/250}$ = 1,80 $H_{1/3}$ assuming the Rayleigh distribution. The diagrams together with the formulae can be found in BSI[31], Goda[88], OCDI[163] and others.

For an area of complicated bathymetry such as ones with bars, troughs and/or reefs, efforts are being made to develop the methodology for prediction of the random wave breaking process. References should be made to most recent research works including Goda[91].

B.5.7 Wave transformations by currents

Interactions between waves and currents are generally evaluated using linear theory. The rate of wave height changes caused by opposing or following currents can be estimated by the works of Jonsson et al.[117] and Brevik and Aas[27]. Mei[147] gives the theoretical treatment of the phenomenon of wave refractions by currents.

For practical applications, several numerical models are available, which include the SWAN model (Booij et al.[25] and Holthuijsen et al.[108]), the STWAVE model (Vincent et al.[253]) or MIKE by Danish Hydraulic Institute, etc. Most of the models have some “shortcuts” and assumptions to save computation time. It is deemed necessary that the model allow for directional wave spectra, especially when the bathymetry is irregular. Each model has considerable strengths and each can be an appropriate choice for wave transformation. However, none of the models can be considered universally applicable and results from all can be inaccurate if the assumptions made in model development are significantly violated. Users of the models must be thoroughly familiar with the models, their assumptions and limitations.

B.5.8 Other transformations

On the coast where a nearly flat and shallow sea extends over a long distance or the seabed is inclined toward the shoreline with a slope gentler than 1/300, waves are gradually attenuated owing to bottom friction; i.e., the loss of wave energy flux by the orbital motion of water particles working against bottom turbulent shear stress. Reliable evaluation of the amount of wave attenuation by bottom friction is difficult however, because there is a wide scatter of the data of the friction coefficient estimated from the field measurements of wave decay. Some efforts are being made to incorporate the term of energy dissipation due to bottom friction into spectral models for wind wave generation and propagation in shallow water.

Another source of possible wave attenuation is the wave-induced motion of soft subsoil layers and associated visco-elastic energy dissipation. There are reports that an appreciable degree of wave damping takes place in coastal waters with the seabed composed of very soft clay. Several theories have been presented and laboratory tests have been made for their verification. No established methodology is available however for quantitative evaluation of wave damping by this mechanism, in the field.

B.6 Wave kinematics

B.6.1 Crest elevation

The crest elevation of the highest wave is one of the key factors in designing pile-supported structures such as piers and oil-drilling platforms, because it determines the upper limit to which the action of waves is exerted. Non-linear theories of monochromatic waves such as the Stokes' 5th wave theory and the stream function theory are often used to calculate the crest elevation and the profile of large waves. The theory of non-linear random waves has not yet developed to accurately calculate the crest elevation of the highest wave among random waves. Comparison of the second order theory with the observed probability distribution of wave crests is found in Forristall[75]. Report of the Technical Committee I.1 "Environment" of the 14th ISSC contains a good source of information on crest height statistics (Ohtusbo and Sumi[165]).

The ratio of the crest elevation above the still water level to the wave height increases from 0,5 for the infinitesimally small waves toward a limiting value at wave breaking as the wave height increases. The upper limit of the crest-to-height ratio at wave breaking is a function of the water depth relative to the wavelength. Table B.1 lists the theoretical breaker limit of progressive waves of permanent type (symmetric profile with a sharp corner at crest) on water of uniform depth, which was computed by Yamada and Shiotani[269]. The crest-to-height ratio at wave breaking is listed in the right-most column. Even though the applicability of permanent wave theory to random sea waves has not yet been proven, Table B.1 provides a guideline for the estimation of the crest elevation of very large waves.

Table B.1 — Characteristics of breaking waves of permanent type

H_b/L_0	h_b/L_A	h_b/L_b	C_b/C_A	H_b/L_b	H_b/h_b	η_c/H_b
∞	∞	∞	1,193	0,141 2	0	□
0,935	0,935	0,768 6	1,189	0,140 9	0,179 1	0,670 6
0,471	0,474	0,401 1	1,181	0,138 6	0,345 6	0,676 5
0,286	0,300	0,259 7	1,154	0,127 7	0,491 9	0,690 8
0,185 6	0,216	0,188 5	1,143	0,111 5	0,591 2	0,716 5
0,111 7	0,151 0	0,133 1	1,134	0,089 97	0,668 3	0,761 9
0,076 3	0,119 8	0,105 0	1,141	0,074 10	0,705 9	0,793 9
0,047 4	0,091 5	0,079 15	1,156	0,057 71	0,729 3	0,839 2
0,028 4	0,069 4	0,059 09	1,174	0,044 30	0,749 6	0,876 6
0,016 69	0,052 5	0,043 98	1,193	0,033 71	0,766 6	0,906 1
0,010 95	0,042 2	0,034 99	1,207	0,027 20	0,777 4	0,924 2
0,005 75	0,030 6	0,248 3	1,231	0,019 62	0,790 4	0,945 3
0,002 39	0,019 53	0,015 70	1,244	0,012 60	0,802 8	0,964 9
0,001 144	0,013 51	0,010 75	1,257	0,008 71	0,809 9	0,975 7

H_b = breaking wave height;

h_b = water depth at breaking;

L_0 = deepwater wavelength by small amplitude wave theory;

L_b = length of breaking wave;

L_A = small amplitude wavelength;

C_b = celerity of breaking wave;

C_A = celerity of small amplitude wave;

η_c = crest elevation above still water level.

B.6.2 Water particle velocities

The velocities and accelerations of water particles under wave action induce drag and inertia forces on cylindrical structural elements and isolated structures. They should be evaluated for waves of large height for which structures are designed. Three approaches have been taken for the estimation of wave kinematics of large waves.

The first approach is the use of the non-linear theories of monochromatic waves, which is applied to individual waves defined by the zero-crossing method. Laboratory measurements of wave kinematics by Chakrabarti and Kriebel[48] among others have demonstrated their applicability in the mid-water zone. Measurements of horizontal velocities around the wave crests have been made by Skjelbreia[202] with laser doppler velocimetry and by Lader[135] with particle image velocimetry. Skjelbreia reported the approximate equivalence of the maximum horizontal velocity to the celerity of a breaking solitary wave, while Lader obtained maximum velocity in the range of $\times$ 0,7 to $\times$ 0,8 for the celerity of transient breaking waves by extrapolation of measured velocity profiles. When a non-linear theory of monochromatic waves is employed, it is recommended to confirm that the theory can predict the horizontal velocity at the crest of a breaking wave being equal to the wave celerity. Table B.1 can be referred to for the estimation of the breaking wave celerity.

The second approach is the spectral computation of wave kinematics by converting the directional wave spectrum of surface elevation to that of wave kinematics by means of the transfer function from the surface elevation to the kinematics. A simple application of the linear wave theory for the transfer function overpredicts the wave kinematics near the wave crest in relatively deep water, because the spectral components of wave kinematics at the high frequency range are excessively amplified. It is customary to employ some stretching of the vertical coordinate. Wheeler's method[262], for example, transforms the vertical coordinate z into $z' = (z - \eta)/(1 + \eta/h)$, where η denotes the instantaneous surface elevation. Gudmestad[97] has presented a review of measured and predicted wave kinematics in deep and intermediate water, including a number of field measurement reports.

The third approach is the hybrid method proposed by Dean[62] in which the prediction of wave kinematics by non-linear wave theories is reduced by taking into account the effect of the directional spreading of wave spectra, which is estimated by the linear transformation theory. Reduction of wave kinematics from two-dimensional wave theories up to 15 % has been observed in several field measurement projects (e.g., Forristall et al.[77]). The ratio of the directional wave-induced water particle velocity to the unidirectional wave-induced water particle velocity is sometimes called the spreading factor. Reference is made to Forristall and Ewans[76] who have presented the value of the spreading factor for various wave conditions in the field.

As to non-linear wave theories, the Stokes' 5th order wave theory and the stream function method by Dean[61] are often used by practitioners in the oil industry. There is another numerical (user-friendly) method for non-linear wave kinematics by Rienecker and Fenton[185], which employs Fourier expansion series of the stream function and applies Newton techniques to solve a system of non-linear simultaneous equations. The latter can also solve the case of waves in water flowing at a specified speed. The Fenton method is user-friendly and applies well to regular shallow water waves.

B.6.3 Wave and current kinematics

The combined kinematics of waves and current are, in principle, required when calculating actions from waves and currents on a slender structure, e.g. Morison type loading, pipelines, vortex induced vibrations, etc.

For the simple case of the following or opposite currents in water of uniform depth, Hedges[106] gave the horizontal and vertical water particle velocities and accelerations for the stationary frame, assuming linear wave theory. Hedges also gave, for similar conditions, the spectrum of the water article velocities and accelerations by a transfer function approach when the scalar water elevation spectrum is given by $S_{\eta\eta}(f_a, U)$, where f_a is the frequency corresponding to the period observed by a stationary observer and U is the current velocity.

Hedges also refers to methods being available for dealing with shortcrested seas for which there will be varying degrees of wave refractions caused by currents, depending on initial wave direction and frequency, as well as on current direction and strength.

However, there have been no investigations on the effect of directional waves and currents on the Morison type force. The recommendation is to use the scalar wave spectrum together with the angle between the mean direction of the waves and the current when evaluating the spectrum of the water particle velocities and accelerations.

Within the oil industry, practise has been to simply add the current velocity, stretched to the instantaneous water level, to the water particle velocities from the waves as obtained from a proper wave theory, e.g. API RP 2A WSD[10] and NORSOK Standard[162]. The Fenton Fourier series theory as mentioned in B.6.2 is also useful and more exact than the engineering approach taken by the oil industry.

Annex C
(informative)

Currents

C.1 General

For bottom-founded structures, the total current profile should be considered. The total current profile associated with the sea state producing extreme or abnormal waves should be specified for structure design.

C.2 Current parameters

Current velocities vary in space and time. The total ocean current velocity is the vector sum of tidal and non-tidal or residual currents. The components of the residual current include circulation and storm generated currents, as well as short and long period currents generated by various phenomena, such as density gradients, wind stress and internal waves. Residual currents are often irregular, but in many locations, the largest residual current to be considered is the extreme storm surge currents.

Tidal currents are regular and predictable and their daily maximum velocities are approximately proportional to the tidal range of the day. They are generally weak in deep water past the shelf break. They are generally stronger on broad continental shelves than on steep shelves. Tidal currents can be strengthened by shoreline and bottom configurations such that strong tidal currents can exist in many inlets and coastal regions.

Circulation currents are relatively steady, large scale, features of the general oceanic circulation. Examples include the North Atlantic Current. While relatively steady, these circulation features can meander and intermittently break off from the main circulation feature to become large scale eddies or rings, which then can drift at a speed of some few miles per day. These circulation features occur mainly in deep water beyond the shelf break and generally do not affect coastal sites. But they may affect wave refraction from deep to shallow water.

Wind generated currents are caused by the wind stress and atmospheric pressure gradients through the storm. These current velocities are a complex function of the storm strength and meteorological characteristics, bathymetry and shoreline configurations, and water density profile. In deep water along open coastlines, surface storm currents may be estimated to up to 3 % of the 1 h sustained wind velocity during storms. As the storm approaches the coastline and shallow water, the storm surge and current can increase.

In the surf zone there exist special currents called the nearshore currents induced by waves. Because the nearshore currents are generated within the surf zone, they transport suspended sediments in areas where sediments are present and cause topographical changes of beaches.

At river outlets and in estuaries the currents can be complex due to the interactions of fresh and salt water.

C.3 Current characteristics

The characteristics of the extreme or abnormal current profile that need to be estimated for the design of coastal structures are particularly difficult to determine since current measurement surveys are relatively expensive and consequently it is unlikely that any measurement programme will be sufficiently long to capture a representative number of severe events. Furthermore, current hindcasting modelling is not as advanced as wind and wave modelling in terms of being able to provide the parameters needed. Also extrapolation of any data set requires account being taken of the three-dimensional nature of the flow.

Site-specific measurements of currents at the location of a structure can be used either as the basis for independent estimates of likely extremes or to check the indicative values of the various components of the total current.

For most design situations in which waves are dominant, estimates of the extreme or abnormal residual current and total current can be obtained from high quality site-specific measurements. These should extend over the water profile, depending on water depth, and over a period that captures several major storm events that generate large sea states. Current models may be used in lieu of site-specific measured data. The period over which the current model is run should be adequate to allow tidal decomposition to be carried out and the residual current to be separated out of the total current. Efforts should be made to ensure that the output of a current model is validated against nearby measured data.

C.4 Current profile

The characteristics of current profiles in different parts of the world depend on the regional oceanographic climate, in particular the vertical temperature structure and the advection of water into or out of an area. Both these controlling aspects vary from season to season. Typically, shallow water profiles in which tides are dominant can often be characterized by a logarithmic profile or simple power laws of velocity versus depth, whereas deep water profiles are more complex and can even show reversal of the current direction with depth.

The logarithmic current profile given in Equation (C.1) or the simple power law, Equation (C.2), may be used where appropriate (e.g. in areas dominated by tidal currents in relatively shallow water as in most coastal waters):

$$U(z) = \frac{u_*}{\kappa} \ln\left(\frac{h+z}{z_0}\right) \tag{C.1}$$

or by a simpler expression, when the velocity at a certain elevation below the still water line, z_1, has been measured

$$U(z) = U(z_1)\left(\frac{z+h}{z_1+h}\right)^{\alpha} \tag{C.2}$$

where

z is the vertical coordinate ($z = 0$ at the still-water line);

u^* is the friction velocity;

z_0 is the bed roughness length;

κ is Van Karman's constant = 0,4;

α is the coefficient, approximately 1/7;

h is the water depth.

Annex D
(informative)

Wave action on rubble mound structures

D.1 Conventional rubble mound breakwaters

D.1.1 Introduction

Rubble mound breakwaters may take various configurations depending on water depth, severeness of wave action, the availability of armour units, core materials, use of the rear area, etc. A special type of rubble mound breakwater allows reshaping of its seaward slope by wave actions. It is called a berm breakwater, the design aspects of which are described in D.2. The present clause deals with conventional types of rubble mound breakwaters in order to supplement 5.1. A general reference is made to Burcharth and Hughes[44], who provide detailed information on design of breakwaters.

A conventional rubble mound breakwater is built with a core mostly made of quarry run, protected by armour layers on the seaward and rear slope surfaces. Armour units are large rocks or concrete blocks of various shapes. Filter layers are usually provided between the armour layers and the core to prevent loss of core materials by being sucked out by wave actions through gaps between armour units.

D.1.2 Failure modes of rubble mound breakwaters

Because of its complex construction and configuration damage to rubble mound breakwaters includes several modes of failure as illustrated in Figure D.1 (according to Burcharth[32]). The major failure mode is the erosion of the seaward slope by removal and/or breakage of armour units by wave actions. If a certain area of the armour layer is removed, the filter layer is subject to direct wave actions and may be destroyed, being followed by sucking-out of core material. Thus, selection of the material and size of armour units is the most important design item.

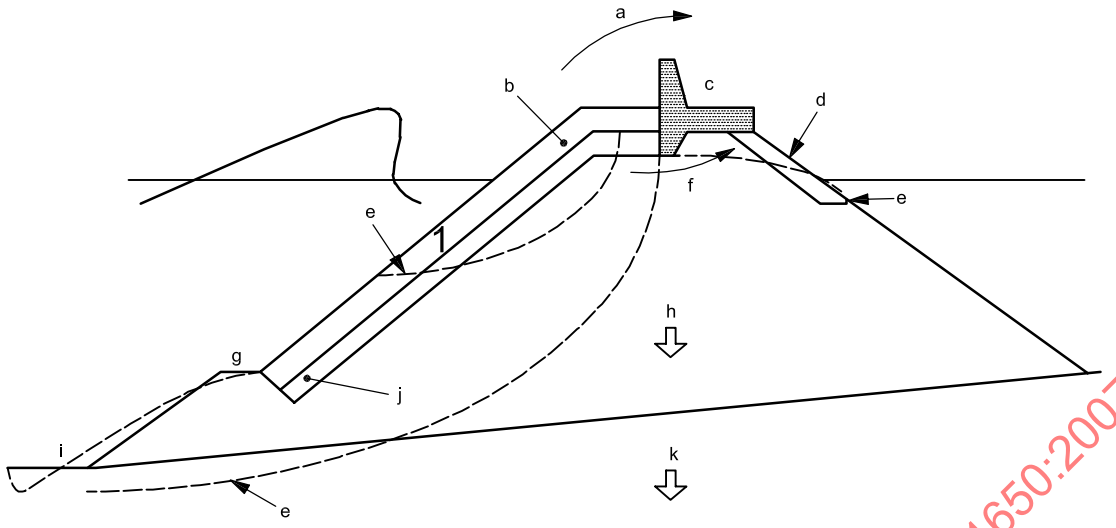

Key

1	armour	f	Venting.
a	Overtopping.	g	Berm erosion.
b	Erosion, breaking of armour.	h	Core settlement.
c	Breakage, sliding, tilting of capping wall.	i	Seabed scour and toe erosion.
d	Erosion of armour.	j	Filter instability.
e	Slip failure.	k	Subsoil settlement.

Figure D.1 — Overview of failure modes for rubble mound breakwaters

D.1.3 Stability of seaward armour units

D.1.3.1 Definition of damage of armour units

Armour layers of rubble mound breakwaters are generally designed with acceptance of a certain amount of armour units being displaced from their original positions. The degree of damage is the input parameter in various empirical stability formulae for the selection of the mass of armour units. The degree of damage of armour layers has been defined differently in several formulae. Three definitions are currently used:

$$D = \frac{\text{number of displaced units}}{\text{number of units in the section}};$$

N_{od} = number of displaced units within a strip along the slope with a width corresponding to the nominal width of armour unit;

$$S = \frac{A_e}{D_n^{\,2}}$$

where

A_e is the eroded area of the cross-section profile of the armour layer;

D_n = $\left(\frac{\text{mass of unit}}{\text{mass density}}\right)^{1/3}$ = (equivalent cube side length).

D.1.3.2 Minimum mass of armour units

The minimum mass of armour units that are stable against wave action within the permissible range of damage can be calculated by the following general formula:

$$M = \frac{\rho_r H^3}{N_s^3 \Delta^3} \tag{D.1}$$

or

$$N_s = \frac{H}{\Delta (M / \rho_s)^{1/3}} = \frac{H}{\Delta D_n} \tag{D.2}$$

where

M is the mass of armour units;

ρ_s is the mass density of armour units;

H is the characteristic wave height used in the design calculation;

N_s is the stability number dependent on types of armour unit and affected by various design factors;

Δ is the relative density of armour units in water = $\frac{\rho_r}{\rho_w} - 1$ with ρ_w being the mass density of water;

D_n is the equivalent cube side length = $(M/\rho_s)^{1/3}$.

For graded materials such as quarried rock and natural stones the 50 % fractile D_{n50} = $(M_{50}/\rho_r)^{1/3}$ is used.

D.1.3.3 Stability number of non-overtopped two-layer rock armoured slopes

There have been proposed a number of empirical formulae based on laboratory tests for the stability number of armour units. The following lists some formulae for seaward slopes.

Hudson[110] formula for head-on waves

$$N_S = (K_D \cot\alpha)^{1/3} \tag{D.3}$$

where

α is the slope angle;

K_D is the stability coefficient.

The 50 % fractile equivalent cube side length D_{n50} is used with Equation (D.1). The formula was based entirely on regular wave tests and there remains some ambiguity on the K_D value applicable for irregular waves. The 1977 edition of the Shore Protection Manual (SPM) by US Army Coastal Engineering Research Center recommends the values listed in Table D.1 with the characteristic wave height $H = H_{1/3}$. However, the 1984 edition of SPM recommends the values listed in Table D.2 with the characteristic wave height $H = H_{1/10}$. When considering the mean relationship of $H_{1/10}$ = 1,27$H_{1/3}$ under the Rayleigh distribution (for non-depth-limited waves), SPM 1984 introduces a considerable safety factor compared to the practice based on SPM 1977.

According to Van der Meer[242],[243], the coefficient of variation of the stability number using Equation (D.3) is estimated to be 18 %. Melby and Mlaker[149] have reported a coefficient of variation of K_D of 25 % for stones and 20 % for Dolosses.

Table D.1 — K_D values for stones by SPM 1977 with $H = H_{1/3}$ for slope angles $1{,}5 \leqslant \cot \alpha < 3{,}0$

Stone shape	Placement	Damage, D [a]			
		0 % to 5 %		5 % to 10 %	10 % to 15.%
		Breaking waves [b]	Non-breaking waves [c]	Non-breaking waves	Non-breaking waves
Smooth, rounded	Random	2,1	2,4	3,0	3,6
Rough angular	Random	3,5	4,0	4,9	6,6
Rough angular	Special [d]	4,8	5,5		

[a] D is defined according to SPM 1984 as follows. The percent damage is based on the volume of armour units displaced from the breakwater zone of active armour units removal for a specific wave height. This zone extends from the middle of the breakwater crest down the seaward face to a depth equivalent to the wave height causing zero damage below still water level.

[b] Breaking waves mean depth-limited waves, i.e., wave breaking takes place in front of the armour slope. (Critical case for shallow-water structures.)

[c] No depth-limited wave breaking takes place in front of the armour slope.

[d] Special placement with the long axis of stone placed perpendicular to the slope face.

Table D.2 — K_D values for stones by SPM 1984 with $H = H_{1/10}$

Stone shape	Placement	Damage, D [a] = 0 % to 5 %	
		Breaking waves [b]	Non-breaking waves [c]
Smooth rounded	Random	1,2	2,4
Rough angular	Random	2,0	4,0
Rough angular	Special [d]	5,8	7,0
[a, b, c, d] See Table D.1.			

Table D.3 — Damage levels, S, for two-layer armour, Van der Meer[242]

Slope	Initial damage (needs no repair)	Intermediate damage (needs repair)	Failure (core exposed)
1:1,5	2	3 to 5	8
1:2	2	4 to 6	8
1:3	2	6 to 9	12
1:4	3	8 to 12	17
1:6	3	8 to 12	17

Van der Meer formulae[242] for breakwaters exposed to non-breaking waves (outside the surf zone) and breaking waves (inside the surf zone).

$$\frac{H_s}{\Delta D_{n50}} = 6,2 C_H S^{0,2} P^{0,18} N_z^{-0,1} \xi_m^{-0,5} : \xi_m < \xi_{mc}, \text{ plunging} \quad \text{(D.4)}$$

$$\frac{H_s}{\Delta D_{n50}} = 1,0 C_H S^{0,2} P^{-0,13} N_z^{-0,1} (\cot\alpha)^{0,5} \xi_m^{P} : \xi_m > \xi_{mc}, \text{ surging} \quad \text{(D.5)}$$

where

C_H is the modification factor due to random wave breaking [= 1,4/($H_{1/20}$/$H_{1/3}$)], which takes a value 1,0 outside the surf zone;

S is the relative area of the eroded area defined in D.1.3;

P is the notional permeability, 0,5, for conventional two layer rock slopes;

N_z is the number of waves (during storm duration); maximum 7 500 waves, after which damage does not develop further;

ξ_m is the Iribarren number defined as equal to tan $\alpha/s_{0m}^{0,5}$, in which s_{0m} is the deepwater wave steepness $H_{1/3}/L_{0m}$ with the deepwater wavelength L_{0m} corresponding to the mean wave period;

ξ_{mc} is the critical Irribarren number (plunging waves for $\xi_m < \xi_{mc}$ and surging waves for $\xi_m > \xi_{mc}$), given by $[6,2P^{0.31}(\tan\alpha)^{0,5}]^{1/(P+0,5)}$.

The characteristic wave height is $H_{1/3}$ and the 50 % fractile equivalent cube side length D_{n50} is used with Equations (D.1) and (D.2). Inclusion of the modification factor C_H in Equations (D.4) and (D.5) is according to the OCDI[163] (p.114), which replaces the 2 % exceedance wave height $H_{2\%}$ (as originally employed by Van der Meer[242] with the one-twentieth highest wave height $H_{1/20}$ (difference of 0,4 %); diagrams of the ratio $H_{1/20}$:$H_{1/3}$ are available in OCDI[163]. Within the surf zone, C_H may take the value up to 1,15 and thus the stability number becomes slightly larger than for the region outside the surf zone.

The coefficient of variation on the factor 6,2 in Equation (D.4) and on the factor 1,0 in Equation (D.5) is estimated to be 6,5 % and 8 %, respectively.

Table D.3 shows damage levels for two-layer rock armour, Van der Meer[242].

The validity ranges for Equations (D.4) and (D.5) are:

— for cot $\alpha \geqslant 4,0$ only Equation (D.4) should be used;

— $0,1 \leqslant P \leqslant 0,6$, $0,005 \leqslant s_m \leqslant 0,06$, 2,0 t/m^3 $\leqslant \rho \leqslant$ 3,1 t/m^3;

— for the eight tests run by Van der Meer[242] with depth limited waves, breaking conditions were limited to spilling breakers which are not as damaging as plunging breakers; therefore Equations (D.4) and (D.5) may not be conservative in some breaking wave conditions.

D.1.3.4 Stability number of non-overtopped concrete block armoured slopes

The stability number of concrete armour units varies widely depending on their shapes and laying methods. The K_D-values for various shapes of concrete blocks in conjunction with Equation (D.1.3) have been proposed by researchers and manufacturers of respective blocks. Some of the available formulae are listed below.

Two-layer concrete cubes

The characteristic wave height is $H_{1/3}$. Brorsen, Burcharth and Larsen[28] have proposed Equation (D.6) for the range of 1,5 ⩽ cot α ⩽ 2,0 for randomly placed cubes in head-on waves.

$$N_s = \begin{cases} 1{,}8 - 2{,}0 : D = 0\% \\ 2{,}3 - 2{,}6 : D = 4\% \end{cases} \quad \text{(D.6)}$$

The damage rate of D = 0 % indicates the onset of damage.

Van der Meer[243] has presented Equation D.7 for two layer cubes randomly placed on 1:1,5 slopes by using irregular head-on waves in the non-depth-limited conditions.

$$N_s = (6{,}7 N_{od}^{0,4} / N_z^{0,3} + 1{,}0) s_{0m}^{-0,1} \quad \text{(D.7)}$$

Uncertainty of this formula corresponds to a coefficient of variation of approximately 10 %.

Two-layer Tetrapods

The characteristic wave height is $H_{1/3}$. Van der Meer[243] has presented Equation (D.8) on 1:1.5 slopes by using irregular head-on waves in the non-depth-limited conditions.

$$N_s = (3{,}75 N_{od}^{0,5} / N_z^{0,25} + 0{,}85) s_{0m}^{-0,2} \quad \text{(D.8)}$$

Uncertainty of this formula corresponds to a coefficient of variation of approximately 10 %.

For depth-limited wave conditions, d'Angremond, Van der Meer and Van Nes[55] have proposed to increase the above stability number by the modification factor C_H.

Two-layer Dolosse

The characteristic wave height is $H_{1/3}$. Burcharth and Liu[40]) have presented Equation (D.9) for two-layer randomly placed Dolosse with a 1:1.5 slope.

$$N_s = (47 - 72r)\varphi D^{1/3} N_z^{-0,1} = (17 - 26r)\varphi^{2/3} N_{od}^{1/3} N_z^{-0,1} \quad \text{(D.9)}$$

where

r is the Dolosse waist ratio (test range of 0,32 < r < 0,42);

φ is the packing density in two layers (test range of 0,61 < φ < 1);

D is the relative number of units displaced more than one dolosse height or more within the zone of the levels SWL ± 6,5D_n (insert D = 0,02 for 2% displacement);

N_{od} is the number of displaced units within a strip width of one equivalent cube length D_n (length of a cube having the same volume as Dolosse).

Tests were made for breaking and non-breaking wave conditions in the range of 2,49 < ξ_m < 11,7. For the number of waves N_z greater than 3 000, N_z = 3 000 is to be used. Uncertainty of this formula corresponds to a coefficient of variation of approximately 22 %.

One-layer Accropodes

Van der Meer[243] found no damage up to N_s = 3,7 and failure at N_s = 4,1. The standard deviation of the factors 3,7 and 4,1 is approximately 0,2.

Burcharth et al.[41] have presented Equation (D.10) for one layer of Accropodes on 1:1,33 slope by using irregular, head-on waves in breaking and non-breaking wave conditions.

$$N_s = A(D^{0,2} + 7,70) \tag{D.10}$$

where A denotes an empirical coefficient having the mean value of $\bar{A}$ = 0,46 and the coefficient of variation of 0,02 + 0,05(1 − D)^6. The minimum stability was observed in the range of 3,5 < ξ_m < 4,5.

D.1.3.5 Stability of overtopped rock armoured slopes

The stability of armour units on seaward slopes slightly increases as the overtopping increases with reduced crest levels. Reference is made to various formulae for low-crested structures given in Burcharth and Hughes[44].

D.1.4 Wave run-up and overtopping

D.1.4.1 Run-up of irregular waves

The run-up, $R_{u,p\%}$, is defined as the vertical distance between the still water level, SWL, and the level of the highest position of the water on the slope which will be exceeded by p% of the waves. For a conventional two-layer rock armoured slope exposed to head-on waves with Rayleigh distributed wave heights, $R_{u,p\%}$ can be estimated by the central fit formula of the following by Delft Hydraulics:

$$\frac{R_{u,p\%}}{H_{1/3}} = \begin{cases} A\xi_{0m} & : 1,0 < \xi_{0m} \leqslant 1,5 \\ B(\xi_{0m})^C & : 1,5 < \xi_{0m} \leqslant (D/B)^{1/C} \\ D & : (D/B)^{1/C} \leqslant \xi_{0m} < 7,5 \end{cases} \tag{D.11}$$

where

ξ_{0m} is the Iribarren number equal to tan $\alpha/s_{0m}^{0,5}$;

s_{0m} is the wave steepness defined as $H_{1/3}/L_{0m}$ with the deepwater wavelength related to the mean wave period.

The coefficients A, B, C and D are listed in Table D.4. The coefficient of variation for A, B, C and D is 12 %.

Table D.4 — Coefficients for estimation of wave run-up

P (%)	A	B	C	D [a]
0,1	1,12	1,34	0,55	2,58
1	1,01	1,24	0,48	2,15
2	0,96	1,17	0,46	1,97
5	0,86	1,05	0,44	1,68
10	0,77	0,94	0,42	1,45
33 (significant)	0,72	0,88	0,41	1,35
50 (mean)	0,47	0,60	0,34	0,82

[a] Only applicable for permeable slopes.

D.1.4.2 Overtopping rate

Wave overtopping occurs when the highest run-up level exceeds the crest freeboard, R_c, defined as the vertical distance from SWL to the crest level of the breakwater. Several formulae exist for the estimation of the time-averaged overtopping rate per unit length, q. For a breakwater with a straight two-layer armoured slope and no crown wall, q can be estimated by the following formula (Van der Meer and Janssen[247]).

$$\frac{q}{\sqrt{gH_s^3}} = 0{,}2 \exp\left(-3{,}7 \frac{R_c}{H_{2\%}}\right) \tag{D.12}$$

where $H_{2\%}$ is the 2 % exceedance wave height and is equal to $1{,}4H_{1/3}$ under the Rayleigh distribution of wave heights. The formula is valid for $\xi_{0p} > 2$, where ξ_{0p} is the Iribarren number defined with the deepwater wave steepness related to the spectral peak wave period as $\xi_{0p} = \tan\alpha/(H_{1/3}/L_{0p})^{1/2}$.

The coefficient of variation on the factor 3,7 in Equation (D.12) is approximately 15 %.

Critical values of average overtopping discharges are shown in Table D.5.

Table D.5 — Critical values of average overtopping discharges
Burcharth and Hughes[44] (CEM)

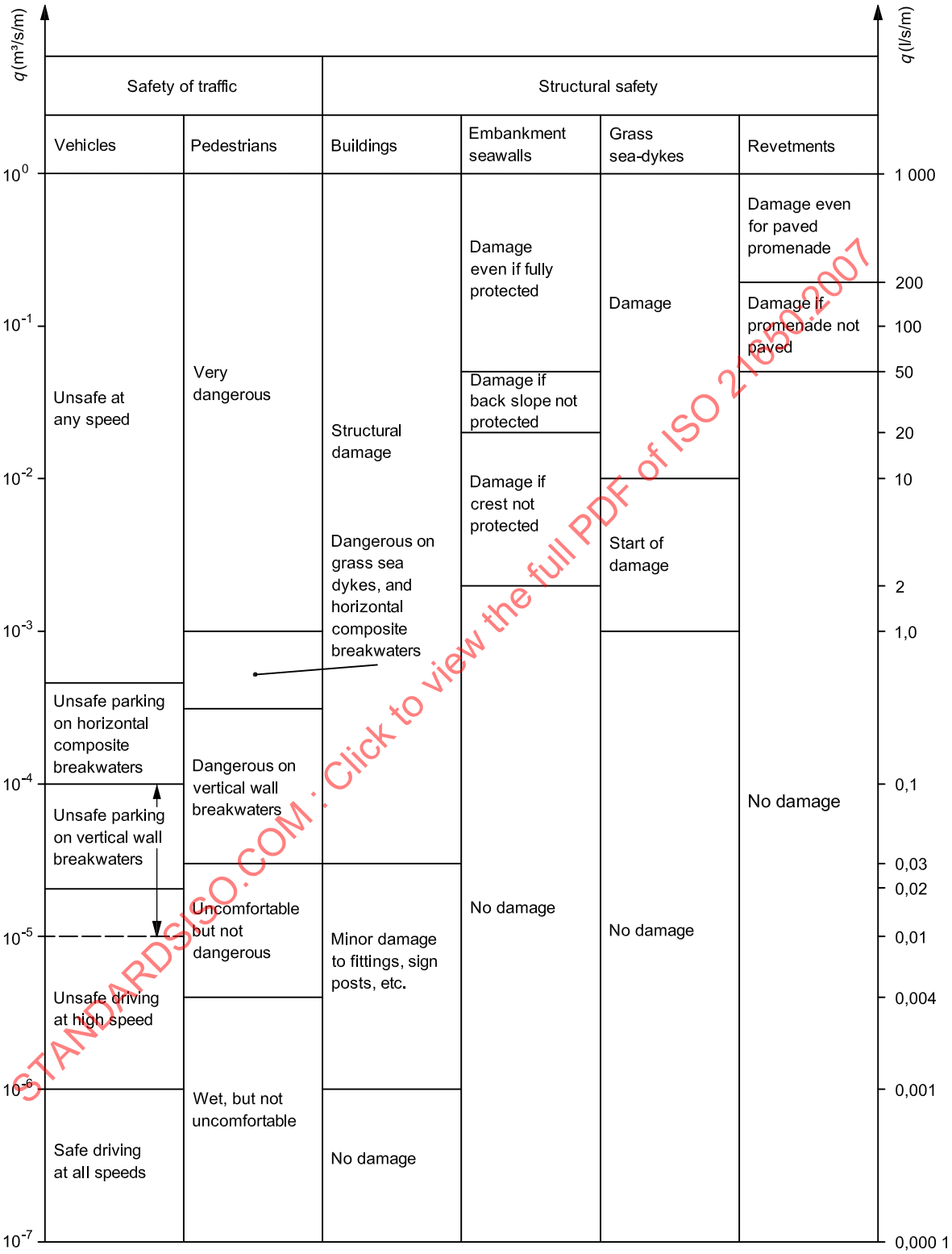

D.1.5 Stability of rear side armour units

Design of lee-side cover layers depends on the extent of wave overtopping and the design of the crest. No general stability formulae are available for leeside armour stability.

For severely to moderately overtopped rubble mound breakwaters without a superstructure, it is good practice to extend the main armour units over the crest down the rear side to a level well below the still water level. Where concrete crown walls are installed, stability of the lee-side armour units should be verified in model tests.

D.1.6 Stability of roundheads

Under similar wave conditions the armour layer in a roundhead is more exposed to damage than the armour layer in the adjacent trunk. This is because the cone shape causes higher overflow velocities and lesser lateral support of the armour units. The most exposed section of the roundhead is indicated in Figure D.2.

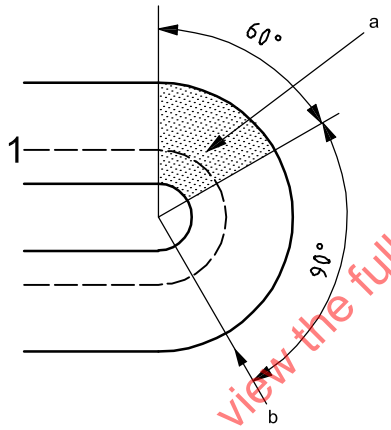

Key

1 still water level

a Critical sector for damage initiation.

b Direction of wave propagation.

Figure D.2 — Illustration of the most exposed section of a cone-shaped roundhead

This is the location where the water jets from the plunging waves hit the cone. Long waves are more damaging than short waves. Within the slope range 1:1,5 to 1:3, it seems that roundheads with steeper slopes can resist larger waves than roundheads with milder slopes for stages of small damage and damage initiation. However, the damage develops faster the steeper the slope.

The weight of the roundhead armour units is in most cases × 1,5 to × 2,5 the weight of the trunk armour units, given the same wave climate and mass density. Alternatively the mass density of the armour units can be increased in the roundhead (Burcharth et al.[46]). Generally, it is recommended to check roundhead stability in hydraulic model tests.

D.1.7 Stability of armour units on toe berm

For a toe berm of two to three layers of quarry rocks with mass density ρ_s = 2,68 t/m^3, the following stability formula has been given by Van der Meer et al.[241] in conjunction with Equation (D.1), based on model tests with a non-overtopped rubble mound structure with front slope 1:1,5 in head-on irregular waves. The characteristic wave height is $H_{1/3}$.

$$N_s = \left(0,24 \frac{h_b}{D_{n50}} + 1,6 \right) N_{od}^{0,15} \tag{D.13}$$

where h_b is the water depth at top of toe berm. The Equation (D.13) is valid for:

$$\begin{aligned} 0,4 &\leqslant h_b / h_s \leqslant 0,9 \\ 0,28 &\leqslant H_s / h_s \leqslant 0,8 \\ 3 &\leqslant h_b / D_{n50} \leqslant 25 \end{aligned} \tag{D.14}$$

in the range of $0,4 < h_b/h_s < 0,9$, $0,28 < H_{1/3}/h_s < 0,8$, and $3 < h_b/D_{n50} < 25$, where h_s denotes the water depth in front of the toe berm.

For a standard toe of about 3 stones to 5 stones wide and 2 stones to 3 stones high, the following N_{od} values can be used:

$$N_{od} = \begin{cases} 0,5 & \text{no damage} \\ 2 & \text{acceptable damage} \\ 4 & \text{severe damage} \end{cases} \tag{D.15}$$

D.1.8 Design of filters

Design criteria for granular filters must ensure that the finer material of the core is not lost by being sucked out through the gaps between coarser materials. Many criteria for filter design exist. The following set of stability criteria is one of those used:

$$\left. \begin{aligned} \frac{d_{15,\text{filter}}}{d_{85,\text{core}}} &< 4 \text{ to } 5 \\ \frac{W_{50,\text{filter}}}{W_{50,\text{core}}} &< 15 \text{ to } 20 \end{aligned} \right\} \tag{D.16}$$

where d and W are the diameter and weight of granular materials, respectively.

A criteria for the internal stability criterion of the filter layer is given by

$$\frac{d_{60,\text{filter}}}{d_{10,\text{core}}} < 10 \tag{D.17}$$

D.1.9 Breakage of concrete armour units

Concrete armour units have limited strength and might break due to too large impact forces when placed, or due to rocking and displacements caused by wave actions. The concrete tensile strength is the limiting factor for unreinforced units. A considerable size effect causes large units to be relatively weaker than smaller units. Critical impact velocities for normal concrete quality (tensile strength $\geqslant$ 2,5 MPa) ranges from 5 m/s to 6 m/s for a 5 t cube to 3 m/s to 4 m/s for a 50 t cube, and 2 m/s for a mid size tetrapod or a Dolos with a waist ratio of 0,4. The stresses in the placed armour units imposed by gravity also contribute significantly to breakage in

case of slender units like tetrapods and Dolosse. The breakage can be predicted by the following formula by Burcharth et al.[43].

$$B = C_0 M^{C_1} f_T^{C_2} H_{1/3}^{C_3} \quad \text{(D.18)}$$

where

B is the relative number of broken units;

M is the armour unit mass in tonnes, $2{,}5 \leqslant M \leqslant 50$;

f_T is the concrete static tensile strength in megapascals, $2 \leqslant f_T \leqslant 4$;

$H_{1/3}$ is the significant wave height in metres;

C_0, C_1, C_2, C_3 are empirical parameters.

The effect of static, pulsating and impact stresses are included in the formula. The values of the empirical parameters fitted to test data are listed in Table D.6.

Table D.6 — Fitted values of empirical parameter for breakage of concrete armour units

Location	Waist ratio	C_0		C_1	C_2	C_3
		Coefficient of variation	Mean			
Trunk of dolosse	0,325	0,188	0,009 73	– 0,749	– 2,58	4,143
	0,37	0,200	0,005 46	– 0,782	– 1,22	3,147
	0,42	0,176	0,013 06	– 0,507	– 1,74	2,871
Round-head of dolosse	0,37	0,075	0,025	– 0,65	– 0,66	2,42
Trunk of tetrapods		0,25	0,003 93	– 0,79	– 2,73	3,84

D.1.10 Stability of crown walls

Wave-induced forces might cause a crown wall to fail as a monolith by sliding or tilting, or by breaking.

With reference to Figure D.3 the wave-induced horizontal force and uplift force can be calculated by the formula by Pedersen[172] given below.

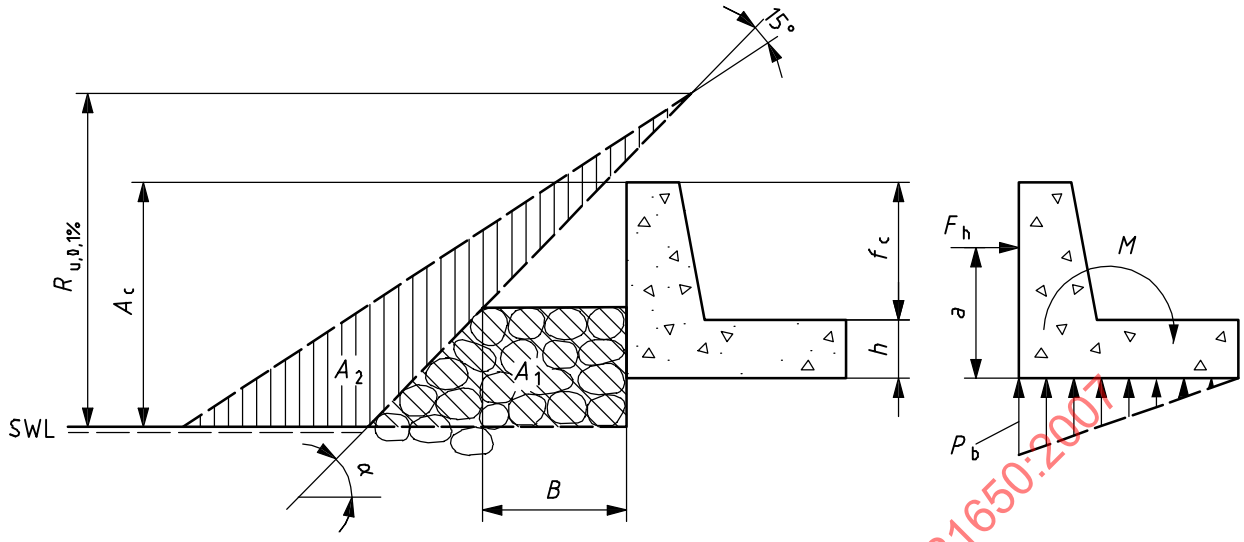

Figure D.3 — Notations for calculating wave actions on crown walls

Figure D.4 is a representation of the tested models and Table D.7 lists the range of test parameters according to Pedersen.

Dimensions in centimetres

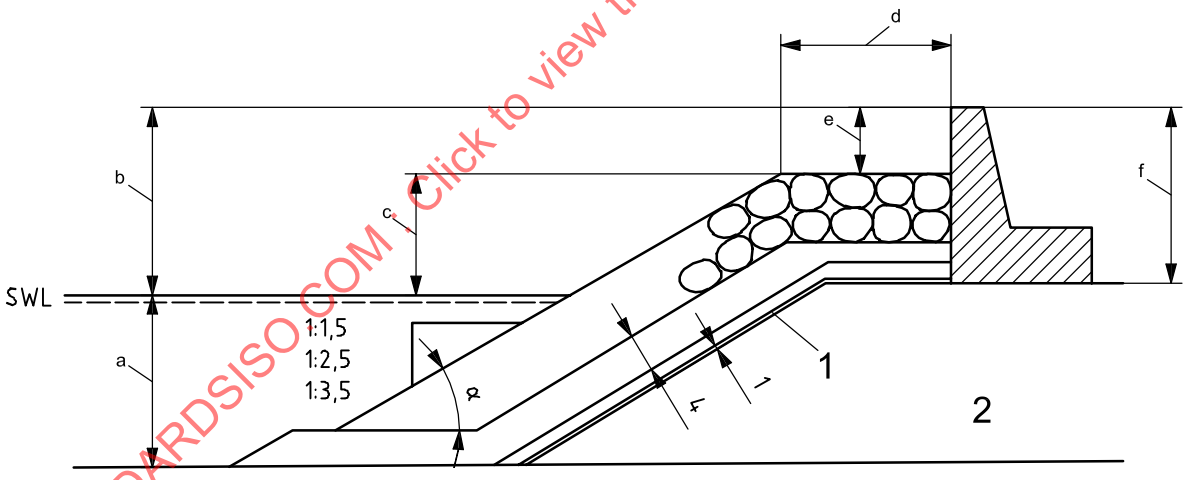

Key

1 geotextile
2 course sand

a 51 cm to 59 cm.

b R_c = 11 cm to 37 cm.

c A_c = 11 cm to 19 cm.

Figure D.4 — Tested models

Table D.7 — Parameter ranges

Parameter	Range
H_s	0, 10 to 0,18
T_{om}	1,07 to 1,94 s
T_{op}/T_{om}	≅ 1,1,3
ξ_{om}	1,11 to 1,51
S_{om}	0,02 to 0,06
R_c/H_s	0,7 to 3,6
H_s/A_c	0,5 to 1,7
A_c/B	0,3 to 1,1
cotα	1,5 to 3,5
Number of waves	> 5 000 per test

$$F_{h,0,1\%} = 0,21\sqrt{\frac{L_{om}}{B}}(1,6\,p_m y_{eff} + A\frac{p_m}{2}h') \tag{D.19}$$

$$M_{0,1\%} = a \times F_{h,0,1\%} = 0,55(h' + y_{eff})F_{h,0,1\%} \tag{D.20}$$

$$p_{b,0,1\%} = 1,00A\,p_m \tag{D.21}$$

where

$F_{h,\,0,1\%}$ is the horizontal wave force per running metre of the wall corresponding to 0,1 % exceedance probability;

$M_{0,1\%}$ is the wave generated turning moment per running metre of the wall corresponding to 0,1 % exceedance probability;

$p_{b,\,0,1\%}$ is the wave uplift pressure corresponding to 0,1 % exceedance probability;

L_{om} is the deepwater wavelength corresponding to the mean wave period;

B is the berm width of armour layer in front of the wall;

p_m is the $\rho_w g(R_{u,\,0,1\%} - A_c)$;

$R_{u,\,0,1\%}$ is the wave run-up corresponding to 0,1 % exceedance probability.

$$R_{u,0,1\%} = \begin{cases} 1,12H_s\xi_m & \xi_m \leqslant 1,5 \\ 1,34H_s\xi_m^{0,55} & \xi_m > 1,5 \end{cases} \tag{D.22}$$

$$\xi_m = \frac{\tan\alpha}{\sqrt{H_s / L_{om}}}$$

where

α is the slope angle of armour layer;

A_c is the vertical distance between MWL and the crest of the armour berm;

A is the minimum $\{A_2/A_1, 1\}$, where A_1 and A_2 are areas shown in Figure D.3;

y_{eff} is the minimum $\{y/2, f_c\}$:

$$y = \begin{cases} \dfrac{R_{u,\,0,1\%} - A_c}{\sin\alpha} \dfrac{\sin 15^\circ}{\cos(\alpha - 15^\circ)} & , y > 0 \\ 0 & , y \leqslant 0 \end{cases} ; \tag{D.23}$$

h' is the height of the wall protected by the armour layer;

f_c is the height of the wall not protected by the armour layer.

The uncertainties of the coefficients in the formulae (D.19) to (D.21) are shown in Table D.8.

Table D.8 — Standard deviation of the coefficients in formulae (D.19) to (D.21)

Coefficients in the formulae	0,21	1,6	0,55	1,00
Standard deviation	0,02	0,10	0,07	0,30

Stability against sliding between the crown wall base and the rubble foundation requires

$$(F_G - F_U)\mu \geqslant F_H \tag{D.24}$$

where

μ is the friction coefficient for the base plate against the rubble stone ($0{,}5 \leqslant \mu \leqslant 0{,}7$);

F_G is the buoyancy-reduced weight of the structure;

F_U is the wave-induced uplift force;

F_H is the wave-induced horizontal force plus force from armour resting against the front of the structure.

A safety factor has to be applied to F_H in deterministic design.

Stability against overturning is maintained if:

$$M_{FG} \geqslant M_{FU} + M_{FH} \tag{D.25}$$

where

M_{FG} is the stabilizing moment of F_G around the heel;

M_{FU} is the antistabilizing moment of F_U around the heel;

M_{FH} is the antistabilizing moment of F_H around the heel.

A safety factor shall be applied to the right hand side of Equation (D.25) in deterministic design.

Stability against geotechnical slip failures shall be demonstrated. Conventional slip failure calculation methods can be used.

Hydraulic model tests are in general recommended for determination of wave-induced loads on crown walls. From the test series must be identified the combinations of simultaneous wave-induced forces that give the minimum crown wall stability.

D.2 Berm breakwaters

D.2.1 Introduction

PIANC[176] issued a report from a working group on “State-of-the-art of designing and constructing berm breakwaters”. The main items for designing berm breakwaters are referenced here.

Berm breakwaters are different from conventional rubble mound breakwaters as indicated in Figure D.5.

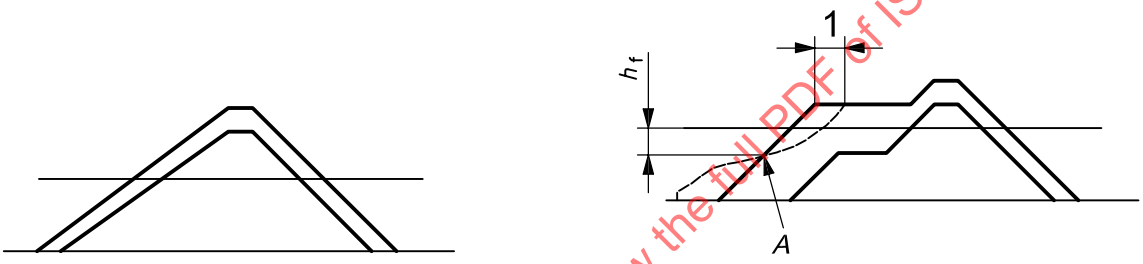

Conventional rubble mound breakwater **Rubble mound berm breakwater with recession**

Key

1 recession

Figure D.5 — Conventional and berm rubble mound breakwaters

A conventional rubble mound breakwater is required to be almost static stable for the design wave conditions, while the berm breakwater has traditionally been allowed to reshape into reshaped static or a reshaped dynamic stable profile as indicated in Figure D.5. Non-reshaping static stable berm breakwaters have also lately been considered. Berm breakwaters may thus be divided in three categories:

a) non-reshaped static berm breakwater, where only a few stones are allowed to move similarly to what is allowed on a conventional rubble mound breakwater, for the design wave conditions;

b) reshaped static stable berm breakwater, where the profile is reshaped into a stable profile where the individual stones are also stable for the design wave conditions;

c) reshaped dynamic stable berm breakwater, where the profile is reshaped into a stable profile, but the individual stones may move up and down the slope for the design wave conditions.

The berm breakwater is normally constructed with a berm that is allowed to reshape into an S-shape. This is because it currently is cheaper to construct the breakwater with an ordinary berm rather than with the S-shape directly. A more stable design has been developed in Iceland in close cooperation between all partners involved: designers, geologists, supervisors, contractors and local governments and Sigurdarson et al.[199]. One reason for this development is the fear that the reshaping process may eventually lead to excessive crushing and abrasion of individual stones as they move on the berm breakwater. The question of allowing reshaping or not has obviously to do with the stone quality and the stones' ability to withstand impact, crushing and/or abrasion. It is however clear that even a non-reshaping berm breakwater requires cover stones with significantly less mass than required on a conventional rubble mound breakwater.

There are methods available to evaluate the suitability of quarried stones against crushing for reshaped static stable type berm breakwaters. There is less information on how to evaluate the suitability of quarried rock for reshaped dynamic stable berm breakwaters. It is not recommended to design for reshaped dynamic stable conditions.

In cases where no quarried cover stones large enough for a conventional rubble mound breakwater can be provided, a berm rubble mound breakwater may be an economic alternative to rubble mound breakwaters with concrete cover blocks.

D.2.2 Stability and reshaping of berm breakwaters

D.2.2.1 Stability and reshaping of the trunk section

Most of the research on the stability and reshaping of berm breakwaters has been for homogenous berms. But lately some work has also been made on the stability and reshaping of multilayer berm breakwaters, (Sigurdarson et al.[200]). The multilayer berm breakwater allows a better and more economical utilization of the quarry yield than does a conventional rubble mound breakwater and it is expected that this will be the future design of berm breakwaters.

There have been several papers presented on the reshaping of berm breakwaters following different routes, e.g. Van der Meer[244], Van Gent[237], Archetti and Lamberti[12] followed a route similar to Van der Meer [242], [243], while Hall and Kao[99] and Tørum et al.[233] followed another route. The reshaped profile is determined with the aid of several length and height parameters depending on simplified description of the sea states, H_s, T and N_z (where N_z is the number of waves) of the geometry of the structure and of the characteristic of the stone (D_{n50}, ρ_s). The dynamic profile is characterized by a number of parameters (Van der Meer[242], [243]).

Tørum[229] and Tørum et al.[233] followed to some extent the route of Hall and Kao[99]. With reference to Figure D.5 the recession, was analysed from several model test series at DHI and SINTEF. It was noticed that for a given berm breakwater all the reshaped profiles intersected with the original berm at almost a fixed point A in Figure D.5.

Tørum et al.[233] arrived at the following simple equation for the mean non-dimensional recession for homogenous berm breakwaters and multilayer berm breakwaters with randomly placed stones, which can be used for conceptual design.

$$\frac{\mathrm{Re_c}}{D_{n50}} = 0{,}000\,027(H_o T_o)^3 + 0{,}000\,009(H_o T_o)^2 + 0{,}11(H_o T_o) - f_1(f_g) - f_2\left(\frac{d}{D_{n50}}\right) \quad \text{(D.26)}$$

The gradation factor function $f\,(f_g)$ is given by:

$$f_1(f_g) = -9{,}9 f_g^{\,2} + 23{,}9 f_g - 10{,}5 \quad \text{(D.27)}$$

and the depth function $f\,(d/D_{n50})$ is given by:

$$f_2(d / D_{n50}) = -0{,}16\left(\frac{d}{D_{n50}}\right) + 4{,}0 \quad \text{for } 12{,}5 < d/D_{n50} < 25. \quad \text{(D.28)}$$

As an approximation h_f in Figure D.5, can be obtained from:

$$\frac{h_f}{D_{n50}} = 0{,}2\frac{d}{D_{n50}} + 0{,}5 \quad \text{for } 12{,}5 < d/D_{n50} < 25. \quad \text{(D.29)}$$

where

D_n is the equivalent cube side length = (W_n/ρ_s);

W_n is the mass of an individual stone

H_o is the stability number = $H_s/(\Delta D_{n50})$;

T_o = $(g/D_{n50})^{0,5}T_z$;

H_oT_o is the period stability number = $[H_s/(\Delta D_{n50})](g/D_{n50})^{0,5}T_z$;

H_s is the significant wave height;

T_z is the mean wave period;

Δ = $(\rho_s/\rho_w)-1$;

f_g is the gradation factor = D_{n85}/D_{n15};

D_{n50} = $(W_{50}/\rho_s)^{1/3}$, W_{50} = median stone mass, i.e. 50 % of the stones have a mass smaller than W_{50};

D_{n15} = $(W_{15}/\rho_s)^{1/3}$, W_{15} = 15 % of the stones have a mass smaller than W_{15};

D_{n85} = $(W_{85}/\rho_s)^{1/3}$, W_{85} = 85 % of the stones have a mass smaller than W_{85};

g is the acceleration of gravity;

ρ_s is the mass density of stone;

ρ_w is the mass density of water;

d is the water depth at the breakwater.

Tørum[229] found that the coefficient of variation for Re_c/D_{n50}, COV, was 0,33 based on the test series at SINTEF and DHI. The COV was found to be independent of H_oT_o.

Tørum et al.[234] came to the preliminary conclusion that orderly placement of the stones on the berm may improve the stability.

Alikhani[2] recommends the following threshold values for long shore transport.

$$H_oT_{op} = \frac{50}{\sqrt{\sin 2\beta_o}} \text{ for the reshaping phase} \quad \text{(D.30)}$$

$$H_oT_{op} = \frac{75}{\sqrt{\sin 2\beta_o}} \text{ after the reshaping phase.} \quad \text{(D.31)}$$

The suggested threshold design criteria for the trunk section, almost head-on waves, for different categories of berm breakwaters are shown in Table D.9.

Table D.9 — Preliminary stability criterion for different categories of berm breakwaters for modest angle of attack, $\beta = \pm 20°$

Category	H_o	$H_o T_o$
Non-reshaping	< 1,75 to 2,0	< 30 to 55
Reshaping, static stable	1,75 to 2,7	55 to 70
Reshaping, dynamic stable	> 2,7	> 70
NOTE The criterion depends to some extent on stone gradation.		

As mentioned before, it is recommended to design for reshaping static stable conditions.

D.2.2.2 Stability and reshaping of the berm breakwater head

Comparing results of tests by Van der Meer and Veldman[246], Burcharth and Frigaard[38],[39], Tørum[228] and Tørum et al.[233], it is concluded that if a berm breakwater is designed as a reshaped static stable berm breakwater, where $H_o T_o < 70$, it seems that by using the same profile for the head as for the trunk the head will be stable, with no excessive movements of the stones in the area behind the breakwater.

D.2.2.3 Rear side stability

Andersen et al.[8] arrived at the following relation for the necessary stone size D_{n50} on the rear side:

$$\frac{R_c}{H_{mo}}\sqrt{s_{02}} > \tan\alpha_f - \left(\frac{H_{mo}}{\Delta D_{n50}}\frac{1}{\sqrt{s_{02}}}\right)^{-1} \times \frac{(\mu\cos\alpha_r - \sin\alpha_r)}{C_D + \mu C_L} \qquad \text{(D.32)}$$

where

R_c is the breakwater crest height;

$H_{mo} \approx H_s$;

C_D is the drag coefficient;

C_L is the lift coefficient;

α_f is the effective slope on the front side (Figure D.6);

α_r is the slope of rear side (Figure D.6);

μ is the friction factor = 0,9 for the material used by Andersen[8];

$s_{02} = 2\pi H_s/(gT_{02}^2)$.

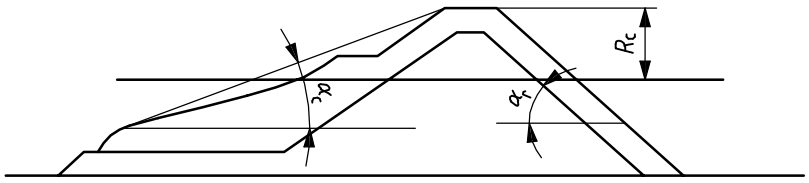

Figure D.6 — Definition of geometrical parameters for rear side stability

D.2.3 Wave overtopping

There are very few measurements of wave overtopping on berm breakwaters. Lissev[139] and Kuhnen[132] have measured average overtopping on a reshaped berm breakwater.

The Kuhnen data compare well with Lissev data, while the Van der Meer[245] relation for a conventional rubble mound breakwater show larger overtopping than the berm breakwater data. The results of Sigurdarson and Viggoson[198] indicate, as expected, that the time mean overtopping discharges for non-reshaped berm breakwaters are less than for reshaped breakwaters.

Burcharth and Andersen[45] gave preliminary results from the first systematic investigation on the wave overtopping of berm breakwaters.

D.2.4 Abrasion and stone crushing

When a berm breakwater reshapes, the stones suffer impact as they roll on the berm. This impact may eventually lead to abrasion and/or breaking of the stones.

Abrasion seems not to be a problem for berm breakwaters as reported by Archetti et al.[13] for Icelandic berm breakwaters.

Impact breaking may be a problem for stones rolling on a berm breakwater. Tørum and Krogh[231] and Tørum et al.[232] developed a method of evaluating the suitability of stones from a specified quarry from the stone breaking point of view, when the stones roll on a reshaping berm breakwater. The method applies to reshaping static stable berm breakwaters. For this condition a stone will basically move once down the breakwater slope and come to rest at a lower level. The speed of the stone will vary as it moves along the slope, but it is anticipated that it will be subjected to one major impact if it hits another stone at maximum velocity. It is well known that a stone that does not break on the first major impact may break after many major repeated impacts, which could be the case for stones on a reshaped dynamically stable berm breakwater.

The probability of breaking of the stones can be evaluated by considering only two variables:

a) the impact energy;

b) the breaking energy required to break the stone.

Although both are dependent on the mass of the stone, velocity and strength are considered to be independent.

D.2.5 Local scour and scour protection

Assessment of local scour should preferably be based on experience. If lacking, then validated semi-empirical formulae or sediment transport theory can be used. Useful guidelines on scour and scour protection may be found in US Army Corps of Engineers Coastal Engineering Manual[235], Whitehouse[268], Sumer and Fredsøe[213], OCDI[163].

Annex E
(informative)

Wave actions on vertical and composite breakwaters

E.1 General

There are several types of wave action on vertical and composite breakwaters as discussed in 6.2.2. Among these types of action, those referred to in the main text are described in Clauses E.2 to E.5.

E.2 Extended Goda formula for wave action on main body of breakwater

Wave pressure exerted upon a front wall of the vertical or composite breakwater is assumed to have a linear distribution as shown in Figure E.1.

The elevation to which the wave pressure is exerted, denoted by η^*, is given by

$$\eta^* = 0{,}75(1+\cos\beta)\lambda_1 H_D \tag{E.1}$$

where

β is the angle between the direction of wave approach and a line normal to the upright wall;

H_D is the wave height to be used in calculation as specified later.

The wave direction should be rotated by up to 15° toward the line normal to the upright wall from the principal wave direction in consideration of inaccuracy in defining the wave direction.

The pressure intensity is given by

$$p_1 = 0{,}5(1+\cos\beta)(\alpha_1\lambda_1 + \alpha_2\lambda_2\cos^2\beta)\rho_w g H_D \tag{E.2}$$

$$p_3 = \alpha_3 p_1 \tag{E.3}$$

$$p_4 = \begin{cases} p_1\left(1-\dfrac{h_c}{\eta^*}\right) & : \quad \eta^* > h_c \\ 0 & : \quad \eta^* \leqslant h_c \end{cases} \tag{E.4}$$

where

α_1, α_2, and α_3 are the coefficients given by Equations (E.5) to (E.7);

λ_1 and λ_2 are the pressure modification factors;

ρ_w is the density of seawater;

g is acceleration due to gravity;

h_c is the crest height of front wall above the still water level.

$$\alpha_1 = 0{,}6 + \frac{1}{2}\left[\frac{4\pi h/L}{\sinh(4\pi h/L)}\right]^2 \tag{E.5}$$

$$\alpha_2 = \min\left\{\left(\frac{h_b - d}{3h_b}\right)\left(\frac{H_D}{d}\right)^2, \frac{2d}{H_D}\right\} \tag{E.6}$$

$$\alpha_3 = 1 - \frac{h'}{h}\left[1 - \frac{1}{\cosh(2\pi h/L)}\right] \tag{E.7}$$

where

$\min\{a, b\}$ denotes the smaller one of a or b;

d is the water depth on top of the armour units (or foot protection blocks);

h is the water depth at the location of the front wall;

h' is the water depth at the toe of the front wall;

h_b is the water depth at an offshore distance of × 5 the significant wave height from the front wall;

L is the wavelength at the water depth h.

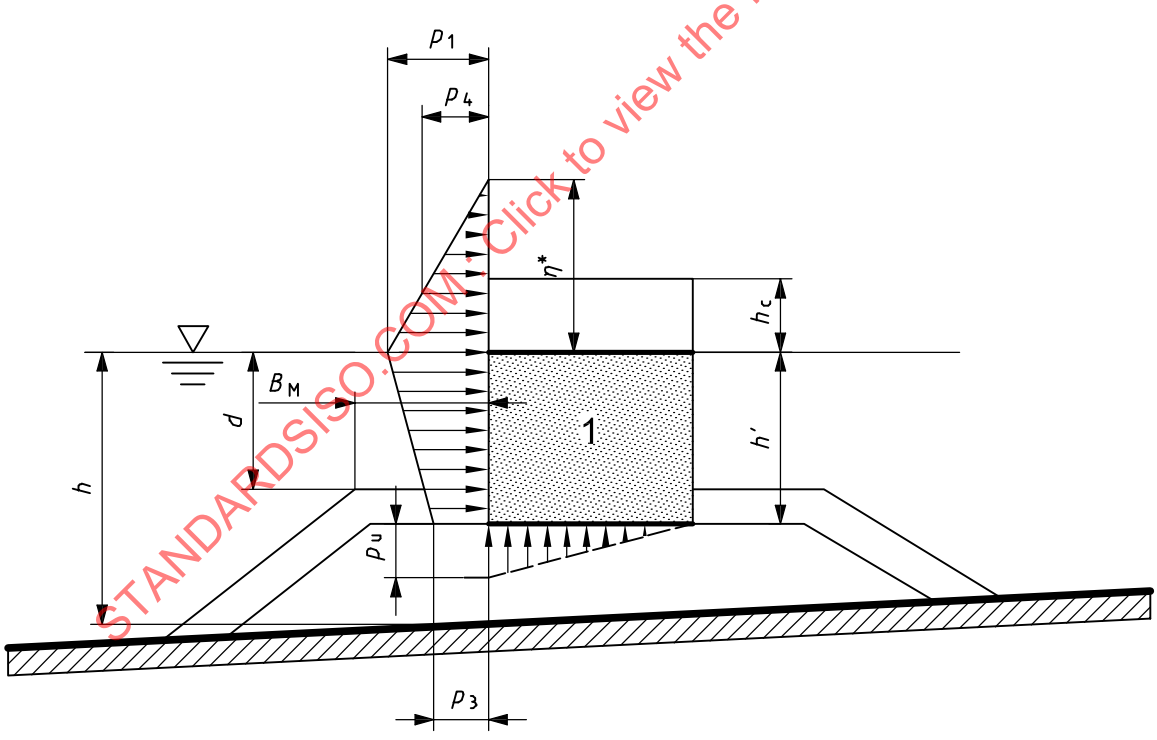

Key

1 buoyancy

Figure E.1 — Distribution of wave pressure and uplift exerted on the main body of the breakwater

The uplift exerted on the bottom of the main body is assumed to have a linear distribution with the maximum intensity as follows:

$$p_u = 0{,}5(1+\cos\beta)\alpha_1\alpha_3\lambda_3\rho_w g H_D \tag{E.8}$$

The buoyancy is applied to the immersed part of the main body regardless of wave overtopping.

The pressure modification factors λ_1, λ_2, and λ_3 are given the values of 1,0 for standard vertical or composite breakwaters, but they are assigned smaller values for composite breakwaters covered with wave-dissipating concrete blocks (see OCDI[163], p. 109 and Tables VI-5-58 and VI-5-59 of Burcharth and Hughes[44]).

The wave height H_D is the height of the highest wave, which is taken as × 1,8 the design significant wave height $H_{1/3}$ when the breakwater is located outside the surf zone. Inside the surf zone, H_D should be evaluated by taking the random wave-breaking process into consideration. The wave period for evaluation of the wavelength L is the significant wave period of the design wave, which is approximately equal to $0{,}9T_p$ and $1{,}2T_m$ for wind waves.

For the cases in which consideration is needed for the exertion of impulsive breaking wave pressures, the coefficient α_2 must be replaced by $\alpha^* = \max\{\alpha_2; \alpha_I\}$, where α_I is the coefficient for impulsive breaking wave pressure and defined below.

$$\alpha_I = \alpha_{IH}\alpha_{IB} \tag{E.9}$$

where

$$\alpha_{IH} = \min\{H/d; 2{,}0\} \tag{E.10}$$

$$\alpha_{IB} = \begin{cases} \cos\delta_2 / \cos\delta_1 & : \delta_2 \leqslant 0 \\ 1/(\cos h\delta_1 \cosh^{1/2}\delta_2) & : \delta_2 > 0 \end{cases} \tag{E.11}$$

$$\delta_1 = \begin{cases} 20\delta_{11} : \delta_{11} \leqslant 0 \\ 15\delta_{11} : \delta_{11} > 0 \end{cases} \tag{E.12}$$

$$\delta_{11} = 0{,}93\left(\frac{B_M}{L} - 0{,}12\right) + 0{,}36\left(0{,}4 - \frac{d}{h}\right) \tag{E.13}$$

$$\delta_2 = \begin{cases} 4{,}9\delta_{22} : \delta_{22} \leqslant 0 \\ 3{,}0\delta_{22} : \delta_{22} > 0 \end{cases} \tag{E.14}$$

$$\delta_{22} = -0{,}36\left(\frac{B_M}{L} - 0{,}12\right) + 0{,}93\left(0{,}4 - \frac{d}{h}\right) \tag{E.15}$$

where B_M is the width of the berm of the rubble mound in front of the main body.

The above formulae are due to Takahashi et al.[216].

Formulae for the total force and overturning moment can be found in Goda[88] p.139, and Table VI-5-55 of Burcharth and Hughes[44].

The Goda formula tends to overestimate the total wave loading on composite breakwaters by about 10 % with the coefficient of variation of 0,1 or so (see Takayama and Ikeda[217] and Table VI-5-55 of Burcharth and Hughes[44]). As such, the bias and uncertainty of the Goda formula should be taken in consideration in the probabilistic design of composite breakwaters.

E.3 Empirical formulae for minimum mass of armour units of rubble foundation

One of the available formulae for designing armour units of the rubble foundation of a composite breakwater is due to Tanimoto et al.[218] and is expressed by Equation (E.16). For other formulae, see Tables VI-5-45 to 48 of Burcharth and Hughes[44].

$$M = \frac{\rho_s}{N_s^3 (\rho_s / \rho_w - 1)^3} H_{1/3}^3 \tag{E.16}$$

where

M is the minimum mass of an armour unit that is stable against the action of waves with a design significant height of $H_{1/3}$;

ρ_s and ρ_w are the densities of armour unit and seawater respectively;

N_s is the stability number to be calculated by use of Equation (E.17).

$$N_s = \max\left\{1{,}8;\ \left(1{,}3\frac{1-\kappa}{\kappa^{1/3}}\frac{h'}{H_{1/3}} + 1{,}8\exp\left[-1{,}5\frac{(1-\kappa)^2}{\kappa^{1/3}}\frac{h'}{H_{1/3}}\right]\right)\right\} : B_M / L' < 0{,}25 \tag{E.17}$$

in which

$$\kappa = \frac{4\pi h'/L'}{\sinh(4\pi h'/L')}\kappa_2 \tag{E.18}$$

$$\kappa_2 = \max\left\{0{,}45\sin^2\beta\cos^2\left(\frac{2\pi x}{L'}\cos\beta\right);\ \cos^2\beta\sin^2\left(\frac{2\pi x}{L'}\right)\right\} : 0 \leqslant x \leqslant B_M \tag{E.19}$$

where

$\max\{a;b\}$ is a function denoting the larger one of a or b;

h' is the water depth at which armour units are placed;

L' is the wavelength of the design significant wave period at the depth h';

β is the wave incident angle;

B_M is the berm width.

The factor 0,45 in Equation (E.19) is due to Kimura et al.[122] and accounts for the effect of the front slope of rubble mound.

E.4 Stability analysis of rubble mound and seabed against geotechnical failures

The rubble mound and the seabed foundation of a composite breakwater might experience geotechnical failure by the eccentric and inclined loading from the main body of the breakwater under wave action. The bearing capacity of the rubble mound and the seabed foundation can be analysed with circular arc calculations based on the simplified Bishop method (OCDI[163], pp. 277-278). The strength parameters of rubble stones of which the mound is composed are preferably estimated through large-scale triaxial compression tests, because they are affected by the stress level. For rubble stones generally used in port construction works however, their strength parameters can be represented with an apparent cohesion of c_d = 20 kN/m^3 and the internal friction angle of ϕ_d = 35°.

E.5 Local scour and scour protection

Assessment of local scour should preferably be based on experience. If lacking, then validated semi-empirical formulae or sediment transport theory can be used. Useful guidelines on scour and scour protection may be found in US Army Corps of Engineers Coastal Engineering Manual[235], Whitehouse[268], Sumer and Fredsøe[213], OCDI[166].

Annex F
(informative)

Wave action on coastal dykes and seawalls

F.1 Coastal dykes

F.1.1 Introduction

Coastal dykes are man-made sloped soil structures parallel to the shore to protect the hinterland against erosion and flooding. They comprise coastal dykes along the shoreline and estuary dykes in a river estuary. These dykes are characterized by flat slopes on the seaward side (usually 1:4 corresponding to an angle of 14° from horizontal and flatter) and on the shoreward side (usually 1:3 corresponding to an angle of 18,3° and flatter). Very often, berms are installed on the seaward and/or shoreward side of the dyke (e.g. dyke access roads). Coastal dykes are generally built of sand and/or clay and are covered by different materials such as grass, asphalt, stone revetments, etc. A summary of relevant hydraulic and geotechnical processes for coastal dykes is given in Figure F.1.

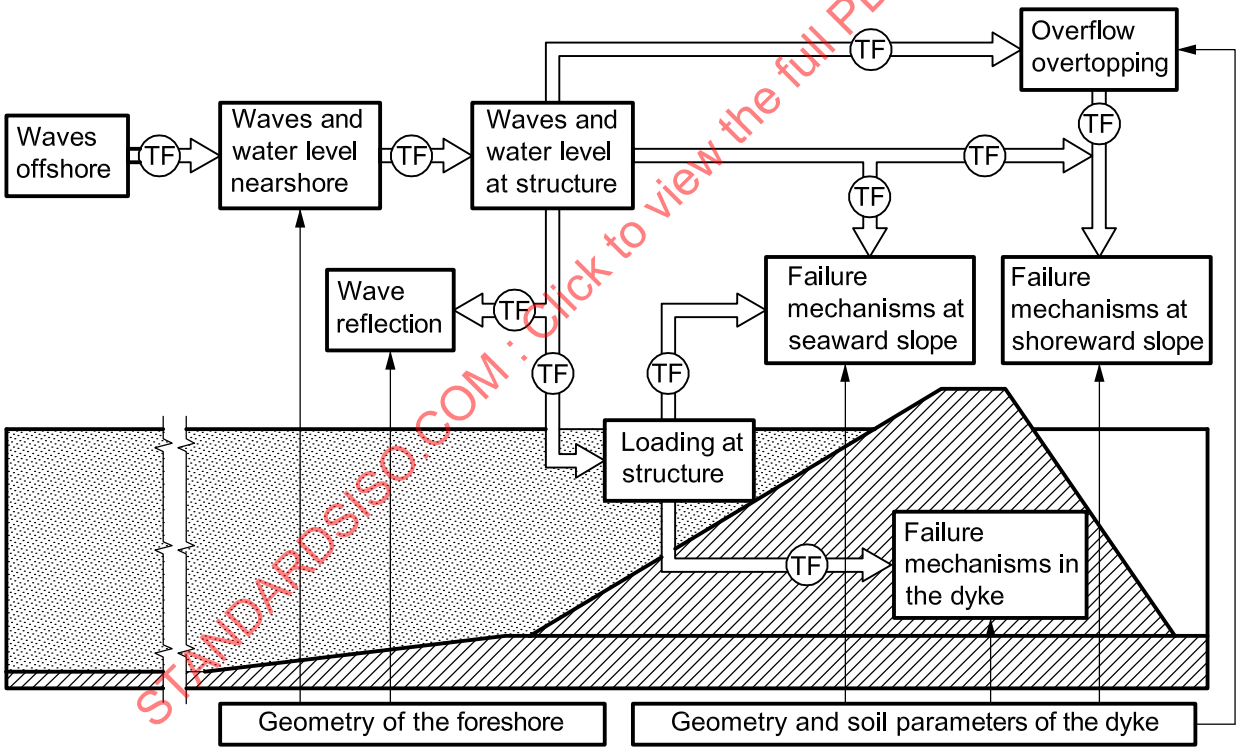

Figure F.1 — Overview of relevant hydraulic processes, loading processes and failure modes for coastal dykes

Figure F.1 shows that the hydraulic processes in the foreshore and the nearshore of the dyke are transferred to processes describing the loading at the structure and the overflow or overtopping, respectively. These "loading processes" can then be used to describe the failure mechanisms at the seaward side, the shoreward side and the interior of the dyke. Some guidance on "loading processes" and failure mechanisms is given in F.1.2 to F.1.5. The main design manuals available are EAK[71], OCDI[163], CIRIA/CUR[52], BSI[30].

F.1.2 Wave action on a seaward slope

For determination of wave run-up height the widely used definition of $R_{u,2\%}$ can be used which is defined as the height of the run-up tongue above still water level, which is exceeded by only 2 % of all waves. It can be determined using Van der Meer[245]:

$$\frac{R_{u,2\%}}{H_s} = 1{,}6 \times \gamma_b \times \gamma_f \times \gamma_\beta \times \xi_{op} \text{ with a maximum of } 3{,}2 \times \gamma_f \times \gamma_\beta \tag{F.1}$$

The surf similarity parameter or Iribarren number ξ_{op} (= tan $\alpha / s_0^{0,5}$) should be determined using the deep water wave steepness s_0 related to T_p and the significant wave height H_s. Empirical parameters γ_b and γ_β, describing the influence of a berm and the angle of wave attack are described in Van der Meer[245] and can be determined as follows:

$$\gamma_b = \begin{cases} 1 - 0{,}5 \times \dfrac{B_A}{L_{berm}} \times \left(\dfrac{R_{u,2\%} + h_h}{R_{u,2\%} - H_s} \right) & \text{for } \dfrac{h_h}{H_s} < -1 \\ 1 - \dfrac{B_A}{L_{berm}} \times \left(1 - 0{,}5 \times \left(\dfrac{h_h}{H_s} \right)^2 \right) & \text{for } \left| \dfrac{h_h}{H_s} \right| \leqslant 1 \\ 1 - 0{,}5 \times \dfrac{B_A}{L_{berm}} \times \left(2 - \dfrac{h_h}{H_s} \right) & \text{for } \dfrac{h_h}{H_s} > 1 \end{cases} \tag{F.2}$$

$$\gamma_\beta = 0{,}35 + 0{,}65 \times \cos\beta \tag{F.3}$$

where

β is the angle of wave attack (0°, if perpendicular);

B_A is the horizontal width of the berm on the seaward slope of the dyke;

h_h is the height of water above the berm;

L_{berm} is the effective length of the berm as described in Figure F.2.

The empirical parameter γ_f can be taken from Table F.1. More parameters can be found in Van der Meer[245].

However, for shallow foreshores, breaking on the foreshore may occur, which changes the type of the wave spectrum. Under these conditions it might be advisable to use a different wave period ($T_{m-1,0}$) for calculation of the surf similarity parameter. Details can be found in Schüttrumpf and Van Gent[194].

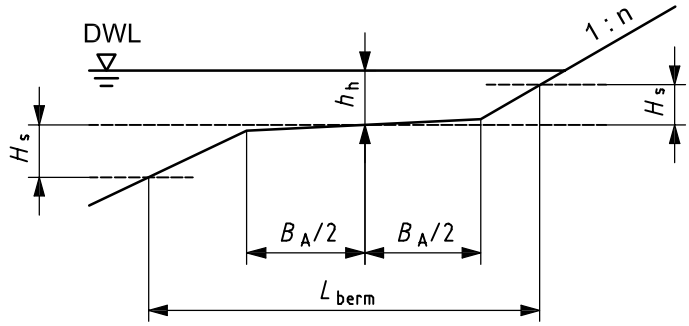

Influence of berms

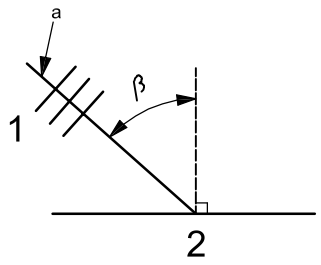

Influence of oblique wave attack

Key

1 wave crests

2 shoreline

a Wave direction.

Figure F.2 — Reduction coefficients accounting for angle of wave attack and berm influence

Table F.1 — Overview of reduction coefficients γ_f accounting for roughness on coastal dykes

Type of dyke cover	Reduction coefficient γ_f
Asphalt	1,0
Grass	1,0
Basalt revetment	0,9

Wave run-down height is defined as the distance of water level elevation during wave trough to still water level. It can be determined using Schüttrumpf[191] or Van Gent[239]. The thickness of the water layer on the dyke changes with the elevation over the still water level and can be determined for the seaward side of the dyke using Schüttrumpf (for crest and shoreward side see F.1.4). Mean run-up velocities on the seaward side, the crown and the shoreward side of the dyke can be estimated using Schüttrumpf and Van Gent[194] or Schüttrumpf.

Infiltration in the dyke body may result from excessive overtopping (from the shoreward side) or wave run-up and overtopping on the seaward side and the crown. Investigation has been made to determine whether this is mostly dependent on the mean layer thickness of the water body on the dyke, see Kortenhaus[124].

The phreatic water level in the dyke body will influence the geotechnical parameters of the dyke in the long term and is therefore more relevant for long-lasting water levels in front of the dyke. The duration for seepage through the dyke body can be estimated using e.g. Kortenhaus (as above).

Wave-induced uplift forces beneath the revetment or cover layer are very relevant for removal failure of revetments and therefore need to be duly considered. They can be estimated using e.g. Bezuijen and Klein-Breteler[23].

Erosion of grass and clay material at the seaward side is difficult to predict and, to date, only empirical formulae exist. However, these formulae are only validated by a very limited number of model tests and variations of relevant parameters may yield different results. The most promising approach is to predict the duration needed for erosion of the respective layers. More detailed information regarding erosion of grass layers is given in TAW[221]; some details on erosion of clay can be found in Möller et al.[156]. Regional data may be available and should then be used because soil, vegetation types and agricultural and construction practices have a large influence on erosion rates.

Wave impact loads on the seaward side of the dyke may cause the revetment or the surface of the dyke to fail, see Müller and Wolters[158]. These loads can be estimated using results from Führböter[80].

F.1.3 Wave overtopping

Mean overtopping discharges over coastal dykes per unit length have been investigated quite intensively in recent years. Influence of various parameters have been investigated and incorporated in formulae available from the literature. The most common formulae for coastal dykes originates from the analysis of a quite significant amount of data of various slopes as given in Van der Meer[245] as follows (see Annex D for comparison for rubble mound breakwaters).

$$\frac{q}{\sqrt{g \times H_s^3}} = \frac{0{,}06}{\sqrt{\tan\alpha}} \times \gamma_b \times \xi_{op} \times \exp\left(-5{,}2 \times \frac{R_c}{H_s} \times \frac{1}{\xi_{op} \times \gamma_b \times \gamma_f \times \gamma_\beta} \right) \quad \text{(F.4)}$$

with a maximum of:

$$\frac{q}{\sqrt{g \times H_s^3}} = 0{,}2 \times \exp\left(-2{,}6 \times \frac{R_c}{H_s} \times \frac{1}{\gamma_f \times \gamma_\beta} \right) \quad \text{(F.5)}$$

In Equations (F.4) and (F.5) the same empirical parameters γ_b, γ_f, and γ_β are used [see Equation (F.1)]. It was however discussed in Schüttrumpf and Van Gent[194]; Oumeraci et al.[170] and Groenendijk and Van Gent[95] that the influence of shallow foreshores and different forms of wave spectra can influence the mean overtopping discharge significantly and therefore has to be accounted for.

Variations of the dyke geometry have been investigated with respect to berms (Van Gent[238]; Pilarczyk[179]), various slopes and different roughness factors (Pilarczyk[179]; Klein-Breteler and Pilarczyk[123]). Oblique wave attack on coastal dykes has been investigated recently (Ohle et al.[164]; Oumeraci et al.[171]) suggesting a simple formula which predicts decrease of wave overtopping due to non-perpendicular wave attack for coastal dykes.

To date, but little information is available on individual wave overtopping volumes. It is however suggested that individual overtopping volumes are relevant for the initiation of failure at the landward side of coastal dykes. Individual overtopping volumes can be estimated from analysis of vertical breakwaters by Franco et al.[78] or rubble mound breakwaters by Sloth and Juhl[206].

Some progress has been made accounting for scale effects which might result from hydraulic model tests and which therefore need to be accounted for in many formulae resulting from model testing. The European CLASH project, De Rouck et al.[69], has delivered guidance on scale effects, but has also brought together a huge database of overtopping tests for various types of structure as described in Van der Meer et al.[249]. From this database a neural network prediction model was derived to predict the mean overtopping rates for various types of coastal structure.

F.1.4 Wave actions on dyke crest and shoreward slope

Actions on the dyke crest and the inner (shoreward) slope can be estimated using simple limits to tolerable overtopping discharges, or formulae describing mean velocities and layer thicknesses of overtopping or overflowing water masses on both the crest and the inner slope as suggested by Schüttrumpf and Van Gent[197]. These formulae are based on large-scale hydraulic model tests with random waves and typical coastal dykes as well as numerical models and also provide information about uncertainties of model prediction and parameters involved. Formulation of both methods is different but results are almost identical so that most simple approaches can be selected from Schüttrumpf and Van Gent. Results of formulae provide input for geotechnical failure modes on the crest and the shoreward slope such as erosion of shoreward slope and infiltration of dyke body (see F.1.5).

F.1.5 Influence of wave action on geotechnical failures

A couple of hydraulic and geotechnical failure modes can be identified for coastal dykes as given in Kortenhaus[124]. Availability of information regarding these failure modes is very different so that future research is required regarding many of them. Table F.2 shows an overview of failure modes, also indicating the background information (model tests, review, etc.), relevant references and whether formulae are available.

Table F.2 — Overview of most important failure modes with respect to coastal dykes

Mode	Based on	Reference	Remarks
Global failure modes			
Breaching	analytical model, breach tests	Visser[254]	analytical formulae available for sand dykes only, expanded to overtopping by Kortenhaus[124]
Seaward side			
Stability revetment	empirical model model tests	Pilarczyk[179]	
Impact	theoretical model	Kortenhaus[124]	magnitude of impacts given by Führböter[80]
Uplift revetment	analytical model	Bezuijen and Klein-Breteler[23]	modified by run-down approach in Kortenhaus[124]
Velocity run-up	analytical model, model tests	Schüttrumpf and Oumeraci[192]	approach for run-down also included in reference
Erosion grass	empirical model, few model tests	Verheij et al.[251]	predicts time for grass erosion
Erosion clay	semi-empirical model	TAW[222]	predicts time for clay layer erosion
Erosion of core	empirical model	Kortenhaus[124]	describes “cliff erosion” at seaward side
Slope stability	analytical model	DIN[60]	based on circular sliding area
Shoreward side			
Erosion grass	empirical model	Kortenhaus[124]	similar to grass erosion at seaward side
Erosion clay	semi-empirical model	Kortenhaus[124]	similar to clay erosion at seaward side
Uplift clay	analytical model	Weißmann[261]	
Sliding clay		Weißmann[261]	
Slope stability		DIN[60]	based on circular sliding area
Shoreward erosion		see breaching	
Internal failure modes			
Piping	semi-empirical model	Van Loon[240]	

Most relevant failure modes are erosion at the seaward side, impact by breaking waves and wave overtopping. Only when significant overtopping occurs does erosion at the shoreward side of the dyke also become relevant.

F.2 Seawalls

F.2.1 Introduction

Seawalls are onshore structures parallel to the shoreline. They are built as vertical face structures such as gravity concrete walls, steel or concrete sheet pile walls, stone filled cribworks or as sloping structures with revetment typically made of concrete slabs, concrete armour units or rubble material. The principal function of seawalls is to reinforce a part of the coastal profile and to protect land and infrastructures from the action of waves and flooding.

Figure F.3 shows that the hydraulic processes in the foreshore and the nearshore of a seawall are transferred to processes describing the loading at the seaward slope and the seawall as well as the overflow or overtopping, respectively. These "loading processes" can be used to describe the failure mechanisms on the slope, the interior of the seawall body and the seawall structure itself. Some guidance on "loading processes" and failure mechanisms is given in F.2.2 to F.2.7. Main design methods are summarised in EAK[71], OCDI[163], Thomas and Hall[224], CIRIA/CUR[52], BSI[30].

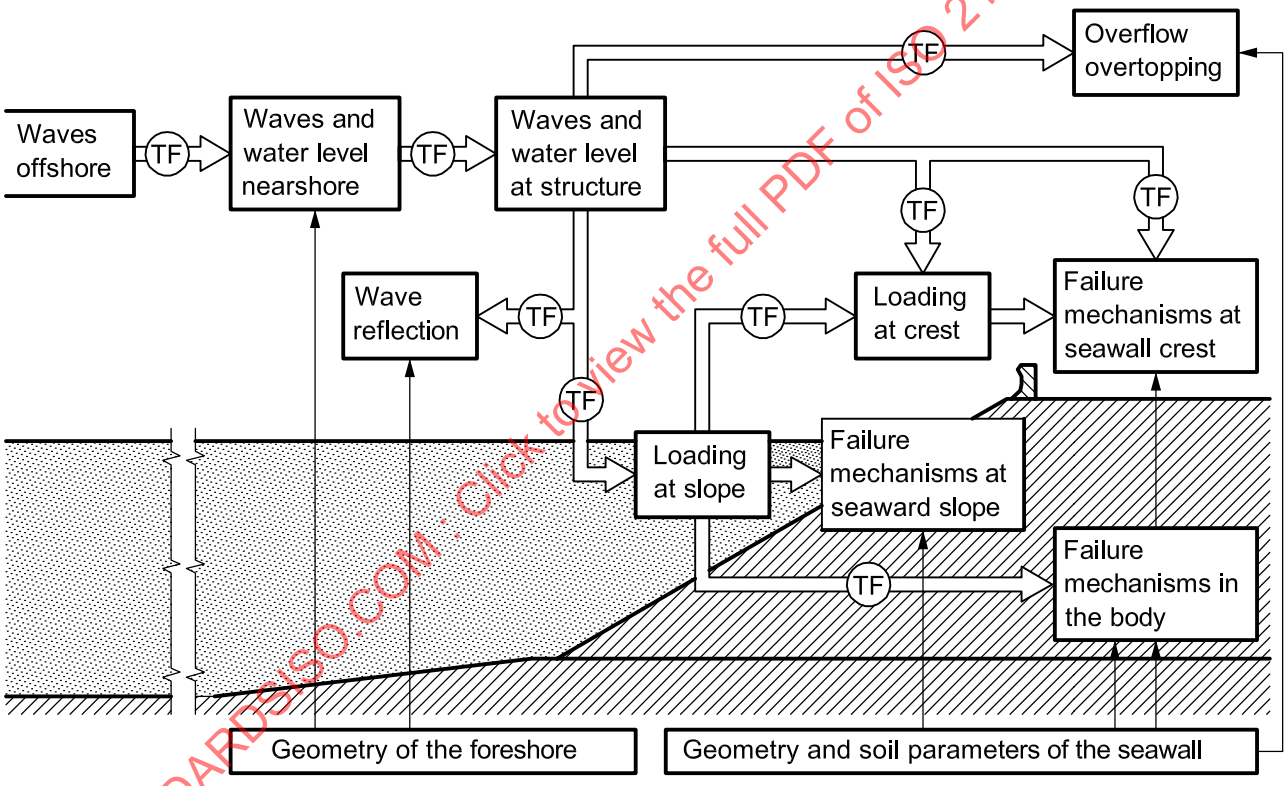

Figure F.3 — Overview of relevant hydraulic processes, loading processes and failure modes for seawalls

F.2.2 Wave reflection

Wave reflections from seawalls may have a significant influence on the coastal regime in front of the structure. Especially vertical or almost vertical constructions may almost totally reflect the waves increasing the wave height in front of the wall quite significantly, see Allsop and McBride[4]. Together with increasing wave heights the sediment transport potential may increase (Miles et al.[148]) and so does the potential danger of scour (Oumeraci[164]). Generally, rough and porous walls will result in lower reflection coefficients due to an increased energy dissipation at the structure (see Bélorgey et al.[20]). Wave reflection is dependent on wave steepness and wave length resulting in longer waves being more reflected than shorter waves. An overview of wave reflection formulae for vertical walls and simple and complex slopes (both porous and non-porous) is available from the literature in Thomas and Hall[224] or Ahrens and Bender[1].

F.2.3 Wave action on seaward slope

The use of different material to be used as armour of the seaward slope is dependent on the wave climate, the required hydraulic performance, visual and access aspects, maintenance and other functional characteristics, see Thomas and Hall[224] or CIRIA/CUR[52]. Rock armour, rip-rap, concrete armour units, gabion mattress, and open-stone asphalt revetments have been used as porous slopes and various constructions are feasible to be used as non-porous slopes comprising stepped slopes, concrete slabs and blocks and many others.

The armour layer of the seaward slope can be designed using the Hudson formula or similar approaches as described in Annex D or Burcharth and Hughes[44]. It should however be noted that hydraulic model tests will be required for special geometries of seawalls where these formulae are not directly applicable or whenever the selection of material on the seaward slope is not covered by any of these empirical formulae.

The design of the underlayer of the seaward slope needs special consideration due to its desired functions such as filtration, erosion control, drainage and energy dissipation. Some advice on the design of granular underlayers (for rip-rap, rock armours and concrete armour units) and geotextiles is given in Thomas and Hall[224].

Run-up on seawall slopes may cause overtopping (see F.2.5) whereas both run-up and run-down may cause erosion damage on the seaward slope depending on the material used for the armour and underlayer. Run-up heights can be estimated using formulae introduced in Thomas and Hall[224]. Run-up and run-down velocities may be determined by methods available for sea-dykes (Schüttrumpf and Van Gent[194]) or revetments (Bezuijen and Klein-Breteler[23]). Very little information is however yet available for critical velocities that are linked to initiation of erosion on the slope so that hydraulic model tests are recommended wherever erosion failure may become critical for the investigated cases.

F.2.4 Wave actions on seaward toe

The main purpose of the toe is to prevent undermining of the body of the seawall. Therefore, the stability of the toe is essential to guarantee the overall stability of the seawall. Various types of toe construction such as sheet-piles, concrete aprons or rubble toes are described in Thomas and Hall[224] together with some recommendation for design. Further types are discussed in Burcharth and Hughes[44] and CIRIA/CUR[52].

F.2.5 Wave overtopping

Wave spray has not yet been simulated in hydraulic model tests and therefore needs to be taken into account by engineering experience whenever needed. Limited information for special cases is available from Kamikubo et al.[119], Hayakawa et al.[102] and Hashida et al.[101].

Wave overtopping volumes are many times greater than spray water volumes and are usually expressed as mean overtopping rate. Wave overtopping will affect the design of the seawall depending on which amount of overtopping is acceptable. Since seawall constructions may differ considerably from one to another, it is not very easy to provide generic prediction formulae for wave overtopping discharges over those walls. However, empirical formulae have been provided in the UK by Besley[22], diagrams of overtopping rates of seawalls of vertical face and armour mound types have been suggested by Goda[88] pp. 170-174, and the European Union research project CLASH has used neural networks, see Van der Meer et al.[249]. A large variety of information from different scales is available for overtopping over seawalls, most of them considering simple or composite (vertical) walls, see e.g. Bruce et al.[29] and Hedges and Shareef[103], or special case situations, see Kamikubo et al.[119], Besley[22] and Thomas and Hall[124].

Oblique wave attack has been considered in a limited number of publications regarding vertical and seawall constructions, see e.g. Napp et al.[159], Daemrich and Mathias[56] and Thomas and Hall[224], suggesting a decrease in wave overtopping with increasing obliquity. Generic prediction formulae for different types of seawall are however not yet available so that hydraulic model tests still need to be performed when needed. Note that for vertical walls Mach stem waves may increase overtopping at appropriate angles of wave attack.

F.2.6 Wave-induced forces

Depending on the type of seawall, the crest and/or the wall may be exposed to wave-induced forces acting horizontally and vertically, which can endanger the stability of the seawall. The distinction between breaking and non-breaking waves is therefore essential and needs to be considered during design of the seawalls. Formulae predicting the breaker type are however only available for simple seawall constructions and vertical walls with and without berm, see Allsop and Kortenhaus[3] or Besley[22]. Wherever the situation is unclear, hydraulic model tests must be performed to determine the breaker type.

For the most simple types of seawall, comprising vertical walls with and without berms, formulae are available mostly based upon hydraulic model tests in USACE[235], ASCE[14], Allsop and Kortenhaus[3], Kortenhaus et al.[125] and Goda[88]. More complex shapes of seawall require hydraulic model tests although a couple of loading investigations have already been performed for special geometries (see e.g. Kamikubo et al.[119] and Schüttrumpf et al.[193]). Oblique wave attack and its effect on wave-induced forces has only been investigated for vertical walls (see Allsop and Kortenhaus[3]). When highly dynamic impact loads are measured in the flume, the problem of scale effect may appear. Initial guidance on how to scale impact loads are given in Oumeraci et al.[169].

F.2.7 Local scour and scour protection

Assessment of local scour should preferably be based on experience. If lacking, then validated semi-empirical formulae or sediment transport theory can be used. Useful guidelines on scour and scour protection may be found in US Army Corps of Engineers Coastal Engineering Manual[235], Whitehouse[268], Sumer and Fredsøe[213], OCDI[163].

Annex G
(informative)

Wave and current actions on cylindrical members and isolated structures

G.1 Current action

The action of a steady current on a single structural element may be determined by use of the following drag force equation:

$$F_D = 0{,}5\rho_w C_{Ds} D l U^2 \tag{G.1}$$

where

ρ_w is the mass density of the water;

C_{Ds} is the drag coefficient for steady flow;

D is the characteristic diameter of the structural member;

l is the characteristic length of the structural member;

U is the current velocity.

For circular members the drag coefficient is a function of the Reynolds number, Re (= UD/ν, where ν is the kinematic viscosity) and the roughness of the cylinder. Steady current drag coefficients at post-critical Reynolds numbers, e.g. $Re > 0{,}5 \times 10^6$, for circular cylinders, are shown in Figure G.1 for "hard" roughness elements. Very frequently, real structures are in the post-critical range for the design current and wave conditions. The parameter e is equal to k/D, where k is the roughness element height. See Figures G.1 and G.2. Note that in case of heavy marine growth the nominal diameter should be increased from D_c to D.

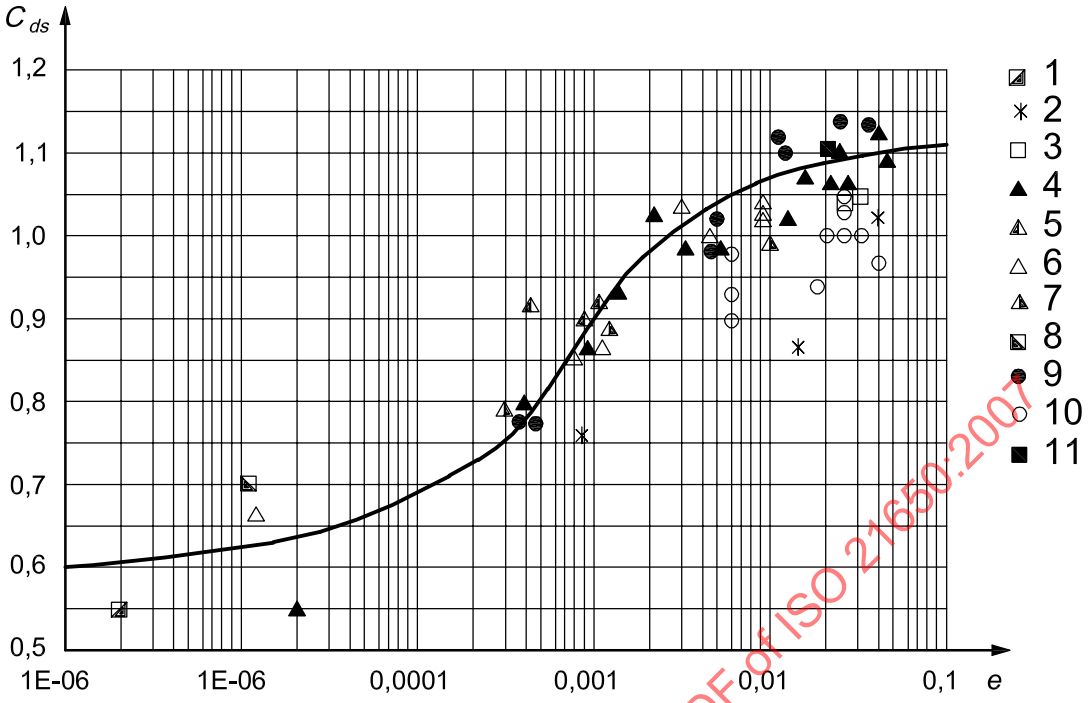

Key

1	Jones (1989)	7	Want (1988)
2	Blumberg (1961)	8	Roshco (1961)
3	Wolfram (1985)	9	Norton (1983)
4	Miller (1976)	10	Nath (1987)
5	Szecheny (1976)	11	Rodenbusch (1983)
6	Achenbach (1971, 1981)		

Figure G.1 — Dependence of steady flow drag coefficient for circular cylinders on relative surface roughness (See ISO 19902[115])

Natural marine growth on piles and platforms will generally have $e = k/D > 10^{-3}$. Thus in the absence of better information on the expected value of surface roughness and its variation with depth for a particular site, it is reasonable to assume C_{Ds} = 1,0 to 1,1 for all elements below high tide level. In order to estimate D, one still needs to estimate the thickness of marine growth that will ultimately accumulate.

All the data in Figure G.1 are for cylinders that are densely covered with surface roughness elements. Load measurements, Madsen[143], Schlichting[190], show that there is little degradation of the effectiveness of surface roughness for surface coverage as sparse as 10 %, but roughness effects are negligible for surface coverage less than 3 %.

The effect of soft, flexible growth on C_{Ds} is poorly understood. Tests indicate that:

a) soft, fuzzy growth has little effect, C_{Ds} being determined predominantly by the underlaying hard growth;

b) anemones and kelp produce drag coefficients similar to those for hard growth.

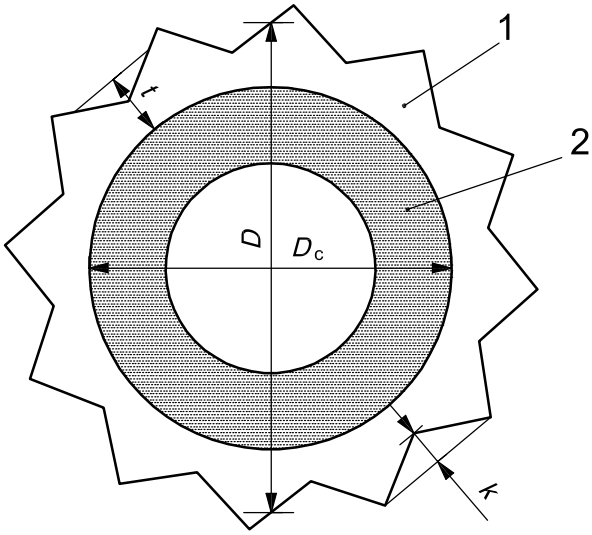

Key

1 hard growth
2 pipe
$e = k/D$
$D = D_c + 2t$

Figure G.2 — Definition of surface roughness height and thickness (See [115])

For sharp-edged elements the drag coefficients are independent of the Reynolds number, depending only on the form of the element. For such elements C_{Ds} may be assumed to be independent of surface roughness.

Hoerner[104], Zdravkovich[271], DNV[65] give current drag coefficients for a number of bodies of different shapes and orientations, different roughness, different Reynolds numbers, etc.

Reed et al.[182] give C_D values for single cylinders as well as for groups of cylinders and for different current directions.

G.2 Wave actions

G.2.1 Wave actions on single slender bodies

When body members are relatively slender, viscous effects are important and the wave/current actions may be expressed as the sum of a drag force and an inertia force, using Morison's equation [154]. The wave actions on a length, dz, of a member is given by:

$$dF = dF_D + dF_I = 0{,}5\rho_w C_D D u|u|dz + \rho_w C_M \frac{\pi D^2}{4}\dot{u}dz \qquad \text{(G.2)}$$

See Figure G.3.

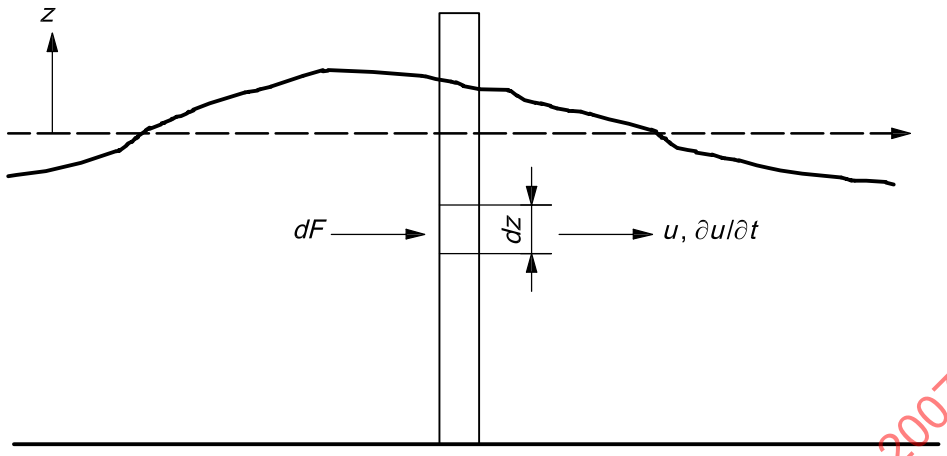

Figure G.3 — Wave actions on a cylindrical pile

where

dF is the action vector normal to the member axis;

dF_D is the drag action vector;

dF_I is the inertia action vector;

C_D is the drag coefficient;

C_M is the inertia coefficient = $1 + C_a$;

C_a is the added mass coefficient;

D is the diameter of the cylinder;

u is the local water particle velocities normal to the member axis;

$\dot{u}$ is the local water particle accelerations normal to member axis = $\partial u/\partial t$;

ρ_w is the mass density of the water;

dz is the length of the considered element.

If important, local velocity should include disturbance from neighbouring large volume elements. When the structural member moves, a modification to account for the velocity and acceleration of the member (structure) must be introduced. The wave actions are then:

$$dF = 0{,}5\rho C_D D|u - \dot{r}|(u - \dot{r})dz + \rho\frac{\pi D^2}{4}(C_M\dot{u} - C_a\ddot{r})dz \qquad \text{(G.3)}$$

where

$\dot{r}$ = $\partial r/\partial t$ velocity of member normal to its axis;

$\ddot{r}$ = $\partial^2 r/\partial t^2$ = acceleration of member normal to axis.

Eddies can be shed from a cylinder alternatively on either side, thus inducing a transversal force normal to the main direction of the water particle velocity direction. The eddies are shed at twice the frequency of the wave. Two eddies are shed when the wave crest passes and two are shed on the return flow when the wave trough passes. The lift force thus induced is expressed as follows:

$$F_L = 0{,}5\rho_w C_L D u^2_{max} \sin 2\omega t \quad \text{(G.4)}$$

where

u_{max} is the maximum water particle velocity in a wave cycle ($u = u_{max}\sin\omega t$);

ω is the radian frequency for the wave = $2\pi/T$;

C_L is the lift coefficient.

The combined effect of simultaneous drag and inertia action is obtained by vector addition.

The drag, inertia and lift coefficients have been obtained from analysis of the results of experimental work. The values of the drag and inertia coefficients depend on the Keulegan-Carpenter (KC) number, the Reynolds number and the cylinder surface roughness.

The Keulegan-Carpenter number, KC, and the Reynolds number, Re, are defined as:

$$KC = \frac{u_{max}T}{D};\ \mathrm{Re} = \frac{u_{max}D}{\upsilon}$$

where ν is the kinematic viscosity.

One of the most extensive investigations on drag, inertia and lift coefficients was carried out by Sarpkaya[186],[187]. The experiments were performed in an oscillating U-tube water tunnel for a range of Reynolds numbers up to 700 000 and Keulegan-Carpenter numbers up to 150. Relative roughness, k/D, for the cylinders varied between 0,002 and 0,02. The roughness k is the average height of the roughness elements glued to the cylinders.

Marine growth is considered to contribute mostly to the roughness of a structural element in the ocean. The cross sectional dimensions of structural elements shall be increased to account for marine growth thickness. Marine growth will depend on the location. The NORSOK standard[162] gives recommendations for marine growth thickness as shown in Table G.1. The marine growth thickness can be different in other locations.

ISO 19902[115] cautions that it takes very little roughness to make the rough value of C_D realistic. Site-specific data should be used to reliably establish the extent of the hydrodynamically rough zones. Otherwise the structural elements should be considered rough down to the sea floor.

Table G.1 — Thickness of marine growth

Water depth[a]	Altitude 56° to 59°	Altitude 59° to 72°
> + 2 m	0	0
+ 2 m to – 40 m	100 mm	60 mm
< – 40 m	50 mm	30 mm

[a] The water depth refers to mean water level NORSOK[162].

Sarpkaya carried out his tests in less than ideal conditions with rectilinear oscillating flow. For "real" waves there is still some controversy on the choice of relevant C_D and C_M values. Different standards, codes and guidelines for the offshore oil industry give different values, NORSOK[162], API[10], DNV[66], ISO 19902[115]. Moe and Gudmestad[153] and Gudmestad and Moe[98] discuss the coefficients and recommend the American Petroleum Institute's recipe on selection of coefficient values, API[10]. The following is quoted from ISO 19901-1[248]:

“For typical design situations, global hydrodynamic loading on a structure can be calculated using Morison’s equation with the following values of the hydrodynamic coefficients for unshielded circular cylinders:

smooth C_D = 0,65 C_M = 1,6

rough C_D = 1,05 C_M = 1,2

NORSOK[162] elaborate somewhat more on the issue of selecting C_D and C_M values and the following is quoted from NORSOK, which again adhere mainly to API[10] for slender tubular structural elements:

“For structures with small motions, the wave action can be calculated as follows:

a) If the Keulegan-Carpenter number (KC) is less than 2 for a structural element, the action may be found by potential theory:

   1) If the ratio between the wave length L and the tubular diameter D is greater than 5, the inertia term in the Morison formula can be used with C_M = 2,0.

   2) If the ratio between L and D is smaller than 5, the diffractions theory should be used.

b) If KC is greater than 2, the wave action can be calculated by means of the Morison formula, with C_D and C_M given as functions of the Reynolds number, Re, and the Keulegan-Carpenter number KC and relative roughness.

   It should be noted that the Morison formula ignores lift forces, slamming forces and axial Froude-Krylov forces.

c) For surface piercing framed structures consisting of tubular slender members (e.g. conventional jackets) extreme hydrodynamic actions on unshielded circular cylinders are calculated by the Morison formula on the basis of:

   — Stokes' 5th order or stream function wave kinematics and a kinematics spreading factor on the wave water particle velocity, which is 0,95 for North Sea conditions. This kinematics spreading factor is introduced in the regular wave approach to account for wave spreading and irregularity in real sea states;

   — drag and inertia coefficients equal to

      — C_D = 0,65 and C_M = 1,6 for smooth members,

      — C_D = 1,05 and C_M = 1,2 for rough members.

These values are applicable for

$u_{max} T_i / D > 3$

where

u_{max} is the maximum horizontal particle velocity at storm mean water level under the wave crest;

T_i is the intrinsic wave period;

D is the leg diameter at the storm mean level.

d) For (dynamic) spectral or time domain analysis of surface piercing framed structures in random Gaussian waves and use of modified Airy (Wheeler) kinematics with no account of kinematics factor, the hydrodynamic coefficients should in the absence of more detailed documentation be taken to be:

C_D = 1,0 and C_M = 2,0

These values apply both in stochastic analysis of extreme and fatigue action effects."

If time domain analysis is carried out with non-symmetry of wave surface elevation properly accounted for, the hydrodynamic coefficients in item c) could be applied.

Taken into account that the codes for offshore oil industry structures are calibrated, which is not the case for structures in shallow water and in the coastal zone, it is recommended to apply the Stokes' 5th order wave theory. For structures in these areas, other approaches are the Fenton method, which is very user friendly, (Rienecker and Fenton[185]), the Stream function method (Dean[61]) or some other high order theory, together with C_D = 1,4 (Kriebel et al.[129]) and C_M = 2,0. For square formed piles ASCE 7-02[14] recommends a C_D value which is approximately 30 % higher than for the circular pile. Note that possible wave slamming actions should be considered.

It should be noted that the wave kinematics have been much more thoroughly explored by measurements for intermediate and deep water irregular waves than for shallow water irregular waves.

All wave theories predict that the maximum water particle velocities are at maximum at the crest height. The Morison equation thus also predicts that the maximum wave force also occurs at the crest height. Dean et al.[63] and Tørum[227] found a slight modification to this due to surface effects.

G.2.2 Wave action on clusters of circular cylinders

Reed et al.[182] give drag coefficients for single cylinder and a cluster of cylinders in a unidirectional back and forth motion and with different orientations. Reed et al. also performed tests with a current superimposed on the waves.

Chakrabarti[49] gives information on the maximum wave forces on cylinders in a single row for different cylinder spacing and different wave direction and different KC numbers.

ISO 19902[115] gives additional information on conductor shielding factors.

G.2.3 Wave action on large-volume bodies

Wave action on large-volume bodies should be calculated on the basis of wave diffraction theory. The incoming waves are reflected and scattered and the wave potential is expressed as the sum of the potential of the incoming waves and those of the reflected scattered waves.

For simple structural shapes like a vertical circular cylinder resting on the sea bottom, the MacCamy and Fuchs[144] analytical solution may be applied. This solution shows that there will be a phase angle between the maximum force and the wave as the wave passes the cylinder. This phase angle is dependant on the D:L ratio. Comparing the MacCamy and Fuchs analytical solution to the general formulae for the inertia force, dF_h on a unit length of the cylinder,

$$dF_h(z) = \rho_w C_M \times \frac{\pi D^2}{4} \times \frac{\partial u(z)}{\partial t} \tag{G.5}$$

where $\partial u/\partial t$ is calculated at the centre of the cylinder, C_M and phase angles are shown in Figure G.4. (according to Dean and Dalrymple[64]).

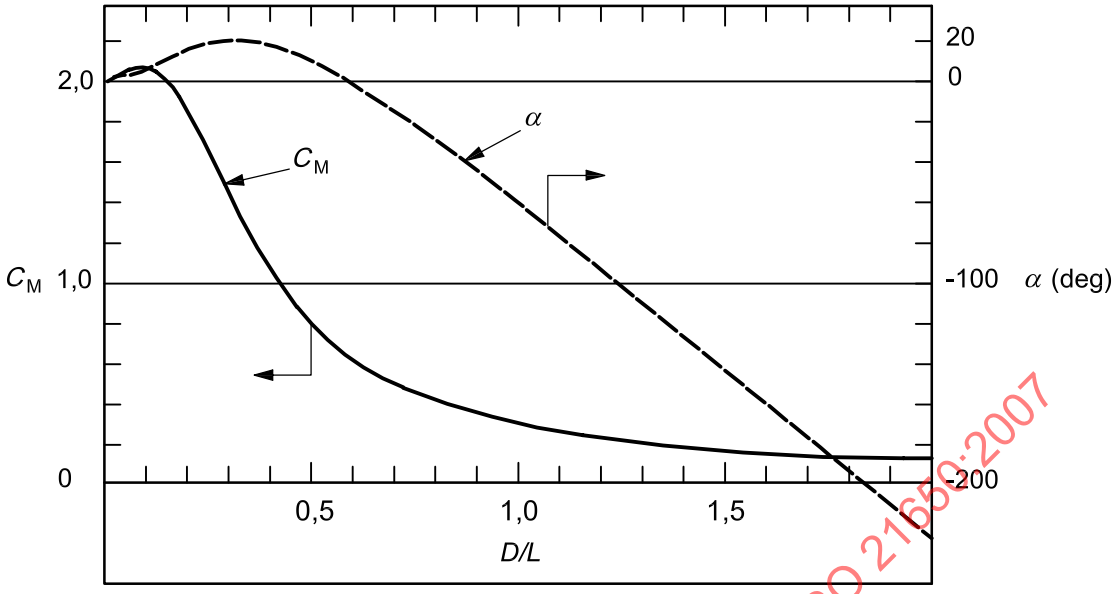

Figure G.4 — Variation of inertia coefficient C_M and phase angle α of maximum force with parameter D/L

For general structures consisting of several large-volume components, boundary element or finite element methods should be used, e.g. Isaacson and Sarpkaya[112], Faltinsen[73].

The MacCamy and Fuchs solution and some computer programs based on boundary element methods are based on linear wave theory. However, in the vicinity of large bodies, the free surface elevations can be increased due to motion, diffraction, radiation, wave/current interaction effects, and other non-linear wave effects, e.g. shallow water effects. These should be accounted for in the wave actions calculation and used to estimate deck clearance and freeboard.

Gjøsund et al.[83], carried out tests on wave forces for a 100 m diameter circular cylinder in 25 m water depth and for waves with periods in the range 7,7 s to 27,3 s and wave heights in the range 4,8 m to 17 m. They also considered the set-down effect due to the influence of radiation stress. The waves with longer periods and greater heights were highly non-linear with regard to water surface elevations. The comparison with the MacCamy and Fuch's theoretical results showed a fair agreement for the horizontal force, especially when the set-down effect was included. The overturning moment was significantly underestimated by MacCamy and Fuch's theory.

G.2.4 Slamming actions

G.2.4.1 General

For a structure in waves, the parts of the structure in the splash zone are susceptible to forces caused by slamming when the member is being submerged in the waves or when the structure is hit by plunging breaking waves.

For circular cylindrical members the slamming actions may normally be calculated as:

$$dF_S = 0{,}5\rho_W C_S D V_R^2 dl \qquad \text{(G.6)}$$

where

dF_s is the slamming force in the direction of the velocity;

ρ_w is the mass density of water;

C_s is the slamming force coefficient;

D is the member diameter;

V_R is the relative velocity of water surface to the surface of the member;

dl is the length of the circular cylinder element.

For 2D circular cylinders the first, simple theoretical approach by von Karman (1929) leads to a C_s value of π. Later theoretical work, e.g. Wagner[259], Puchanov and Korobkin[181], Armand and Cointe[6], Faltinsen[73], Wienke and Oumeraci[266] lead to $C_s = 2\pi$. This value is also to some extent confirmed by experiments. 3D effects will lead to smaller C_s values than obtained from 2D considerations, but the reduction factor is not exactly known.

The Goda approach [84], leads to time duration of the wave slamming actions of $\tau = 0{,}5D/v_r$, while Wienke and Oumeraci[266] theoretically found the duration time to be $\tau = 0{,}20D/v_r$, see Figure G.5. This is close to what Tanimoto et al.[219]) found experimentally. The slamming force versus time, $(f_1/\rho RV^2)$ versus t, where R is the cylinder radius, for different theories and approaches are also shown in Figure G.5. In which "own model" is by Wienke and Oumeraci.

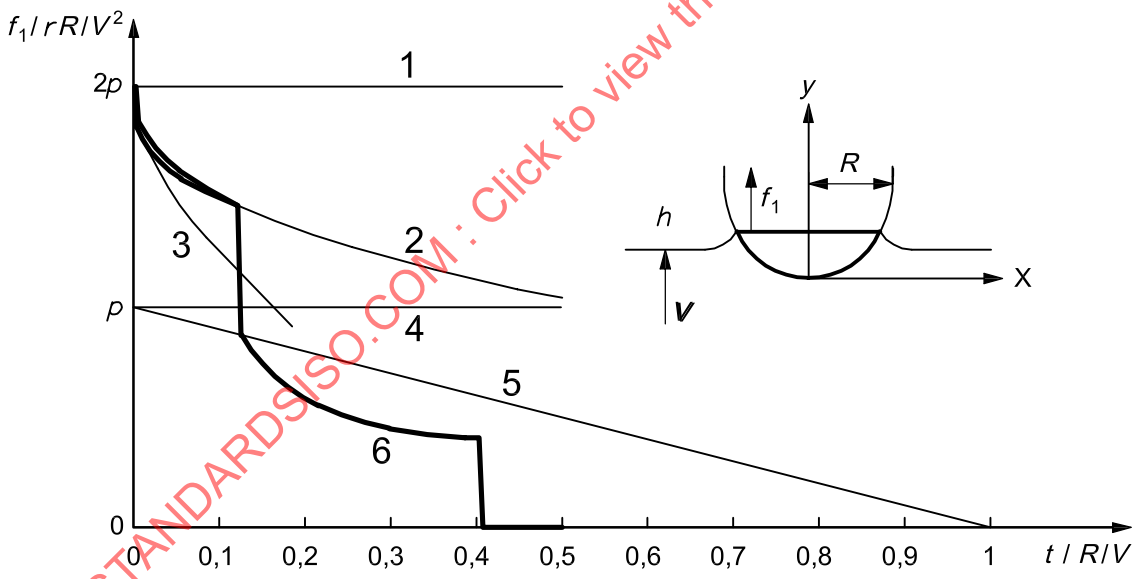

Key

1	Wagner	4	von Kaman
2	Cointe	5	Goda
3	Fabula	6	own model

Figure G.5 — Slamming coefficients and slam time histories according to different theories

G.2.4.2 Slamming action on vertical and inclined cylinders on uniformly sloping or horizontal bottoms

For vertical or nearly vertical piles exposed to plunging breaking waves, slamming action occurs in a limited region from the wave crest and downward as indicated in Figure G.6. The total wave force on the pile is

$$F = F_D + F_I + F_S \tag{G.7}$$

where $F_D + F_I$ are the Morison force and F_S is the slamming force.

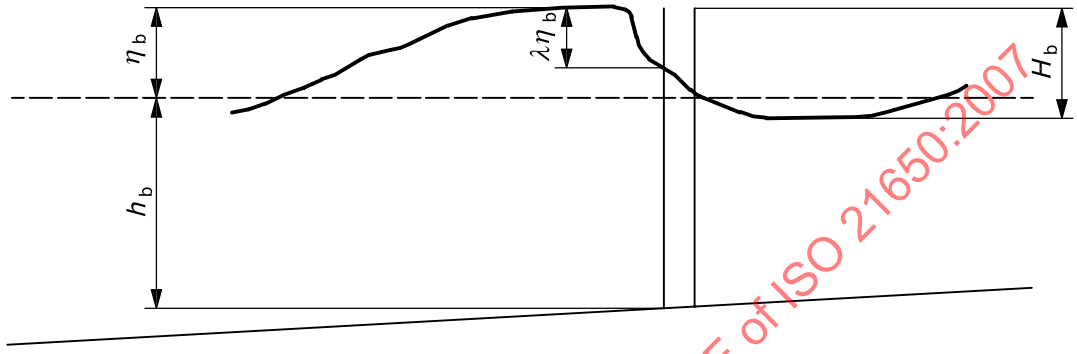

Figure G.6 — Sketch of a plunging wave hitting a vertical pile

Goda et al.[84] measured the total slamming force on a vertical pile. They introduced the term "curling factor" λ and assumed that the slamming force intensity was uniformly distributed over the height $\lambda\eta_b$ where η_b is the wave crest elevation. The total slamming force was then obtained as:

$$F_I = 0{,}5\rho_w C_S D C_b{}^2 \lambda\eta_b \tag{G.8}$$

where

C_b is the wave celerity at the breaking point;

C_s is assumed to be $C_s = \pi$ (von Karman theory).

Goda et al. arrived at a curling factor of $\lambda = 0{,}5$ for plunging breakers and $\lambda = 0{,}1$ for spilling breakers.

Sawaragi and Nochino[188] measured the slamming forces from breaking waves along a vertical cylinder. They found a considerable scatter in the forces and larger forces than those obtained by Goda et al. The maximum curling factor they obtained was 0,9 with $C_s = \pi$, which complies with the findings of Wienke and Oumeraci[266] (maximum curling factor is approximately 0,45 with $C_s = 2\pi$). Sawaragi and Nochino found that the slamming force intensity distribution along the pile had a triangular form and not a uniform form, while Wienke and Oumeraci inferred from their wave pressure measurements on their test cylinder that the slamming force intensity was uniformly distributed.

Tanimoto et al.[219] investigated the slamming force along a pile with different inclinations and with detailed measurements of the slamming force intensity along the pile. They also found that the slamming force intensity distribution along the pile had triangular form, and the maximum measured forces were comparable to the forces obtained by Goda et al.[84]. Apelt and Pierowiez[9] obtained total breaking wave forces and overturning moments on a vertical cylinder on a sloping bottom as a function of D/H_o and H_o/L_o, where D is cylinder diameter, H_o is deep water wave height and L_o is deep water wave length.

Oumeraci et al.[170],[171], Wienke[264] and Wienke and Oumeraci[266] analysed their large scale laboratory flume test results according to the Goda approach, i.e. they analysed their measured total slamming force, but used a slamming coefficient $C_s = 2\pi$ and a force-time history as given in Figure G.5 when calculating the curling factor λ. The breaking waves during Wienke and Oumeraci's tests were generated by superimposition of several waves with different frequencies or so-called Gaussian wave packets. Wienke and Oumeraci subdivided the experiments into five different loading cases. From their measurements Wienke and Oumeraci found that impact occurs almost simultaneously at the different levels of the front line (violent spreading). They obtained curling factors λ as shown in Figure G.7 for loading case 3, which was the case that gave the largest slamming force. For vertical cylinders, $\alpha = 0$, Equation (G.8) may be used to estimate the total wave slamming force. Wienke and Oumeraci also present a method of obtaining the total wave slamming forces on an inclined cylinder, taking the angle of inclination into account.

For a vertical cylinder Wienke et al. obtained a maximum curling factor of 0,46 with a slamming force coefficient of $C_s = 2\pi$, which leads to a force twice the force obtained by Goda et al. and by Tanimoto et al., but the same as Sawaragi and Nochino obtained as the maximum slamming force. Since short duration forces are tricky to measure, a possible explanation for the discrepancies may be because of the different force and pressure measuring method and the analysis methods used.

Ircschik et al.[111] carried out similar tests as Wienke and Oumeraci with a foreshore 1:10 in front of the pile. The results on the force measurements have not been examined and published yet.

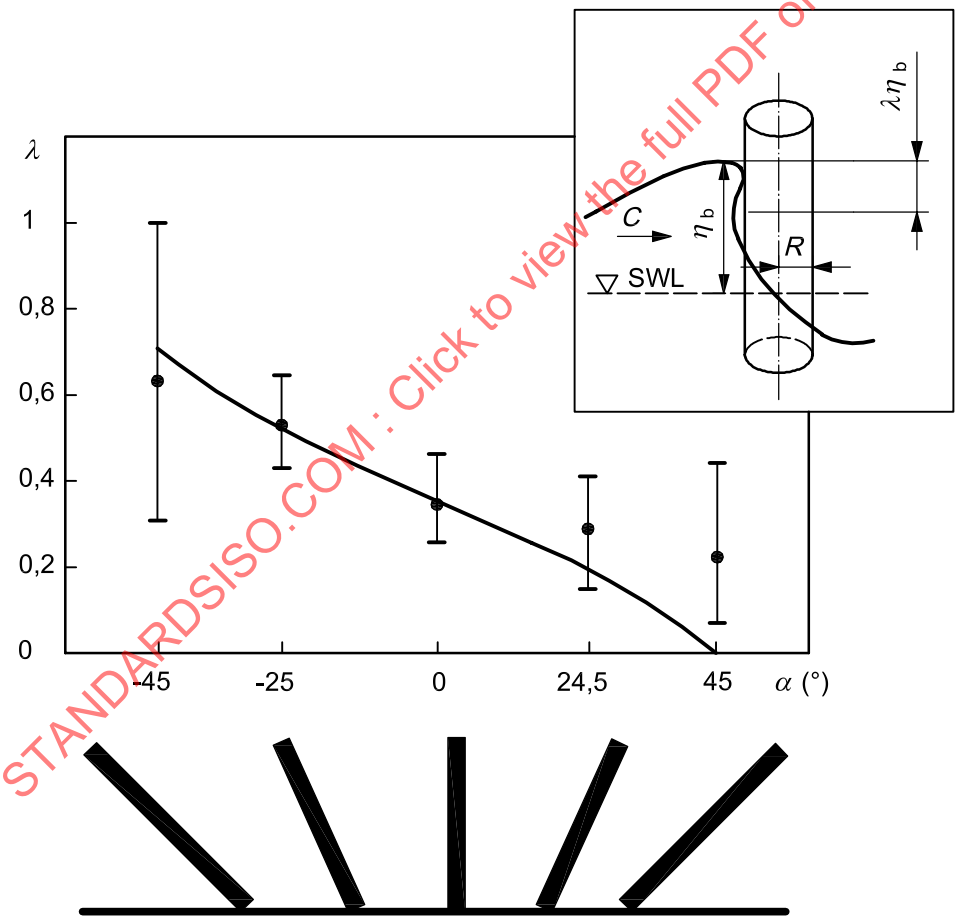

Key

a Still water level.

Figure G.7 — Curling factor λ for loading case 3

G.2.4.3 Wave action, including slamming action, on vertical cylinders on reefs and shoals

Special attention should be given to vertical structures erected upon reefs subjected to breaking waves. See Figure G.8, Goda[85], Hovden and Tørum[105], Kyte and Tørum[134], Hanssen and Tørum[100]. The height of breaking waves over shoals, Lie and Tørum (1991), and the wave kinematics (Goda; Hanssen and Tørum), differs considerably from the uniformly sloping bottom. No numerical wave programme on the wave heights and wave kinematics is yet available to cover the breaking wave conditions on peaky shoals. Hence the general results from laboratory wave flume investigations should be used with care and not for conditions deviating too much from the shoal configurations used during the laboratory tests. However, the obtained results can be useful for conceptual designs. For important structures, it will be necessary to carry out site-specific hydraulic model tests.

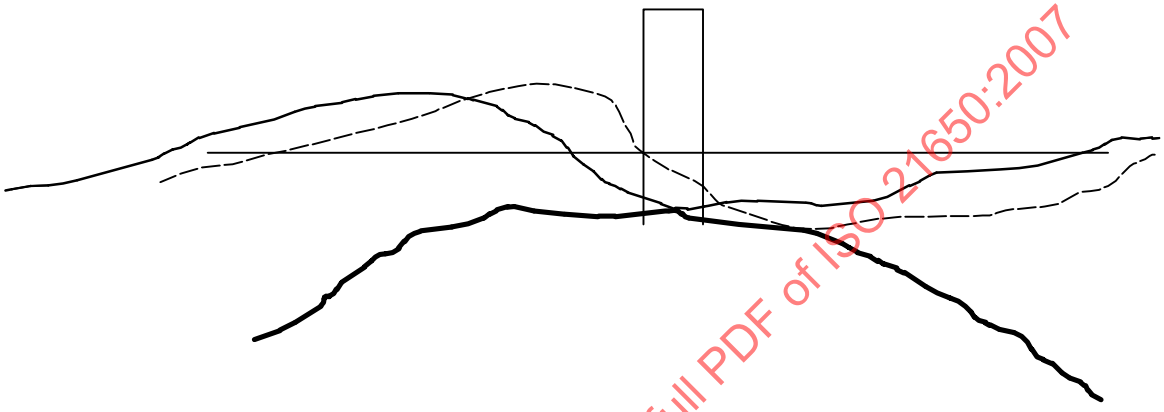

Figure G.8 — Waves over shoals

Goda[85] investigated the wave forces on vertical circular cylinders on cylindrical and ledged reefs. The short duration slamming actions were of no concern for the structures Goda considered and the slamming forces are not included in his results. Goda also gives results on the wave crest elevations.

Kyte and Tørum[134] carried out tests on a cylinder on a site-specific shoal, but which was almost circular and rather peaky, i.e. the water depth increased rapidly in front of the cylinder. The water depth over the shoal was kept constant during the tests. The slamming actions were also measured. Kyte and Tørum derived equations almost similar to those derived by Goda, but the force coefficients Kyte and Tørum arrived at was larger than those obtained by Goda. This difference is mainly attributed to 1) differences in wave force measuring systems; i.e. Goda did not, on purpose, pick up the high intensity, short duration slamming force, and 2) the topography of the shoals differs. This indicates again that local effects may be significant and that site-specific tests should be carried out for important structures. An example of such tests is the tests that Hansen and Tørum[100] carried out for a tripod on a shoal.

G.2.5 Wave action on piers and platform decks

Many types of wave loads should be considered in the design of piers. See Figure G.9.

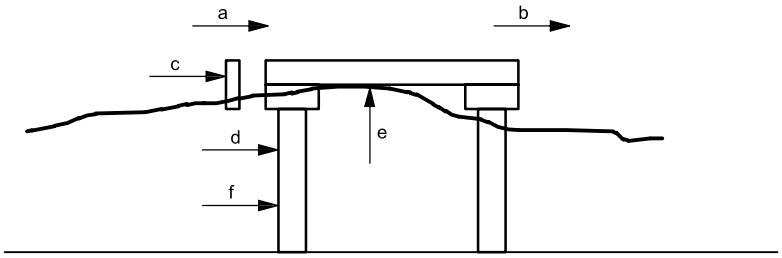

Key

a Overtopping.
b Overall drag.
c Structure slam.
d Pile slam.
e Uplift slam.
f Pulsating pile load.

Figure G.9 — Wave loads on piers

The main types of action to be considered are:

— wave action on pile (as described in previous clauses);

— horizontal wave action on beams, fenders or other projecting elements;

— wave uplift action on decks;

— wave uplift action on beams, fenders or other projecting elements;

— wave downward action on decks (inundation and suction).

These forces, with the exception of pile loading, are called “wave-in-deck forces”.

There have been several investigations on wave action, including wave slamming actions on the underside of smooth horizontal platforms, e.g. El Ghamry[72], French[74], Shih and Anastasiou[195], Baarholm[15], Ren and Wang[183],[184].

Shih and Anastasiou derived very simple empirical formulae for wave uplift pressures on horizontal platforms.

Kaplan[120], Kaplan et al.[121] and Murray et al.[155] developed a set of equations to calculate the wave actions on almost any form of the platform. According to HSE[109], Kaplan’s approach is state-of-the-art in predicting impact loads on platform decks.

OCDI[163] provides an estimated order of magnitude of slamming force on the underside of a horizontal platform deck, expressed as an equivalent static load with uniform upward pressure of $2\rho_{ws}gH$ for progressive waves and $4\rho_{ws}gH$ for standing waves (in case of open-type wharf with a retaining wall behind), where ρ_w is the mass density of water, g acceleration due to gravity and H the wave height.

Stansberg et al.[210] give results from a study on deck wave impacts on a gravity base structure at a depth of 150 m water.

Most of the referenced recent research on wave forces on platform decks is related to oil platform decks. However, Tirindelli et al.[225], McConnell et al.[145], Tirindelli et al.[226] and Cuomo et al.[54] give preliminary results from a research project related to exposed jetties at HR Wallingford, UK, while, based on this research, McConnell et al.[146] give guidelines for loadings on piers, jetties and related structures.

G.2.6 Dynamic amplification and vibrations

Slamming actions are characterized by high peak intensity and a very short duration. Depending on the elasticity and damping characteristics of a structure subject to slamming action, the effect of slamming action depends on the dynamic response of the structure and its foundation, which may amplify or dampen the peak force. Thus a structure should be investigated for the dynamic response to slamming action.

Slamming action may also cause vibrations in the structure. Some light beacons for navigation aids can be vulnerable to such vibrations.

G.2.7 Wave and current actions on pipelines

Wave and current actions on pipelines are most extensively dealt with by the oil industry and are treated in different standards and guidelines, i.e. DNV[67],[68].

Wave and current actions on pipelines on or close to the bottom, Figure G.10, are calculated with a Morison equation approach.

The horizontal action on a pipe length dl is given by:

$$dF_{\mathrm{h}} = 0{,}5\rho_{\mathrm{w}} C_{\mathrm{D}} D u|u| \sin\alpha\, dl + \rho_{\mathrm{w}} C_{\mathrm{M}} \frac{\pi D^2}{4} \frac{\partial u}{\partial t} \sin\alpha\, dl \qquad \text{(G.11)}$$

and the lift actions are given by:

$$dF_{\mathrm{v}} = 0{,}5\rho_{\mathrm{w}} C_{\mathrm{L}} D u^2 \sin\alpha\, dl \qquad \text{(G.12)}$$

where α is the angle between the wave direction and the pipeline axis.

The model given by Equations (G.11) and (G.12) predicts that vertical action is in phase with the water particle velocities. But measurements show that the vertical action is ahead of the undisturbed water particle velocities above the pipeline. More refined methods have been developed to obtain the horizontal and vertical action that more accurately predicts the phases; see Lambrakos et al.[137], Verley et al.[252]. However, these methods are cumbersome to use and are not employed unless it is very critical for pipeline stability considerations.

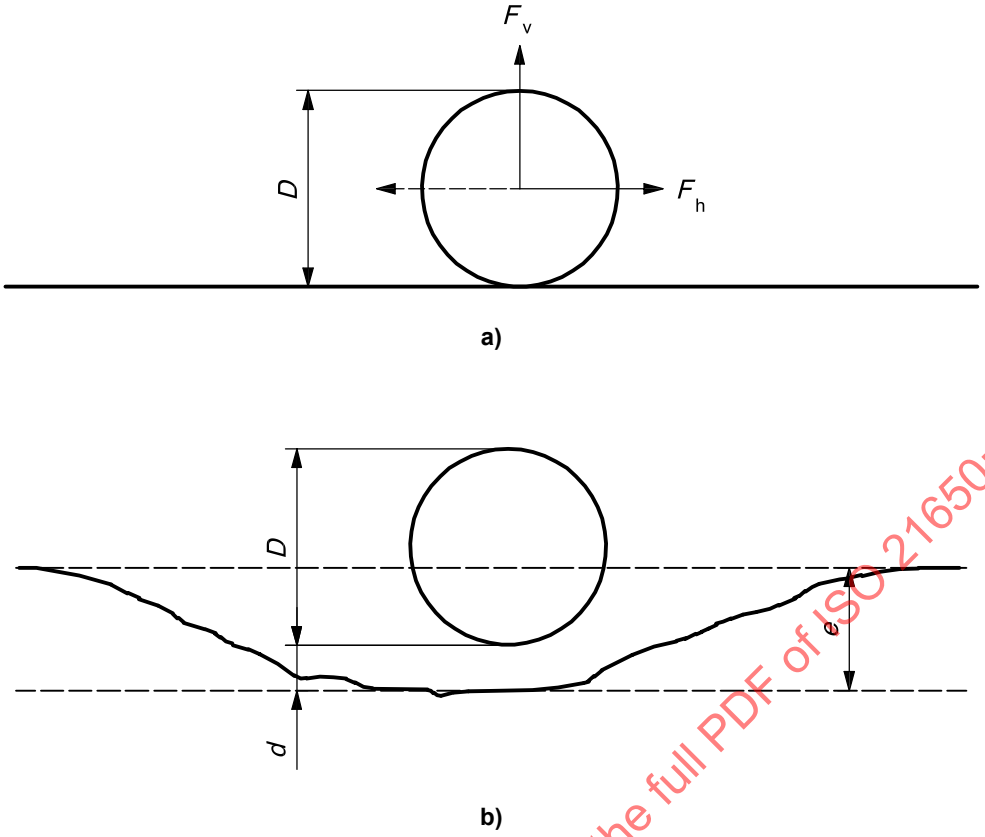

Figure G.10 — Pipeline on a) the sea bottom or b) in a trench

The drag, inertia and lift coefficients C_D, C_M and C_L are dependent on the Reynolds number, the Keulegan-Carpenter number, the gap to diameter ratio, $e{:}D$, the ratio α between the current velocity and the wave water particle velocities, and the pipe roughness.

DNV[68] gives a detailed recommendation of the C_D and C_M coefficients depending on the ratio between the current velocity and the wave particle velocity amplitude, the seabed proximity, pipe roughness, the pipe in trench and cross-flow vibrations.

There are no values given in DNV for the lift coefficient C_L. Sumer and Fredsøe[212] give values of C_L as a function of seabed proximity, pipe roughness and Keulegan-Carpenter number.

G.2.8 Vortex induced vibration (VIV) of pipelines

Water or any fluid past a slender member can cause unsteady flow patterns due to vortex shedding. At certain critical flow velocities the vortex-shedding frequency may coincide with, or be a multiple of, the natural frequency of motion of the member, resulting in harmonic or sub-harmonic excitations, either in line with the flow or with the cross flow.

These effects may be investigated by using semi-empirical methods based on model tests and full scale data. The other alternative is to use computational fluid dynamics (CDF) methods by direct numerical solution of the fluid/structure interactions problem.

The vortex shedding frequency may be calculated as follows:

$$f = St\frac{V}{D} \tag{G.13}$$

where

f is the vortex shedding frequency;

St is the Strouhal number;

V is the flow velocity normal to the slender member axis;

D is the diameter of the member.

For circular cylinders the Strouhal number, St, is a function of the Reynolds number, Re. In a wide range of Reynolds numbers the Strouhal number is $St \approx 0{,}2$.

For determination of the velocity ranges where vortex induced vibration (VIV) can occur, a parameter V_r, called the reduced velocity is used. V_r is defined as:

$$V_r = \frac{V \cos\varphi}{f_{iD} D} \tag{G.14}$$

where

V is the flow velocity;

f_{iD} is the natural frequency of vibration of the structural member;

D is the diameter of the member;

φ is the angle between the current direction and the pipeline axis.

Another parameter controlling the motions is the stability parameter, K_s, defined as

$$K_s = \frac{2 m_e \delta}{\rho D^2} \tag{G.15}$$

where

m_e is the effective virtual mass;

δ is the generalized logarithmic decrement ($2\pi\xi$) of damping defined by, $\delta = \delta_s + \delta_{soil} + \delta_h$;

in which

δ_s is the logarithmic decrement of structural damping;

δ_{soil} is the logarithmic decrement of soils damping or other damping;

δ_h is the generalized logarithmic decrement of hydrodynamic damping.

The amplitude of vibration ratio, $A{:}D$, where A is the vibration amplitude, is primarily a function of the reduced velocity. For reduced velocities in the range V_r = 2 to 4 in-line vibration occurs, while for V_r = 4 to 12, cross-flow oscillation occurs. The maximum amplitude of cross-flow oscillation is approximately one pipe diameter, while the maximum amplitude of in-line oscillation is approximately 0,15 pipe diameter.

DNV[68] give vortex-induced pipeline vibration amplitudes for in-line as well as for cross-flow oscillations. The oscillation amplitudes are given as functions of the reduced velocity, stability parameter, flow angle, turbulence intensity and trench proximity.

G.3 Local scour and scour protection

Assessment of local scour should preferably be based on experience. If lacking, then validated semi-empirical formulae or sediment transport theory can be used. Useful guidelines on scour and scour protection may be found in US Army Corps of Engineers Coastal Engineering Manual[235], Whitehouse[268], Sumer and Fredsøe[213], OCDI[163].

Annex H
(informative)

Wave interaction with floating breakwaters

H.1 Introduction

The wave height reducing effect of a floating breakwater is to a large extent governed by the ratio breakwater width:wave length. Thus the floating breakwater concept easily becomes uneconomical for coasts exposed to ocean waves. But floating breakwaters can be economically used for marinas etc in areas with limited fetch lengths and large depths. Floating breakwaters have also successfully been used on open coast to protect fish farms. They will let the longer period waves pass through, but reduce the heights of the shorter period waves that can be devastating to the fish farm cages.

A large variety of floating breakwater concepts has been presented. PIANC[174] gives an overview of different types. probably the most frequently used is the box type floating breakwater, an example of which is shown in Figure H.1.

Dimensions in metres

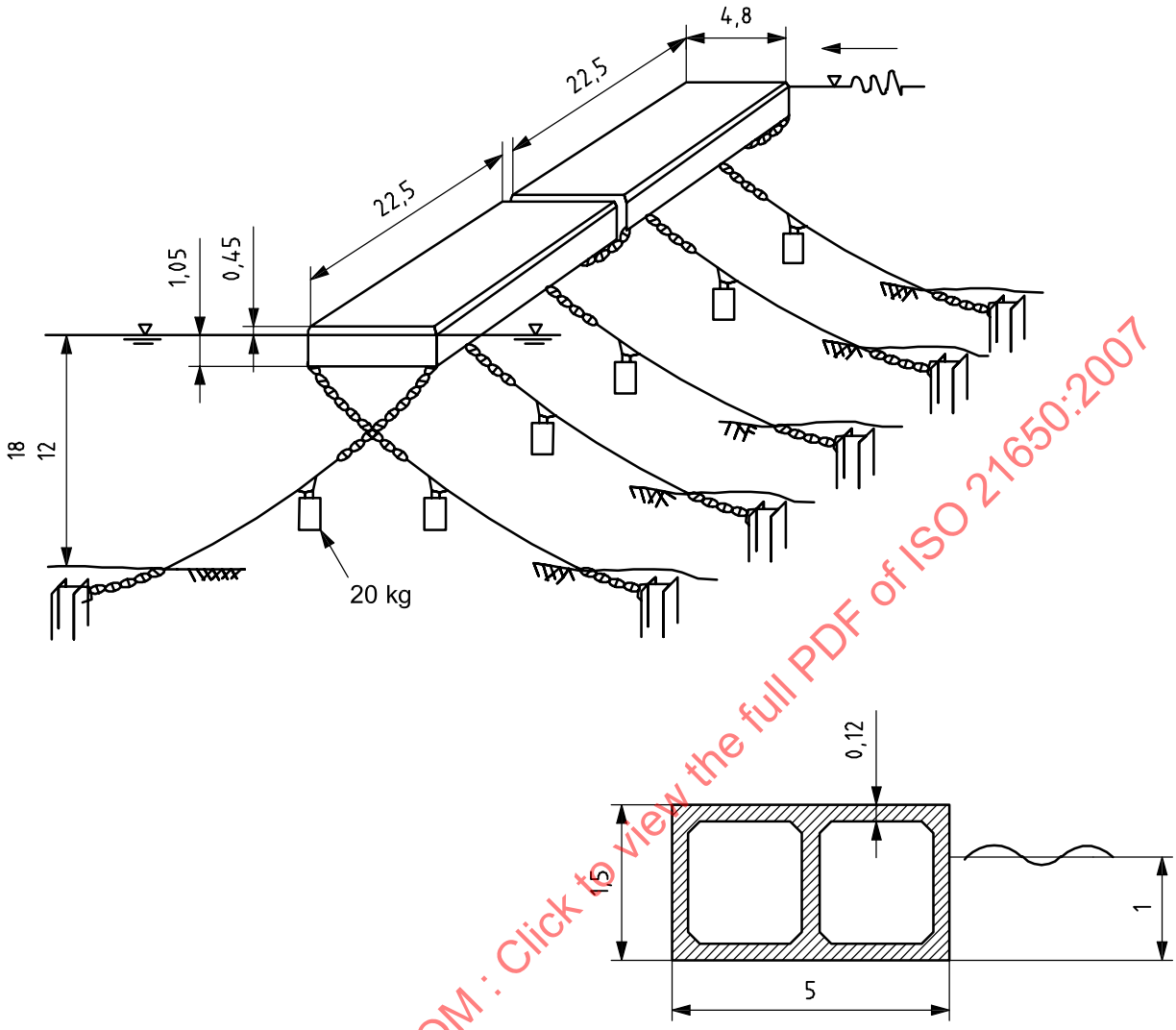

Key

a Still water level.

NOTE Not to scale.

Figure H.1 — Box type floating breakwater

Araki and Chujo[11] and Yoshida and Isozaki[270] show an example of a floating breakwater to protect fish farm cages. It dampens the shorter period waves while the longer period waves of the wave spectrum are not damped. This floating breakwater is 450 m long and is located in 65 m of water. The breakwater has experienced at least 11 m high waves; see PIANC[174].

H.2 Wave-reducing effects of floating breakwaters

H.2.1 General

When waves meet a floating breakwater they will basically be partly transmitted under the breakwater and partly be reflected from the breakwater. Some of the wave energy is lost due to turbulence and friction, depending on the breakwater type.

The wave transmission coefficient for a floating breakwater is defined as:

$$C_T = \frac{H_t}{H_i} \tag{H.1}$$

and the wave reflection coefficient as

$$C_R = \frac{H_R}{H_i} \tag{H.2}$$

where

H_i is the height of the incoming wave;

H_t is the height of the transmitted wave;

H_r is the height of the reflected wave.

In case of irregular waves the significant wave height is commonly used as the wave height parameter.

The transmission coefficient is dependent on many parameters, but, as mentioned, the most significant parameters for box type floating breakwaters are the width:wave length ratio and the draft:wave length ratio. To give an idea of the wave attenuation characteristics, a breakwater with seven units similar to the ones shown in Figure H.1 will attenuate waves with a peak period of T_p = 5 s by 10 % and waves with T_p = 3 s by approximately 65 %; see Stansberg et al.[209].

H.2.2 Calculations of transmitted and reflected waves and mooring forces

A floating breakwater is a complex structure from a hydrodynamic and motion point of view. No satisfactory analytical solutions exist on the motion and wave transmission. Most operational numerical models rely on assumptions of small waves and small motions.

The assumption of small structure motions does not appear to be a major limitation, for if the breakwater should attenuate the waves effectively, its motion should be small. However, this is not the case if a floating breakwater, designed for short wave periods, is exposed to a swell coming from the open sea. In this case roll, heave and sway can become relatively important and for this special case, the adequacy of the mooring system should be checked. Also the small motion assumption cannot be applicable to the case for “resonant systems” which are designed so as to attenuate waves through destructive interference between incident and radiated waves; see Bowley[26].

Lei[138] developed a computer model that is capable of simulating the dynamic performance of a group of interconnected, moored floating structures subjected to harmonic wave action. In addition to the elasticity and damping of the mooring system and the constraints of the interconnections, linearized viscous damping, especially roll damping, was taken into account. Results from the computations and model tests confirmed the validity of the assumptions used in the modelling of the wave forces and the mooring line forces, excluding the slow drift forces and motions.

Other non-linear effects are effects from non-linear waves and non-linear damping. The latter is especially the case for large motions when viscous effects and turbulence can become more important.

In addition to the forces mentioned above, a wave drift force that is proportional to the incident wave energy flux acts on the floating breakwater and will especially influence the horizontal motion and the mooring line forces. The mooring line forces and anchor's holding capacity should be evaluated with the inclusion of the wave drift forces and the resulting breakwater motion.

Stansberg et al.[208] and Stansberg[207] deal with non-linear slow drift oscillations of moored floating structures with some reference to floating breakwaters, according to Stansberg et al.[209]. There is, as yet, no readily

available theory to handle the slow drift oscillations. The findings from the experiments of Stansberg et al.[208] are the following:

a) the slow drift oscillations are dominant with respect to mooring forces;

b) the slow drift motion is larger on a long breakwater than on a short one;

c) the low frequency drift sway motion oscillations get significantly reduced in multidirectional irregular waves compared to those in unidirectional irregular waves.

The mean offset is, however, the same.

PIANC[174] refers to results of several test programmes on wave damping by and mooring forces for different types of floating breakwater.

Annex I
(informative)

Wave action on wave screens

I.1 Types of wave screen

A definition sketch of a wave screen is given in Figure I.1. Wave screens are generally built in one of three types.

a) Single impermeable wall: consists of a single vertical wall that is impermeable, and which extends from above the still water level down to near mid-depth (or deeper) with a gap at the bottom to permit some water circulation and wave transmission. Wall panels are usually built from pre-cast concrete panels.

b) Single permeable wall: consists of a single vertical wall which is permeable, and which extends from above the still water level down to near the sea floor (gap at bottom) or to the sea floor (no gap at bottom). Wall panels are usually built from pre-cast concrete panels or from timber boards with gaps or slits between boards.

c) Multiple walls: consists of two or more parallel wall sections of either the impermeable or permeable type. The most common configuration includes a permeable wall in front with an impermeable wall at the back. Wall panels are usually built from pre-cast concrete panels.

In all types of wave screen, wall panels are then attached to a pier or pile-supported structure.

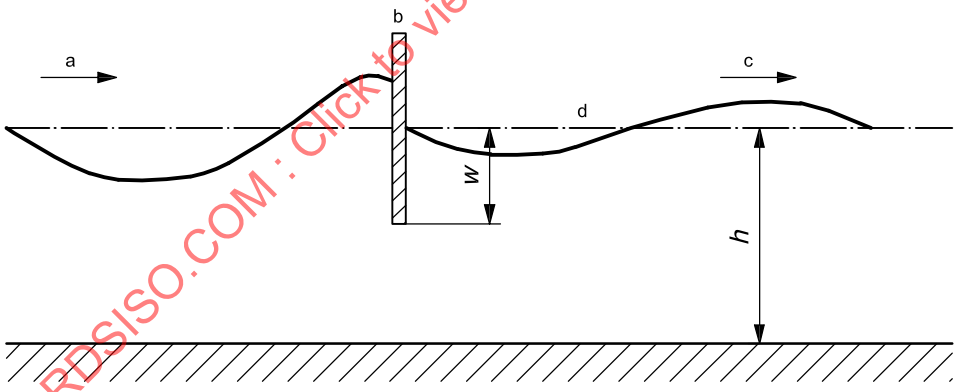

Key

a Incident wave.
b Wave barrier.
c Transmitted wave.
d Still water level.

Figure I.1 — Definition sketch for generic wave screen or wave barrier
{Coastal Engineering Manual (2003)}

I.2 Applications of wave screens

Wave screens may be used as a type of breakwater in areas of restricted fetch within bays, estuaries, harbours, lakes and other enclosed or semi-enclosed water bodies. They are not recommended in areas where impact loads due to breaking waves are expected. Typical design wave conditions include significant wave heights of one metre to two metres and peak wave periods of less than 6 s.

I.3 Functional design for wave transmission, reflection and overtopping

The function of a wave screen is to reduce wave heights transmitted into the harbour or marina while at the same time minimizing adverse effects of wave reflection from the structure. Wave screens dissipate some wave energy but designs yielding low wave transmission are usually accompanied by high wave reflection. Multiple wall designs can yield the best reduction in transmitted waves while keeping reflection to a minimum.

Incident waves, transmitted and reflected waves should be specified in terms of the wave spectrum, or may be specified in terms of the significant wave height and peak wave period. In random waves, wave screens preferentially reduce transmission of high frequency waves in the spectrum and allow more transmission of low frequency waves in the spectrum. The tolerable level of transmitted wave height within a harbour or marina depends on the usage of the water area, but transmitted waves should usually be reduced to a significant wave height of 0,3m or less.

The transmission and reflection coefficients of a wave screen are affected by many factors including the wall draught (gap at the bottom), permeability, incident wave periods (wavelength), water depth and others. Because single walls are usually thin relative to the wave length, wall thickness is not a major factor in determining wave transmission. For multiple walls, spacing between walls relative to wavelength is an important factor.

Waves will also be diffracted around the ends of a wave screen. The configurations and layout of a wave screen need to be determined by taking into consideration both the transmitted waves and the diffracted waves.

Wave screens are generally designed to prevent overtopping. Some overtopping may be allowed for waves larger than the significant height, and the adverse effects of occasional overtopping on harbour performance should be examined.

Water levels (tidal elevations) affect functional performance. As a result, wave transmission and wave loading should be checked for a complete range of expected water levels. The highest wave transmission sometimes occurs at a low tide condition.

Some design diagrams are available for typical configurations. Wave transmission past impermeable wave screens are given for regular waves by Wiegel[263] and by Kriebel and Bollmann[128], and for random waves by Gilman and Kriebel[82], Kriebel[127], and by Losada et al.[141],[142]. Wave transmission past permeable or slotted wave screens extending to the sea floor are given by Grune and Kohlhase[96], and Kriebel[126]. A method of estimating transmission past partial depth permeable wave screens is given by Isaacson et al.[113]. Wave transmission past multiple walls is difficult to generalize. Gardner et al.[81] and Cox et al.[53] present results of physical model test programmes of some typical designs, while Tillman et al.[223] present a theoretical approach. In general, hydraulic model tests are recommended for evaluating the functional performance of multiple wave screens.

Oblique incidence of waves results in some reduction in wave transmission, but it may usually be disregarded in functional design considerations unless the angle of incidence is large.

I.4 Structural design considerations

I.4.1 Waves for structural design of wave screens

Structural design of wave screens should consider the complete wave spectrum and should be based on the largest waves in a design sea state. Kriebel[127] shows that forces on impermeable wave screens due to non-breaking waves in a random sea follow a Rayleigh probability distribution. Following Goda[88], a design wave height of 1,8 H_s should be used for computing wave forces and overturning moments.

Wave screens are usually designed for non-breaking waves and are usually not used in areas where high impact loads due to breaking waves are expected. If breaking waves are expected, appropriate wave slamming or impact loads should be considered through hydraulic model tests.

Wave screens are also subject to repeated wave loadings of small to medium storm waves that have a high frequency of occurrence. A fatigue analysis of structural members should be conducted based on the joint frequency tables of wave heights and periods.

I.4.2 Wave-induced pressures, forces and moments

Structural design of wave screens should include consideration of wave-induced pressures, depth-integrated wave forces, and wave-induced overturning moments. Because wave screens have water on both sides, hydrostatic pressures are normally equal on each side of the wave screen. Wave-induced pressures on the front and rear faces of the vertical walls must be evaluated with due consideration of the wave phase on each side of the wall.

For an impermeable wave screen with a small gap at the bottom, an approximation to the wave pressure exerted on the front surface can be made by applying the modified Goda formula (Annex E). It provides an upper limit to the actual wave pressure, because it neglects a reduction of pressure caused by partial wave reflection and by the bottom gap. The maximum horizontal force is then obtained from the vertical integration of the wave-induced pressures along the height of the wall over one cycle of wave period. The maximum overturning moment about the sea floor by wave actions is similarly obtained.

Some design diagrams are available for the maximum forces and moments for wave screens. Kriebel[126] and Bergmann and Oumeraci[21] provide information on wave loads for full-depth permeable (slotted) wave screens. Kriebel et al.[130], Gilman and Kriebel[82], Kriebel[127], and Losada et al.[141],[142] provide information on wave loading on partial-depth impermeable wave screens. For wave screens of other configurations, hydraulic model tests are required for evaluation of wave pressures, forces and moments.

For the case of an impermeable wave screen, of the type shown in Figure F.1, the U.S. Army Corps of Engineers Coastal Engineering Manual[235] presents an empirical design method for computing wave forces. Large-scale physical model test data of Kriebel et al.[130] were used to develop an expression for significant force. Results are shown in Figure I.2 and are given by

$$F_{MO} = F_O \left(\frac{w}{h} \right)^{0{,}386\left(h/L_p\right)-0{,}7} \tag{I.1}$$

in which

$$F_O = \rho g H_{MO} \frac{\sin h(k_p h)}{k_p \cos h(k_p h)} \tag{I.2}$$

where

F_{MO} is the significant force per unit width on a partial-depth impermeable wave screen;

F_O is the significant force per unit width on a full-depth wall;

H_{MO} is the significant wave height;

h is the water depth;

w is the wave screen draught or penetration;

L_p is the wavelength associated with peak spectral wave period, T_p;

k_p is the wave number associated with peak spectral wave period, $2\pi/L_p$;

ρ is the water mass density;

g is acceleration due to gravity.

The USACE method should be used within the limits of data for which it was developed: $0{,}4 < w/h < 0{,}7$ and $0{,}14 < h/L_p < 0{,}5$. See Figure I.2.

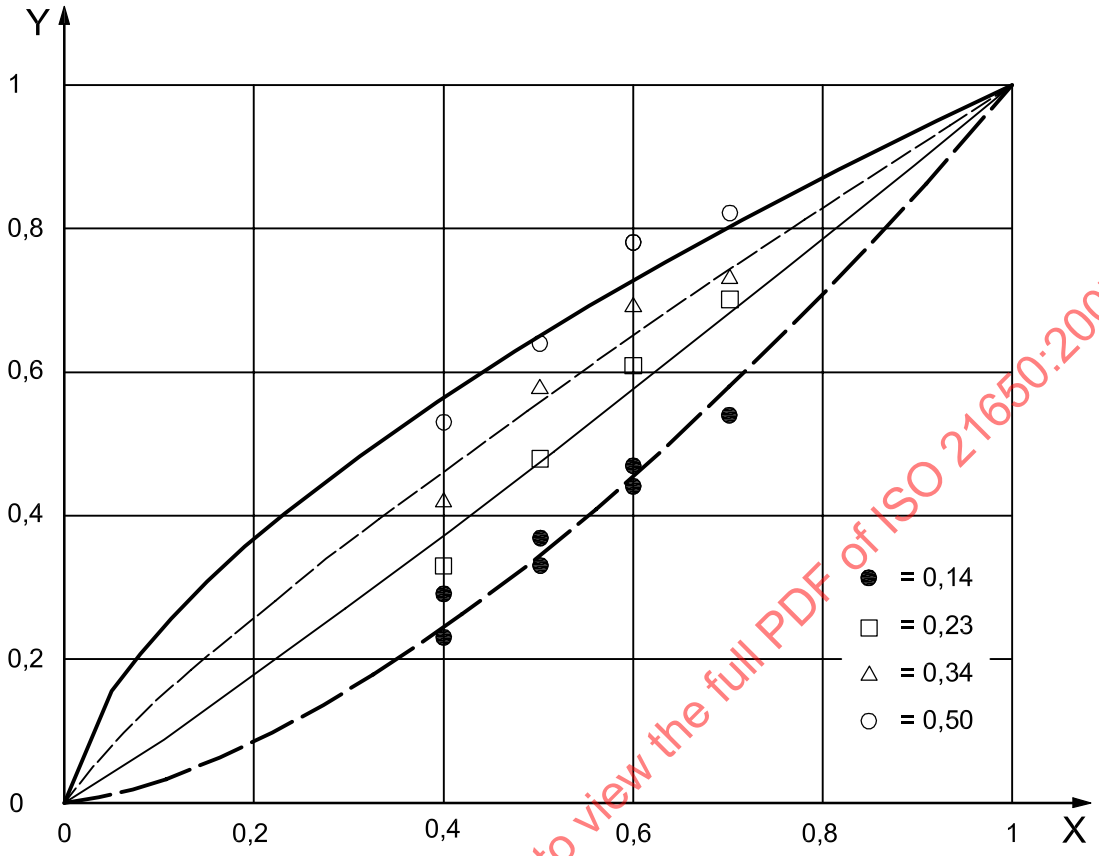

Key

X wall penetration, w/h

Y relative force, F_{MD}/F_O

Figure I.2 — Dimensionless wave forces on impermeable wave screen
(USACE[235])

The design force per unit width on the wave screen should be the load corresponding to the design wave height recommended by Goda[88], of 1,8 H_{MO}. The appropriate design force is then given by

$$F_{Design} = 1{,}8H_{MO} \tag{I.3}$$

Horizontal wave forces vary dynamically in time over the wave cycle. When an incident wave crest is at the wall, dynamic wave loads are landward (toward the harbour side). When an incident wave trough is at the wall, dynamic wave loads are seaward. Equations (I.1) to (I.3) and Figure I.2 give the magnitude of the dynamic force. This can be coupled with sinusoidal time dependence. In some conditions, wave loads associated with the wave trough can be larger than those associated with the crest.

The expressions above are also valid for 0° wave incidence where incident wave crests are parallel to the wave screen. Waves generally approach wave screens obliquely and wave loads are then reduced for non-zero angles of incidence. The Goda formula in Annex E, includes a simple expression to account for the effect of oblique incidence on the pressure intensity. Gilman and Kriebel[82] and Grune and Kohlhase[96] suggest a cosine dependence in oblique waves in which wave loads at 90° incidence are reduced to one-half of those for 0° incidence.

In addition to a reduction in the force per unit length, oblique waves also cause a variation in loading along the length of the wave screen. This longitudinal variation should be considered when designing the structural support (pier or pile supports) for the wave screen.

I.4.3 Connections between wall panels and supporting structures

The method of attachment of the wall panels to the supporting structure is critical due to the oscillatory nature of wave loading on the panels. Loose connections will permit relative movement between the wall panels and the supporting structure, leading to rocking or impact of the panels against the supporting structure. It is important to remember that loads will act in two directions and that connections must work in both compression and tension. Periodic inspection and maintenance is required to prevent damage due to corrosion and/or undesired structural motions.

I.5 Local scour and scour protection.

Assessment of local scour should preferably be based on experience. If lacking, then validated semi-empirical formulae or sediment transport theory can be used. Useful guidelines on scour and scour protection may be found in US Army Corps of Engineers Coastal Engineering Manual[235], Whitehouse[268], Sumer and Fredsøe[213], OCDI[163].